Design and optimisation of adhesively bonded overlap joints

Guido Fessel

A thesis submitted in partial fulfillment of the requirements of Oxford Brookes University for the degree of Doctor of Philosophy.

18th Mai 2009

Abstract

Adhesive bonding is used increasingly by the automotive industry to join structural components of metallic and composite materials. The most common joint configuration is the lap shear joint, which has been investigated widely and several ideas have been proposed to improve its performance. For example, the introduction of fillets at the overlap ends or tapering of the substrates can reduce the peel stresses at the overlap end.

This work reviews the most common joint optimisations and compares the stress distribution of a selection of joint improvements numerically. A parametric study was carried out using FEA showing trends influencing stresses in the adhesive layer and the substrate materials. This resulted in a novel joint design that was called the reverse-bent joint.

Experimental tests were conducted to evaluate the assumptions used in, and the findings of, the FEA. Different metallic materials, as well as fibre reinforced composites, were chosen to be joined with various adhesives. The joint strengths of reverse-bent joints were found to be up to 40% higher compared to flat joints when metallic substrates were used. Due to the significant decrease of through-thickness stresses at the overlap ends the joint strength of composite lap shear joints increased up to 190% using the reverse-bent joint configuration depending upon the chosen fibre layup.

Acknowledgements

I would like to thank Dr. James Broughton and Dr. Neil Fellows for their supervision throughout this investigation.

I would also like to thank Professor Allan Hutchinson and Dr. John Durodola for their help and support in completing this thesis. For the assistance in the laboratory I would like to thank Mike Hartman.

I would also like to thank the support of T. Bharj (Ford Motor Company), M. Birrell (BI-Composites), R Davidson (Crompton Technology), M. Collier (Hodgson and Hodgson), A. Atkins (Siemens Magnet Technology) and M. Burnett (Motor Industry Research Association - MIRA) who were industrial collaborators in the the Faraday Advance, Engineering and Physical Sciences Research Council (EPSRC GR/S27245/01) project, under which this research was carried out.

Finally, many thanks to my family for their support and my friends Srinivasan Puri and Adolfo Lopez Castro.

Contents

List of Figures

List of Tables

List of symbols and abbreviations

δ	Relative displacement
ϵ	Strain
$\acute{\epsilon}$	Strain rate
ν	Poisson's ratio
σ_{ult}	Tensile strength
τ	Shear stress
τ_m	Average shear stress
b	Width
CFRP	Carbon fibre reinforced plastic
DCB	Double cantilever beam
E	Young's modulus
E_a	Adhesive Young's modulus
E_s	Substrate Young's modulus
F	Force
FCGR	Fatigue crack growth rate
FCP	Fatigue crack propagation
FE	Finite Element
FEA	Finite Element Analysis
G	Shear modulus
G'	Strain energy release rate
k	Bending moment factor
l_o	Overlap length

t_a	Adhesive thickness
T_g	Glass transition temperature
t_s	Substrate thickness
UD	Unidirectional
UTS	Ultimate tensile strength
v_s	Volume fraction

1 Introduction

Most industrial products consist of a number of several individual components which require different methods of assembly. This chapter introduces basic joining techniques used in the automotive industry, illustrating the relevance of adhesive bonding and gives the aims and objectives as well as the novelty of this investigation.

1.1 Adhesive bonding

Modern industrial products such as vehicles, trains and airplanes are required to meet demands in addition to their primary function which in this case is the transport of persons and goods. Customers desire more comfort, less noise and vibrations, more safety and also less fuel consumption which requires on one hand the use of various additional components, i.e. small engines or airbags. On the other hand, lighter materials need to be used in order to maintain the same weight. Joining the individual parts is essential as the strength of complex structures usually depends on the strength of the weakest part, which is often the connection between components where loads are transferred.

Adhesively bonded joints can be applied to a wide range of materials and structural adhesives are designed to maintain the stiffness and the strength of the structure. The main advantages of adhesively-bonded joints are:

- an ability to join dissimilar materials, such as polymers, various metallic materials and wood

- the entire contact area is used for bonding and localized stress concentrations, present in spot-welds and bolted joints, are avoided
- holes, which may cause damage or corrosion problems, are not required. The electrical isolation properties of the adhesives act as a galvanic corrosion inhibitor
- due to the large contact area, bonded joints increase the stiffness of the structure compared to discontinuous joining techniques (i.e. spot-welding). Hence, the use of adhesives can lead to weight reduction
- structural adhesives act as a seal against moisture and chemical ingress
- the bondline is not necessarily visible, hence, the aesthetics of the assembly are improved.

Disadvantages need to be understood if bonding is to be used. These are:

- durable bonds require expensive surface treatment
- nondestructive testing is limited in application and therefore quality assurance is difficult
- the integration of curing time and temperatures into the manufacturing process can be problematic as well as applying the required pressure (jigs and fixing) during the cure in order to hold the components together
- structural adhesives are often expensive
- disassembly is difficult
- most adhesives are sensitive to environmental effects
- can be problematic for joining thick substrates.

The most common and extensively studied bonded joint configuration is the traditional lap shear joint, shown in Figure 1.1. Due to the low costs this joint is commonly used in the automotive industry, often with additional spot welds. However, despite the more uniform stress distribution in comparison to mechanical fastenings, bonded lap shear joints may still generate high-localized stresses at the joint ends with very little stress carried in the large central region when a relatively stiff adhesive is used.

Figure 1.1: Lap shear joint

1.2 Aims and objectives

The overall aim of this work was to develop a new overlap joint design, which increased the joint performance significantly without increasing the complexity of production.

The objectives therefore were to:

- review the current optimisation approaches for lap joints available in the literature
- compare a selection of joints using numerical techniques
- develop an existing joint design or novel joint configuration
- develop a joint that is beneficial for a wide range of substrate materials and material combinations
- establish whether the new joint exceeds the static and fatigue performance of the traditional lap shear joint for selected materials

- provide simple tools to estimate the joint strength of the new joint and to provide general design recommendations for its practical application.

1.3 Novelty of this work

Various optimisation methods have already been employed to improve joint strength. Amongst these are the reverse-bent joint (McLaren and MacInnes 1958), the joint with prebent substrates (DasGupta and Sharma 1975) and the wavy joint (Zeng and Sun 2000). In this work these joint configurations were chosen to be investigated in more detail using Finite Element Analysis (FEA). An optimisation of the three joints based upon the stress distribution within the bondline, resulted in a novel joint design. This was similar to the reverse-bent joint and hence, the new joint was also called reverse-bent joint for simplicity.

Further key investigations that were not found in the literature include:

- comparison of the stress distribution within the overlap area of joints with prebent substrates, reverse-bent joints, wavy joints and lap shear joints
- parametric FEA study of the wavy joint for metallic substrates
- parametric studies of the improved reverse-bent joint for various substrate materials, overlap lengths and adhesives
- experimental evaluation of the fatigue performance of the 'new' reverse-bent joint compared with the lap shear joint.

1.4 Outline of the thesis

The literature study provided the background information, including the empirical methods and optimisation approaches. A selection of joint types was consequently analysed and compared using Finite Element Analysis to show the resulting different stress distributions. A final joint configuration was chosen, based on the FEA

results, to be analysed experimentally in comparison with the traditional lap shear joint. Figure 1.2 illustrates the research strategy and the following list gives details of each chapter:

Chapter 2 reviews the literature that developed an increasing understanding of the important mechanisms determining the behaviour of lap shear joints. A few attempts to optimise its stress distribution are presented. Finally, previous work on the fatigue behaviour of bonded joints is discussed.

Chapter 3 characterises the substrate and adhesive materials and manufacturing details that were chosen for the experimental investigation.

Chapter 4 analyses the stress distribution using FEA and discusses failure mechanisms based upon different substrate materials, which leads to a parametric study on certain joint types. This shows the influence of the design variables on the stress distribution within the overlap area.

Chapter 5 presents the results of the experimental investigation, which includes the static tests of metallic and composite joints, as well as the fatigue performance of certain joint types using metallic substrates.

Chapter 6 discusses the experimental results in comparison with the findings of the FE Analysis.

Chapter 7 draws some general conclusions for the recommended joint design and suggests some ideas for future investigations.

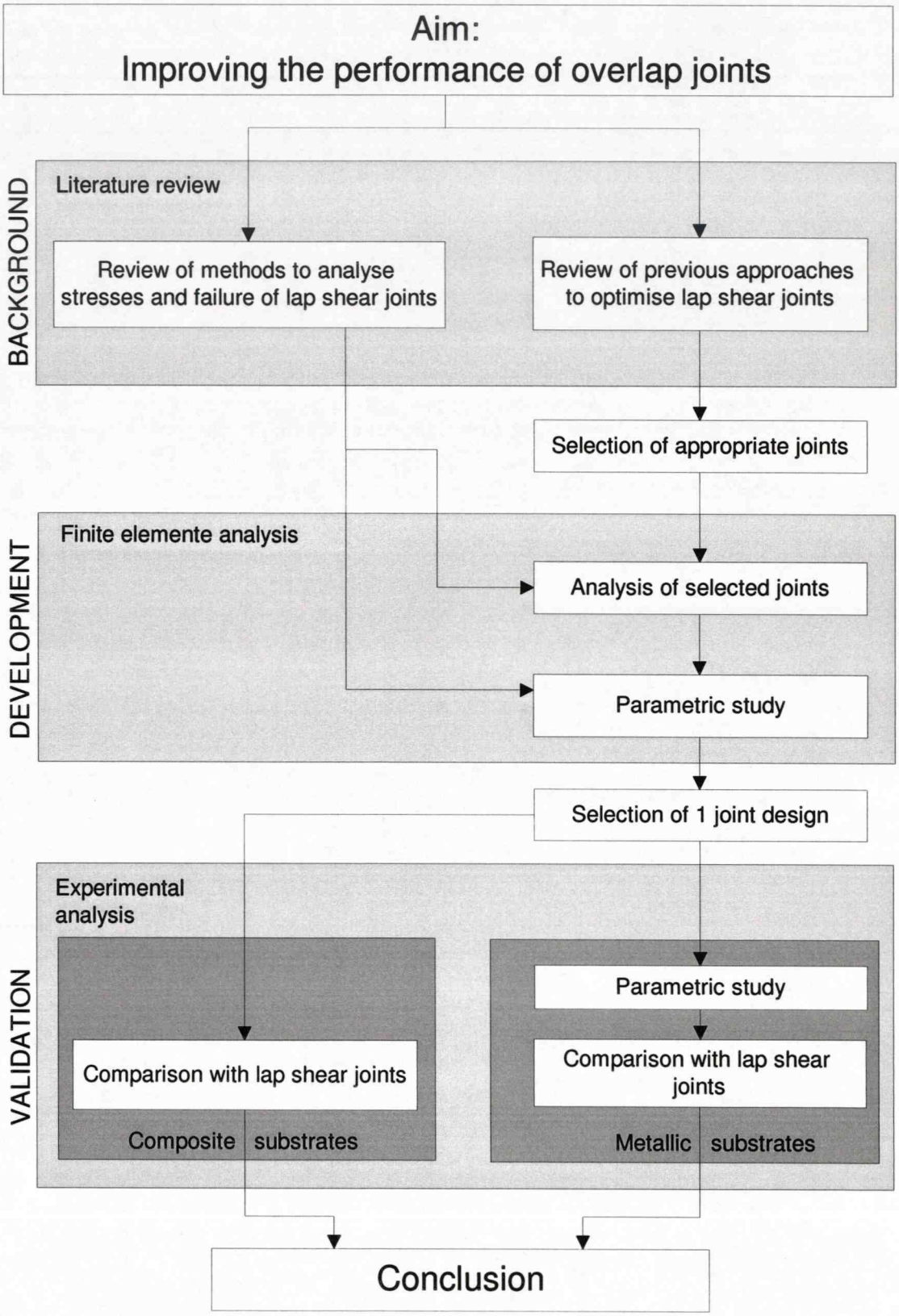

Figure 1.2: Flowchart of the research strategy

2 Review of the analysis and optimisation of adhesively bonded lap joints

Lap shear joints have been investigated extensively and several methods have been developed to predict the stresses generated within the bondline. With an understanding of the failure mechanisms, the joint design focus was to minimize the stresses and to improve the joint strength. This chapter will discuss the main contributions available in the literature although, due to the large variety of joining methods, this survey only focuses on bonded overlap joints.

2.1 Stress and failure prediction methods

Since 1938 bonded joints have been investigated extensively using, initially, closed-form solutions and later, with growing computational resources, Finite Element Analysis (FEA). A review of the key findings of the lap joint analysis show an increasing understanding of the stresses and failure mechanism on which, later, optimisation attempts were based upon.

2.1.1 Closed-form solutions

Various models were developed to predict the joint strength, beginning with the basic Linear-Elastic Approach. Volkersen (1938) then took differential straining into account and Goland and Reissner (1944) the nonlinear behaviour of the joint geometry. Hart-Smith (1973b) later refined the consideration of the joint rotation. This work had significant impacts on joint analysis and was constantly developed further with increasing complexity (Adams et al. 1997).

Linear elastic analysis

The simplest analysis considers rigid substrates and the adhesive only deforming in shear (Figure 2.1). The average stress is calculated by dividing the applied force, F, by the bonded area, bl_o (width and overlap length).

$$\tau_m = \frac{F}{bl_o} \tag{2.1}$$

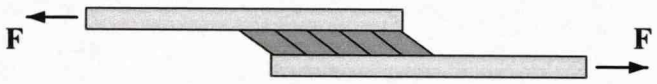

Figure 2.1: Shear stress in the linear elastic analysis assuming stiff substrates

Volkersen's analysis

Volkersen assumed that the adhesive deformed in shear but also that the substrates deform in tension, as shown in Figure 2.2. Both materials are assumed to be linear elastic. With respect to the upper substrate the straining at the loaded overlap end (see A in Figure 2.2) is larger, and decreases towards the unloaded end (see B in Figure 2.2) which results in *differential shear stresses* along the adhesive bondline.

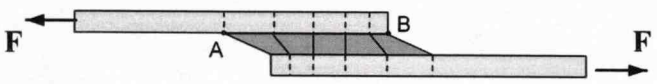

Figure 2.2: Joint with elastic substrates

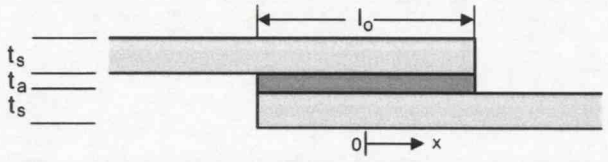

Figure 2.3: Geometry of the lap shear joint

Volkersen's model is based on the relative displacement, δ_x, of the substrates

$$\delta_x = \delta_0 - \int_{-l_o/2}^{x} \epsilon_1 dx + \int_{-l_o/2}^{x} \epsilon_2 dx \tag{2.2}$$

where δ_0 is the relative displacement at $x = -l_o/2$ (see Figure 2.3) and ϵ_1 and ϵ_2 are the strains of the substrates, which are given by:

$$\epsilon_1 = \frac{1}{E_s t_{s1}} \left[F - \int_{-l_o/2}^{x} \tau_x dx \right] \tag{2.3}$$

and

$$\epsilon_2 = \frac{1}{E_s t_{s2}} \int_{-l_o/2}^{x} \tau_x dx \tag{2.4}$$

where E_t is the substrate Young's modulus. The shear strain in the adhesive is derived from:

$$\delta_x = \frac{t_a}{G_a} \tau_a \tag{2.5}$$

where

$$\gamma_a = \frac{\tau_a}{G_a} \tag{2.6}$$

where G_a is the shear modulus, γ_a the shear strain and t_a the thickness of the adhesive. The following equation was obtained by substituting the equations (2.3),(2.4) and (2.5) in equation (2.2):

$$\frac{\partial^2 \tau_x}{\partial x^2} = \omega^2 \tau_x \tag{2.7}$$

which has a solution:

$$\tau_x = A_1 \cosh(\omega x) + A_2 \sinh(\omega x) \tag{2.8}$$

where A_1 and A_2 are constants depending upon the boundary conditions. By substituting (2.1) and (2.8) into 2.9

$$\overline{\tau} = \frac{\tau_x}{\tau_m} \tag{2.9}$$

the following adhesive shear stress distribution can be obtained:

$$\overline{\tau} = \frac{\omega}{2}\frac{\cosh(\omega X)}{\sinh(\omega/2)} + \left(\frac{\Psi - 1}{\Psi + 1}\right)\frac{\omega}{2}\frac{\sinh(\omega X)}{\cosh(\omega/2)} \tag{2.10}$$

where

$$\omega^2 = (1 + \Psi)\Phi \tag{2.11}$$

$$\Psi = \frac{t_{s1}}{t_{s2}} \tag{2.12}$$

$$\Phi = \frac{G_a l_o^2}{E_s t_{s1} t_a} \tag{2.13}$$

$$X = \frac{x}{l_o} \tag{2.14}$$

$$-\frac{1}{2} \leq X \leq \frac{1}{2} \tag{2.15}$$

For the case of equal substrate thickness the maximum adhesive shear stress is given by:

$$\overline{\tau}_{max} = \sqrt{\frac{\Phi}{2}}\coth\sqrt{\frac{\Phi}{2}} \tag{2.16}$$

Consequently, the joint strength is reached when the maximum applied shear stress is equal to the failure shear stress of the adhesive.

Volkersen showed that the stress within the adhesive is not constant along the overlap. He also showed that the substrates had differential straining, predicting

shear stresses within the adhesive that varies along the bondline with a maximum value located at the overlap ends. Equation 2.13 accounts for the substrate properties suggesting a material with a high Young's modulus and a high thickness in order to maximise the joint strength. This was an important step in understanding the failure mechanism of lap shear joints. Later, new joint types were introduced that were aimed at reducing Volkersen's effect of differential straining in order to increase the joint strength, such as joints with tapered substrates.

However, equation 2.13 shows that the joint strength should be approximately proportional to t_a, meaning thicker adhesive layers should be stronger than thin ones, which contradicts experimental evidence (Adams 2001). Furthermore, the analysis does not consider that the applied loading was not collinear, which causes the overlap area to rotate under loading conditions. This had the effect of introducing a bending moment in the substrates and causes high peel stresses at the overlap ends.

Goland and Reissner's analysis

Goland and Reissner (1944) recognised the importance of the rotation of the overlap area (see Figure 2.4) and consequently the resulting through-thickness stresses at the overlap ends. They, subsequently, introduced a bending moment factor, k, that accounts for substrate eccentricity resulting in the overlap rotation:

$$M_0 = kF\frac{t_s}{2} \tag{2.17}$$

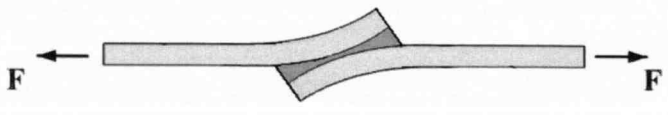

Figure 2.4: Lap shear joint under loading

If the load on the joint is small the bending moment is large ($k = 1$). With higher loads the overlap area rotates until eventually the substrates are aligned. During

this process the bending moment decreases, reducing the k-factor. The value of the bending moment factor was given by:

$$k = \frac{1}{1 + 2\sqrt{2}\tanh\theta/2\sqrt{2}} \tag{2.18}$$

where

$$\theta = l_o\sqrt{\frac{3F(1-\nu_s^2)}{bE_s t_s^3}} \tag{2.19}$$

and ν is the Poisson's ratio. Goland and Reissner included the bending moment factor as a function of the maximum shear stress in order to account for its decreasing effect when the applied load increased:

$$\tau_{max} = \frac{F}{8}(1+3k)\sqrt{8\frac{G_a}{E_s}\frac{t_s}{t_a}} \tag{2.20}$$

Furthermore through-thickness stresses, σ_t, were taken into account, when:

$$\sigma_t = \frac{\sigma t_s^2}{C^2 R_3}\left[\left(R_2\lambda^2\frac{k}{2} + \lambda k'\cosh\lambda\cos\lambda\right)\cosh\frac{\lambda x}{C}\cos\frac{\lambda x}{C}\right] +$$

$$\frac{\sigma t_s^2}{C^2 R_3}\left[\left(R_1\lambda^2\frac{k}{2} + \lambda k'\sinh\lambda\sin\lambda\right)\sinh\frac{\lambda x}{C}\sin\frac{\lambda x}{C}\right] \tag{2.21}$$

where

$$C = \frac{l}{2}$$

$$\lambda = \frac{C}{t_s}\left(\frac{6E_a t_s}{E_s t_a}\right)^{1/4}$$

$$k' = k\frac{C}{t_s}\left(3(1-\nu_s^2)\frac{\sigma}{E_s}\right)^{1/2}$$

$$R_1 = \cosh\lambda\sin\lambda + \sinh\lambda\cos\lambda$$

$$R_2 = \sinh\lambda\cos\lambda - \cosh\lambda\sin\lambda$$

$$R_3 = \frac{\sinh 2\lambda\sin 2\lambda}{2}$$

The analysis of Goland and Reissner (1944) showed that a load dependent nonlinear joint deformation affects the stress distribution within the adhesive. Figure 2.5 shows the bending moment factor, k, decreasing with increasing load. Hence, when the joint is subjected to cyclic loading at low load levels (fatigue) the bending of the substrates significantly affects the failure of the joint and may, in certain cases, produce failure within the substrates. Consequently, the influence of the bending moment on the static strength of the lap shear joint is smaller.

Equation (2.20) illustrates that lower k-values can decrease the maximum shear stress occurring within the adhesive layer. Based upon this fact new joint types were introduced that reduced the joint rotation to minimise the bending moment in order to increase the joint strength, as in the case of the joint with prebent substrates (DasGupta and Sharma 1975).

Hart-Smith analysis

Hart-Smith (1973b) believed that Goland and Reissner overestimated the bending moment in the substrates and developed a different approach to calculate the factor, k, where:

$$k = \frac{1}{1 + \theta + \theta^2/6} \tag{2.22}$$

Figure 2.5 shows a comparison of the k-factor determined by Goland and Reissner (1944) and Hart-Smith (1973b).

The work done by Volkersen, Goland and Reissner and Hart-Smith was refined subsequently. Later work accounted for substrate stresses in greater detail and included material non-linearities. The closed-form solutions became more complicated and thus difficult to apply in practice. Today, numerical techniques are commonly used to analyse the stresses within joints. However, the main mechanisms that lead to the failure in lap shear joints were described by Volkersen (1938)

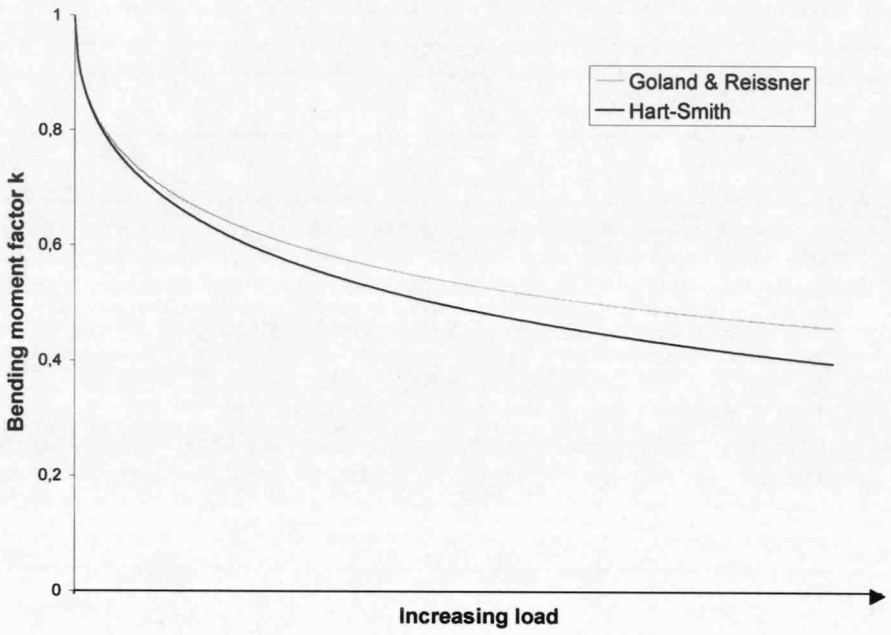

Figure 2.5: Bending moment factor, k, given by Goland and Reissner and Hart-Smith

and Goland and Reissner (1944).

2.1.2 Numerical solutions

Increasing computer power enabled the use of numerical techniques to simulate adhesive joints. Arguably, the most common method is Finite Element Analysis (FEA) where structures are divided into small finite regions to solve the overall complex problem. In this work FEA will be used to study the stress distribution occurring in lap joints, although certain limitations need to be considered.

Modelling lap shear joints

In lap shear joints the bondline is relatively thin compared to the substrate thickness. However, to achieve accurate results the adhesive layer needs to be modelled with a fine mesh. The substrates can though be meshed using larger elements in areas away from the overlap in order to save computational time.

Hildebrand (1994) showed the importance of allowing geometric and material

non-linearities, as first shown by Goland and Reissner (1944) and Hart-Smith (1973b). Geometric nonlinearities need to be modeled accurately because the stress distribution within the adhesive and substrates changes significantly under various loading conditions.

Furthermore, the adhesive and substrate can plastically deform before ultimate failure occurs. This may affect the stress distribution of the overlap area and thus, the materials should be modelled including their non-linear stress-strain behaviour. Suitable data can be obtained from material tests.

Plane strain versus plane stress

3D models provide the most accurate results but require high computational resources due to the high number and higher order of elements required, and it is often possible to simplify the analyses by using 2D models. Krueger et al. (2002) compared a 3D model with 2D plane stress and plane strain solutions for joints with composite substrates. They suggested using the results of the plane stress and plane strain solutions as upper and lower bounds.

Richardson et al. (1993) proved the plane strain assumption to be reasonably accurate for most joint geometries. The central part of the joint, i.e. over about 80% of the joint width, are effectively in a state of plane strain. The stress in the substrates has been shown to be non-uniform across the width of the substrates. A method was developed to apply the load profile obtained from the 3D analysis to the 2D model which can subsequently be of greater detail. However, for the purpose of this investigation this was neglected. Thus, a 2D-plane-strain analysis appeared to be appropriate.

Stress singularities

An additional complication for the modeling of bonded joints are stress singularities. At particular points where geometry and material properties change abruptly

discontinuities occur which in linear elastic models produce singularities. Greater mesh density just increases the stresses at the ends of the overlap length in the case of lap shear joints. Volkersen (1938) and Goland and Reissner (1944) predicted the highest stresses at these singular points, where numerically predicted stresses vary with the mesh density. Thus, it appears to be difficult to predict stresses and failure in this area, without altering the geometry to suit experimental results. In this study stress distributions of various lap joints were only compared and therefore stress singularities can be ignored as discussed further on.

2.1.3 Failure modes

Although, in many cases the adhesive itself appears to be the weakest link in lap joints, the failure can occur initially and also totally within the substrates depending upon the chosen materials and overlap geometries. The most common failure modes are (see also Figure 2.6):

- *Cohesive failure of the adhesive layer.* This occurs when a crack runs only through the adhesive.
- *Adhesion failure.* This occurs at the interface between substrate and adhesive, which can be prevented using adequate surface preparation techniques.
- *Interlaminar substrate failure.* This can cause composite joints to fail within the substrate due to the low through-thickness strength of the composite and high peel stresses located near to the overlap ends of lap shear joints.
- *Plastic deformation of metallic substrates.* This significantly affects the ultimate failure of the joint, introducing high strains into the adhesive.

Joints can also fail by a combination of the above.

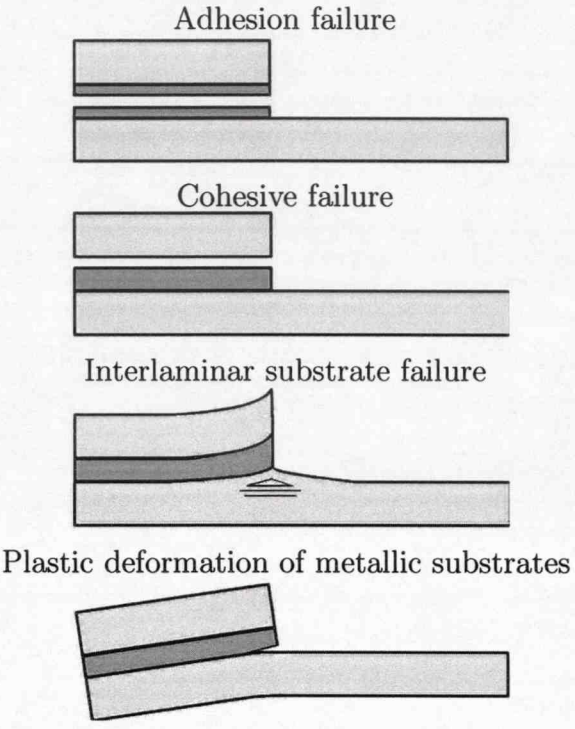

Figure 2.6: A selection of failure modes of adhesive joints

2.1.4 Failure criteria

The application of closed-form solutions and failure criteria is often time consuming and requires a detailed analysis. To estimate the strength of metallic joints Adams et al. (1997) suggested a practical attempt based on the yield strength of the metallic substrates, σ_y, and the ultimate shear strength, τ_u, or yield shear strength, τ_y, of the adhesive. When the overlap area rotates under loading the metallic substrates bend and may yield adjacent to the adhesive interface, which introduces high strains into the adhesive leading to failure of the joint. The maximum load, F_{max}, that can be applied to the joint before plastic deformation of the substrates occurs, was given by:

$$F_{max} = \frac{\sigma_y b t_s}{4} \tag{2.23}$$

where b is the joint width and t_s the substrate thickness.

If the overlap is very short the joint may fail in the adhesive before the substrates

yields:

$$F_{max} = \tau_y l_o b \tag{2.24}$$

Additionally, the use of a safety factor of at least 5 and preferably 20 to account for environmental effects was suggested (Adams et al. 1997).

Renton and Vinson (1975) gave some simple design recommendations to maximise the static and fatigue load carrying capability of bonded lap shear joints such as preferable ratios between overlap length and substrate thickness. Chamis and Murthy (1991) summarised step-by-step procedures for the preliminary design of composite joints. Simple equations were used to estimate the influence of the most important factors on the joint such as applied loads, environmental effects, material properties and different geometries. This can be helpful for the initial design of joints. When structures require joints with higher strength more accurate results for the strength prediction of joints can be achieved with the use of FEA, together with appropriate failure criteria applied to the adhesive and substrates, particularly fibre reinforced composites, which tend to fail by delamination before failure in the adhesive occurs.

Adhesive failure criteria

The properties of adhesives can vary over a wide range and therewith the applicability of chosen failure criterion is important. Fracture and Damage mechanics can be used for brittle or semi-britle adhesives with minimal plastic deformation before failure. Maximum stress or strain criteria are based on peel stresses, principal tensile stresses or strains. However, these criteria are not suitable for adhesives that yield significantly before failure. Neither are the commonly applied von Mises or Tresca criteria as the hydrostatic stress component also needs to be taken into account. The Drucker-Prager yield criterion (Drucker and Prager 1952) is a pressure dependent model which distinguishes between tensile and compressive stresses. Figure 2.7 shows a comparison of the yield surfaces of the von Mises and Drucker-

Prager criterion.

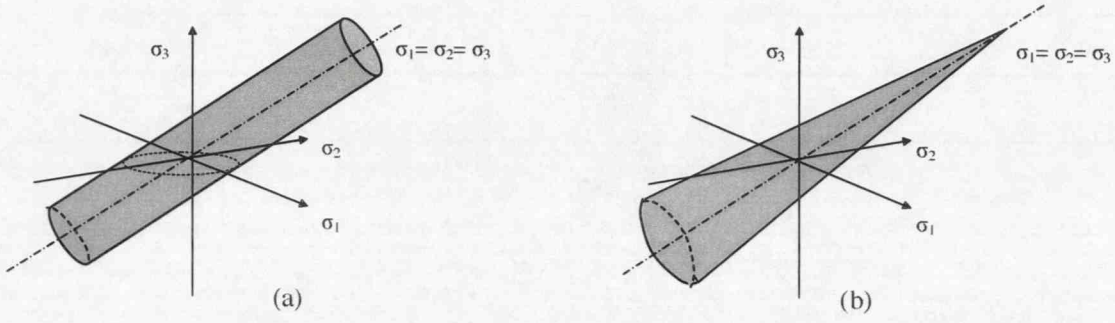

Figure 2.7: Yield surface of the von Mises (a) and Drucker-Prager (b) yield criterion

Criteria for failure in the composite substrate

There are macroscopic failure criteria used to predict failure in plies of composite materials. Apparently, the failure criteria most applied to composites are maximum strain and maximum stress criteria, the Tsai-Hill criterion (Tsai 1965), the Tsai-Wu criterion (Tsai and Wu 1971), the Yamada and Sun criterion (Yamada and Sun 1978) and the Hashin criterion (Hashin 1981).

However, predicting failure of composite structures with varying geometries and loading conditions, where the composite material is made of several plies in certain directions, is complex and often experimental work is required to validate the analyses.

Due to the large variation of failure criteria and the ongoing discussion about their applicability to lap shear joints, the optimisation in this study is only based upon the distribution of stresses within both the adhesive and the substrates.

2.2 Lap joint designs and optimisation attempts

In order to develop a joint with a high strength that also meets cost and weight requirements it is essential to review and compare the current joints and optimi-

sation methods available in the literature beginning with the standard lap shear joint.

2.2.1 A selection of lap joint types

Traditional lap shear joint

Lap shear joints (see Figure 1.1) are the simplest joints to manufacture and, as such, are commonly used to bond structures together. Despite the more uniform stress distribution compared to mechanical fastening techniques like riveting or spot-welding, high stresses at the overlap ends still occur. Figure 2.8 shows the shear stress distribution along the overlap length with peaks at the overlap ends caused by the differential straining of the substrates. As discussed previously in Section 2.1.1, the overlap area rotates under loading conditions due to the misalignment of the substrates. This causes high peel stresses in the through-thickness direction, also shown in Figure 2.8.

The adhesive properties, the overlap geometry and substrate material can influence the joint strength significantly. Metallic substrates may plastically deform in bending when the overlap area rotates which introduces high strains into the adhesive and may cause failure of the joint. In the case of composite substrates high through-thickness stresses can cause the fibre layup to fail in delamination due to typically low strengths in this direction. Hence, bonded lap shear joints often fail at average stresses which are considerably lower than the shear strength of the adhesive. Increasing the overlap length is only beneficial for very small overlaps. Beyond a given overlap length the peel stress reduction is only marginal (Adams et al. 1997).

Double lap joint

In symmetrical double lap joints, shown in Figure 2.9, the inner substrate experiences no bending moment but the outer substrates bend under loading which

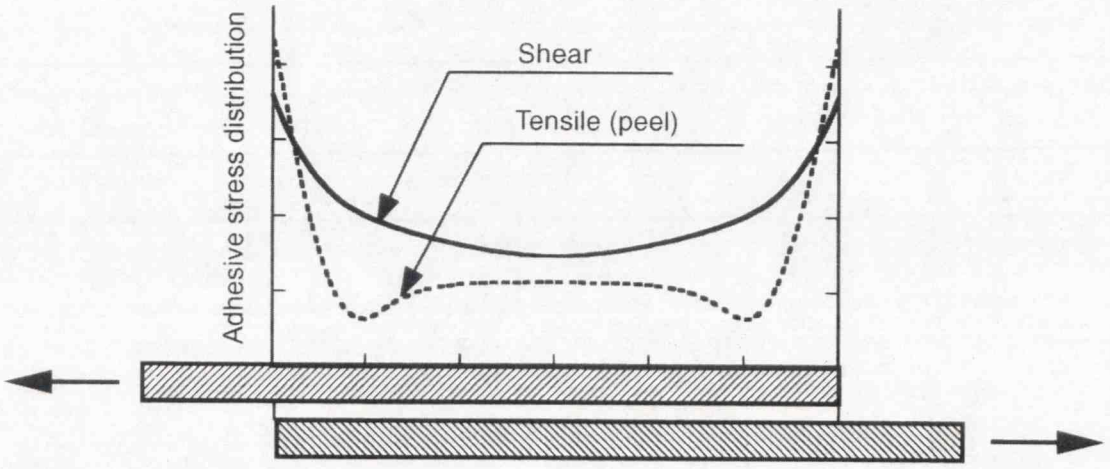

Figure 2.8: Ideal shear and tensile stress distribution within lap shear joints (Harris 2003)

results in tensile through-thickness stresses at the unloaded overlap end of the outer substrates and compressive stresses at the loaded end. The analysis of this joint may help to understand the failure mechanisms of other joints such as co-axial joints.

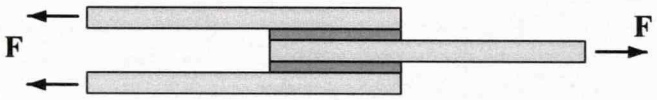

Figure 2.9: Double-lap joint

Scarf joint

The main advantage of scarf joints with very low scarf angles (see Figure 2.10) over lap shear joints is the avoidance of substrate eccentricity and thus reduced bending moments. The distribution of shear stress is almost constant along the overlap length as well as through-thickness stresses which are, compared to shear stresses, low depending on the scarf angle (Gleich et al. 2000). Due to the expensive manufacturing of the substrates especially for long overlaps or thin substrate materials the scarf joint is rarely used in mass production.

Figure 2.10: Scarf joint

Stepped scarf joint

The stepped scarf joint (see Figure 2.11) provides well distributed stresses in the overlap area similar to the scarf joint, but at points where the substrate thickness changes stress concentrations still occur. The aligned substrates reduce critical peel stresses which normally results in higher joint strength compared to similar lap shear joints, but again this joint type is expensive to manufacture.

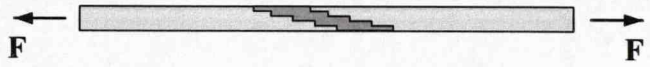

Figure 2.11: Stepped scarf joint

Joggle lap joint

In joggle lap joints, as shown in Figure 2.12, the misalignment of the substrates is avoided but the substrates also bend under loading conditions and introduce high stresses into the adhesive. Givler and Pipes (1981) performed a parametric study on composite substrates and concluded some design rules for joggle joints. It was shown that the load was transferred through a small part of the overlap and large areas were subjected to low stresses similar to stresses within lap shear joints. This joint is beneficial for esthetic applications where a flat surface finish is preferred.

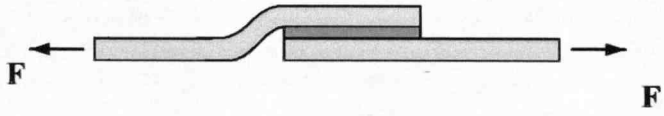

Figure 2.12: Joggle lap joint

Reverse-bent joint

McLaren and MacInnes (1958) investigated the influence of the bending moment factor, k, introduced by Goland and Reissner (1944), on the stress distribution within the overlap area of lap shear joints. A photoelastic analysis was carried out where the load was applied at different angles to the overlap area to obtain the distribution of stresses resulting from different k-factors. Compared to the analytical model of Goland and Reissner (1944) this analysis allowed a wider range of k-factors to be analysed.

The bending moment factor, k, was given by:

$$k = \frac{DE}{DB} \tag{2.25}$$

where DE and DB are dimensions defined in Figure 2.13. The dashed line displays the direction in which the load, T, was applied on the joint.

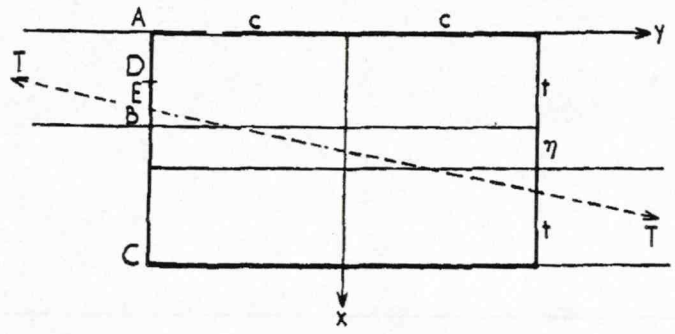

Figure 2.13: Direction of load applied to the joint
McLaren and MacInnes (1958)

The experimental study using photoelasticity showed the best distribution of stresses for the bending moment factor $k = -0.5$, which reduced the stress peaks at the overlap ends significantly. It was consequently suggested to create such a joint, named the reverse-bent joint, with a uniform stress distribution along the overlap area. The joint is shown in Figure 2.14.

Greenwood et al. (1966) produced reverse-bent joints with steel substrates comparing various positive and negative k-factors. The highest failure loads were ob-

tained from joints with a k-value of about -0.5. However, an overlap length of 76mm and a substrates thickness of 13mm was used, which is quite unrealistic for current automotive applications.

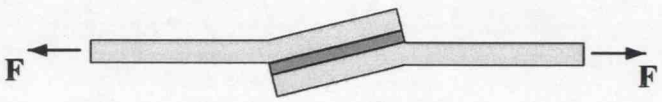

Figure 2.14: Reverse-bent joint

Joints with prebent substrates

DasGupta and Sharma (1975) also tried to reduce the stresses concentrations with variations in the joint geometry. In contrast to the reverse-bent joint, the substrates were bent outside of the overlap to angles of 5° and 10°, as shown in Figure 2.15. Reduced stresses within the overlap area were shown using closed form solutions. Experiments with 3.2 mm thick metal substrates and a structural adhesive (E = 2.5 GPa) resulted in 60% joint strength improvement over the lap shear joint for the 5° bend angle and 120% for the 10° bend angle. However, due to the flattening of the joint under loading, a large displacement before failure of the 10° joints was reported which may or may not be acceptable for certain applications.

DasGupta (1979) carried out a Finite Element Analysis (FEA) on joints with prebent substrates and compared the results with the analytical solution and experimental results. Both methods were found satisfactory for calculating the joint strength.

Sancaktar and Lawry (1980) applied photoelasticity to the joint showing reduced stresses for prebent substrates. The use of large prebent angles was not recommended due to a possible substrate failure.

Sawyer and Cooper (1981) deployed a modified analytical model, FEA and photoelasticity to study the influence of various parameters, which included applied load, substrate and adhesive material properties, and the joint geometry, on maximum stresses within the overlap. Experiments showed the greatest improvement

for a 15° prebend angle.

The substrate bend that is required prior to the bonding process can presumably be integrated in the metal-forming or in the manufacturing process of the composite components. Thus, a significant increase of the production costs is not expected and the tensile joint strength may increase significantly compared to the lap shear joint, though overall joint stiffness can be reduced.

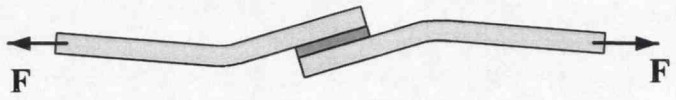

Figure 2.15: Joint with prebent substrates

Wavy joint

Zeng and Sun (2000) introduced a novel lap joint geometry that they named wavy joint. The substrates were shaped as shown in Figure 2.16 which is actually the exaggerated shape of highly loaded lap shear joints. It was shown numerically that critical tensile through-thickness stresses at the overlap ends, typically associated with lap shear joints, were replaced by compressive stresses. The remaining tensile stresses are more uniformly distributed over the central region of the joint.

An experimental study using a structural adhesive ($E = 2.2$ GPa) and carbon-fibre epoxy substrates validated the improved stress distributions resulting in significantly higher failure loads. Depending on the fibre layup of the composite substrates, the joint strength of the wavy joint showed improvements of between 56% and 113% over the lap shear joint.

The fatigue behaviour of the wavy joint was subsequently compared with the lap shear joint using the same adhesive and unidirectional carbon epoxy substrates (Zeng and Sun 2004). Both joint types where tested in fatigue at about 53% and 40% of the static joint strength, which gave similar results when the load was normalised to the static joint strength. When comparing absolute load levels of both joint types the load applied to the wavy joint would need to be doubled to

produce a similar fatigue life.

Additionally, Zeng (2001) carried out a parametric study using FEA which included the overlap length, l_o, the radius, R, the initial proportion of the overlap, P, and the angle, α (for details see Figure 4.4 and the FE Analysis in chapter 4). Stress distributions, plotted along the overlap length, were used to show the influence of the various design variables. The influence of design changes on the failure load of the wavy joint was then investigated experimentally, showing the following trends of the design variables:

- Larger initial proportion of the overlap, P, reduced interfacial stresses and increased joint strength
- Smaller angles, α: increased the failure load but compressive through-thickness stresses at the overlap end disappeared as the wavy angle approached zero
- The larger the radius, R, the better.

Although the improved wavy joint (Zeng 2001) showed almost 30% higher failure loads compared to the initial design, the comparison of static and fatigue performance (Zeng and Sun 2000; Zeng and Sun 2004) against the lap shear joint was carried out with the initial wavy joint design where no justification for their values for the design variables could be found.

Avila and Bueno (2004) argued that Zeng and Sun considered an overlap length of 25.4 mm measured at the horizontal line whereas the bondline that follows the wavy shape is actually 3% longer. Thus, Avila and Bueno (2004) carried out a similar investigation using woven E-glass/epoxy composites where they considered the real overlap length. As expected, they also concluded a significant increase in joint strength, similar to the analysis of Zeng and Sun (2000).

In contrast, Melograna and Grenestedt (2004) showed a poor performance using a similar wavy joint configuration with different composite and adhesive materials and with a comparable overlap geometry. They argued that high through-thickness

stresses, although located more centrally, remained the main cause of delamination within their chosen material combination. Zeng and Sun (2000) used materials which failed in delamination mainly due to high stress intensities at the overlap ends. These stress intensities were reduced in the wavy shape providing improved performance. The material used by Melograna and Grenestedt (2004) was tougher and thus, failure was not initiated near the substrate ends, but by the remaining tensile through-thickness stresses in the central regions of the overlap.

The wavy joint appears to be a promising design to increase joint strength although fabrication and assembly tolerances of the joined components may result in mismatches in the overlap area of the wavy joint. Further investigations of the design variables and especially using different substrate and adhesive materials are required to obtain conclusive results.

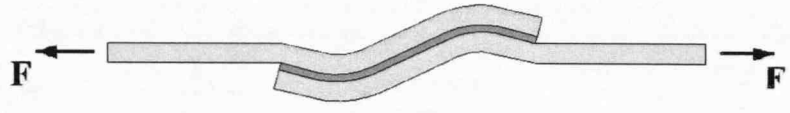

Figure 2.16: Wavy joint

2.2.2 Variable adhesives and adhesive properties

Joints with multi-modulus bondline

Stress concentrations at the overlap ends should be avoided especially for brittle adhesives which do not allow large straining before failure. Hennig (1965) suggested the variation of the shear modulus along the bondline inversely proportional to the stress distribution which results in constant shear stress distribution across the overlap area. Experimentally, a more flexible adhesive was used at the overlap ends which was able to relieve the stress peaks, whereas, in the centre a high-modulus adhesive gave a high shear strength. Using metallic substrates a joint strength improvement of 20% was reported where a high-modulus adhesive was used over 50% - 75% of the overlap length in the centre of the joint.

Raphael (1966) investigated multi-modulus bondlines theoretically using closed form solutions aiming to predict the highest possible joint strength. Pires et al. (2003) carried out an experimental study using aluminium substrates. An increase of joint strength up to 22% was reported.

Fitton and Broughton (2005) used the same approach for composite substrates where the low though-thickness strength of the composite mostly causes delamination failure within the substrates. Experiments showed an increase of joint strength up to 100% for certain material combinations.

Hart-Smith (1973a) expected a greater potential of this technique for the application of bonded joints at large temperature ranges where the brittle adhesive performs at high temperatures and the flexible adhesive carries the load at low temperatures. Da Silva and Adams (2007) investigated this idea and showed experimentally benefits for applications in certain temperature ranges.

Due to the expensive application of 3 different adhesive sections and the required separation methods within the overlap area that are usually not longer than 20 mm and the small potential of increasing the joint strength, the joint has not so far been used in industry.

Rubber toughening

The formulation of many adhesives has been varied using additives like solvents, plasticisers or reinforcing fillers. Especially for lap shear joints a compromise between brittle adhesives with high shear strengths and more ductile adhesives resisting high peel stresses is required.

Elastic particles, such as rubber, are commonly added to high-modulus adhesives to increase the crack growth resistance and toughness of the adhesive. Sancaktar and Kumar (2000) showed advantages of toughening the adhesive either over the entire overlap area or limiting it to the outer regions of the overlap, where high stresses in lap shear joints may cause cracks to initiate.

2.2.3 Geometric optimisation of the end of the overlap

With the understanding of the poor distribution of stress within lap shear joints many researchers tried to relieve these stress concentrations with small changes in the shape of the joint geometry at the end of the overlap.

Adhesive fillets and tapered substrates

Stress peaks at the overlap ends of lap shear joints can be reduced by local concentrations of adhesive. This can be implemented using adhesive fillets and tapered substrates at the overlap ends. Adams and Harris (1987) investigated various fillet sizes and radiused substrates and recommended the design, shown in Figure 2.17, to improve the joint strength. Typical stress peaks at the overlap ends were distributed over a larger area and the magnitudes reduced significantly.

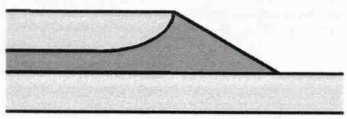

Figure 2.17: Radiused substrates and adhesive fillet

Hildebrand (1994) used hybrid joints with composite and metal substrates to show the effect of different overlap end geometries on joint strength. Various fillet angles in combination with radiused or tapered substrates were tested, as can be seen in Figure 2.18. Best results were produced with design G, with a joint strength 260% higher compared to geometry A. The joint always failed in the composite substrate, similar results may, subsequently, be expected for composite-composite joints.

A numerical method to optimise the shape of fillets was developed by Rispler et al. (2000). A Finite Element model of the lap shear joint with a large fillet at the overlap end was created and subsequently loaded. Elements of the adhesive layer which were lowly stressed and had free edges were progressively deleted. The driving criterion was the mean maximum principal stress. An optimum was found

for fillets with an angle of 45° similar to geometry F in Figure 2.18.

However, tapered substrates are difficult to manufacture or impractical with thin substrates and thus expensive. Controlling the size of adhesive fillets is also complicated when applied to industrial processes. Hence, these approaches are rarely relied upon in practice.

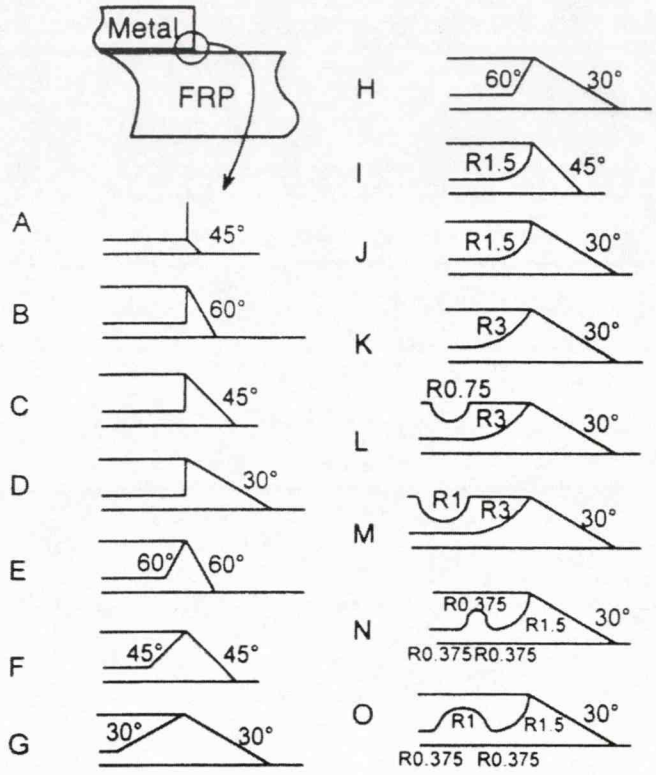

Figure 2.18: Modified geometry of the joint edges
Hildebrand (1994)

Tapered substrate overlap ends with constant bondline thickness

Cherry and Harrison (1970) presented a method to produce a uniform shear stress distribution along the bond line. The substrate thickness was reduced starting from the loaded substrate towards the unloaded end where the thickness approached zero. Figure 2.19 illustrates this method. A uniform substrate deformation along the loading direction reduced the differential straining and resulted in a more uniform distribution of shear stresses.

Ojalvo (1985) used a more advanced model for double lap shear joints that

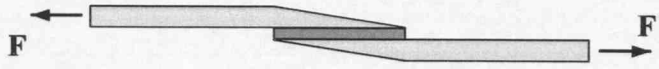

Figure 2.19: Joint with tapered substrates and constant bondline thickness

included peel stresses. Groth and Nordlund (1991) and Nirantar and Sancaktar (2002) used Finite Element Analysis (FEA) to improve the substrate shape. Hu et al. (1998) applied a method based on fracture mechanics for the optimisation of the substrate shape.

Once again, tapering of the substrates over the entire overlap length is expensive, or impractical with thin substrates and only the effect of differential straining is reduced. If thick substrates are used scarf joints can be used that may produce the same costs but scarf joints also avoid the misalignment and the resulting problems.

Notched Substrates

Notched Substrates (Figure 2.20) were investigated by Sancaktar and Simmons (2000). The idea was to allow joint rotation without introducing large straining into the substrates and thus into the adhesive.

Under loading conditions the substrates of lap shear joints tend to bend at the overlap ends. At this point Sancaktar and Simmons (2000) notched the substrates which reduced the tensile strains adjacent to the adhesive significantly.

On one hand notched substrates reduce strains caused by bending but on the other hand the reduced cross section area of the substrate at the critical point may cause plastic deformations or ultimate failure of the metal due to the high tensile stresses over the remaining substrate thickness at the notch section. Thus, only a few applications may benefit from this idea.

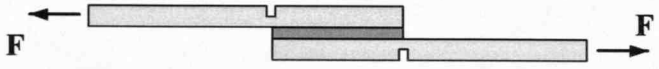

Figure 2.20: Lap shear joint with notched substrates

Nested overlap joints

Coates and Armanios (2000) extended the idea of co-cured joints for composite substrates by altering the fibre layup within the overlap area. The increasing number of planes can transfer more load from one substrate to the other. Figure 2.21(a) shows a single nested overlap joint where one layer of each substrate is used to increase the contact area. The design can be extended further to double nested overlap joints, as shown in Figure 2.21(b), where 2 layers of fibres of each substrate are laid up in an alternating sequence which again increases the area for load transfer.

The third design involves slicing both contacting plies at one end along the axial direction. An additional ply with fibres orientated in the width direction is then placed at the interface between the slices in a weave manner, as shown schematically in Figure 2.21(c).

Test data showed a strength increase of up to 70% for nested overlap joints. The results were strongly dependent on the selected composite materials and chosen fibre orientations. A general conclusion as to which design was preferable appeared difficult.

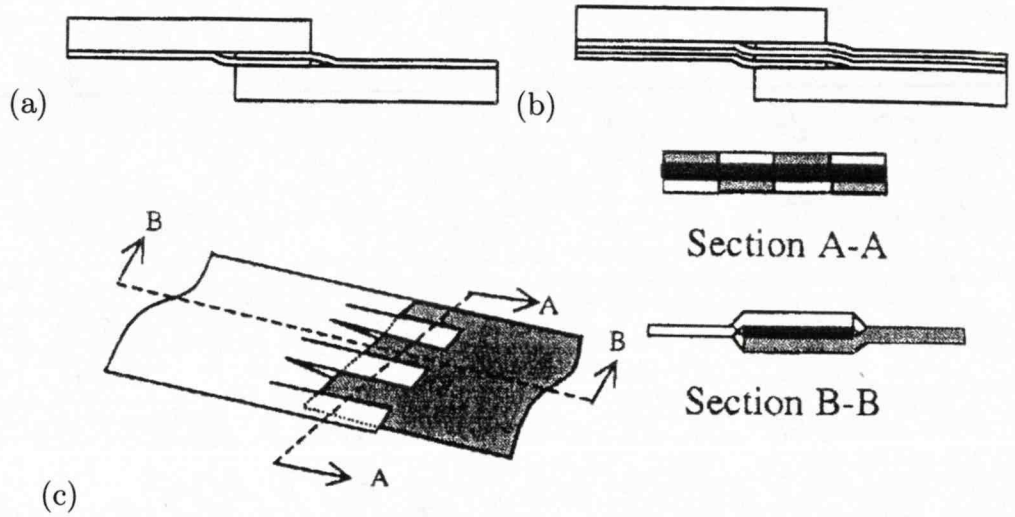

Figure 2.21: Nested overlap joints: (a) Single nested (b) Double nested (c) Transverse Interfacial Layer
Coates and Armanios (2000)

2.2.4 Lap shear joints with additional elements

Weld-bonding

Weld-bonding is now commonly used in the automotive industry for joining metallic structures. Generally, weld-bonding appears to give higher static, fatigue and impact joint strength than each method alone (Chang et al. 1999). A major advantage is the instant fastening which gives functional integrity during the assembly process.

Disadvantageous are the small compatibility of substrate materials and during the production process of weld-bonds adhesive located at the spot-weld is squeezed out or burned which also affects the material close to the spot weld.

Rivet-bonding

Rivet-bonding combines mechanical fastening (rivets) with adhesive bonding. Due to the applicability to various materials and material combinations the automotive industry uses self-pearcing rivets and adhesives for joining aluminium structures. Self-piercing rivets were designed to assemble structures without the need for a hole. The tool drives the rivet into the top layers of the joint and then spreads and forms the rivet within the bottom layer of the joint without penetrating it (see Figure 2.22). In comparison to spot-welded joints rivets are weaker in static and impact conditions (Miller et al. 1998).

Lap shear joints with adhesively-bonded columns

Liu and Sawa (2002) investigated bonded lap shear joints which were reinforced by metallic columns bonded in holes that were drilled through both substrates, similarly to bolted-adhesive joints (see Figure 2.23). This technique was developed to increases the strength of joints with thick substrates. Compared to alternative techniques such as additional bolts or rivets joints, adhesively-bonded columns are not limited by the substrate thickness and can reduce the weight since the weight

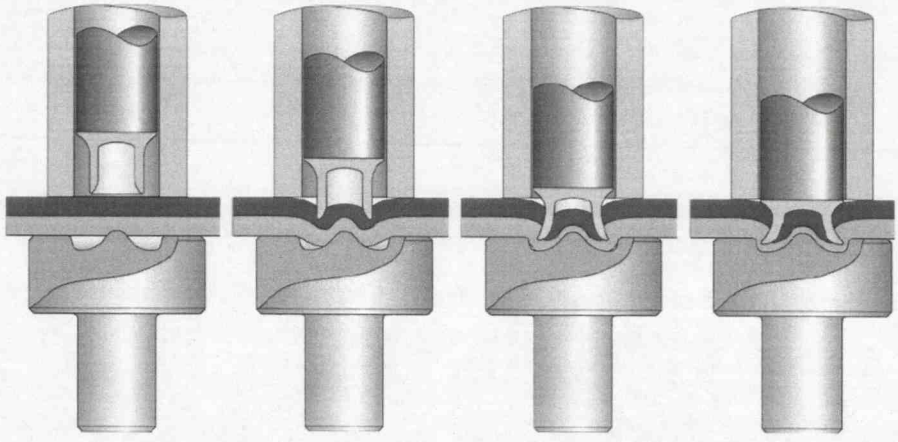

Figure 2.22: Setting process of self piercing riveting
AEROBOLTS (2007)

of columns is lower than of bolts.

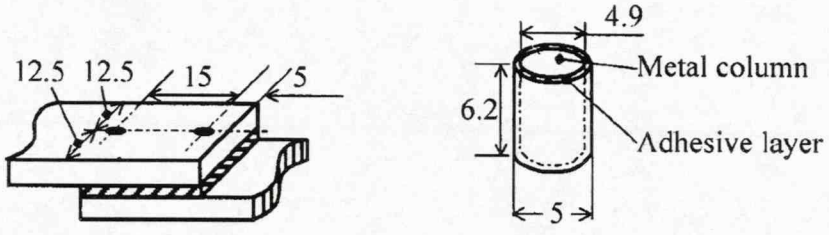

Figure 2.23: Lap shear joints with adhesively-bonded columns
(Liu and Sawa 2002)

However, the implementation of metal columns into production processes appears to be unrealistic and thus this joint configuration may only compensate the high assembly costs in a few applications.

Lap shear joints with attachments

Turaga and Sun (2003) added stepped attachments, shown in Figure 2.24, to each end of the lap shear joint. They showed an increase in strength up to 60% for aluminum joints with attachments compared to lap shear joints. Despite the increase in load capacity the application of attachments increases the weight and the assembly costs.

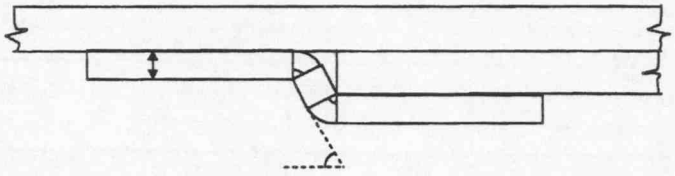

Figure 2.24: Geometric details of the attachment region
(Turaga and Sun 2003)

Reinforcement by Z-pinning

The technique of Z-pinning is used for composite materials to avoid delamination failure by creating a mechanical link between the different plies of the composite laminate. Cartie et al. (2006) applied this reinforcement to T-joints. Rigid cured carbon fibre reinforced rods were inserted in the uncured plies, effectively nailing the different plies together.

Pull-off tests, as schematically shown in Figure 2.25, were used to determine the strength of the T-joint with and without reinforcement. The Z-pins delayed the crack initiation and increased the maximum load necessary to break the joint. In both cases the crack initiated at the resin-rich area where the 3 composites meet. This particular point could not be reinforced by the carbon fibre rod due to geometric limitations.

The application of Z-pins to reinforce composite substrates of lap shear joints may delay or avoid delamination if Z-pins are used at the overlap ends where peel stress concentration usually occurs.

Lap shear joints with stitched substrates

Sawyer (1985) also tried to increase the through-thickness strength of composite substrates. Compressive transverse forces were applied by stitching the substrates close to the critical overlap end together using a Kevlar thread. An increase in joint strength up to 38% was reported although they used a needle with a diameter of 2.5 mm, which caused fibre damage that may have limited the improvement.

Tong et al. (1998) increased the failure load of lap shear joints by 20% when the

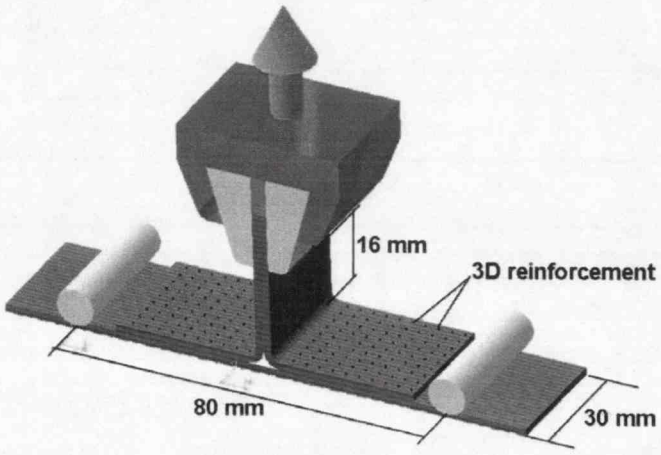

Figure 2.25: Sample geometry and test configuration
(Cartie et al. 2006)

substrates were stitched but the joint still failed predominantly in mode 1 (peel).

Cartie et al. (2006) simplified the stitching process with a technique called tufting. A hollow needle carries the thread totally through the thickness of the preform. When the needle retracts, the thread is retained by simple friction, forming a loop, as can be seen in Figure 2.26. This technique requires access only from one side of the structure and a second thread is not necessary. Experiments showed good results for T-joints; failure loads were higher compared to standard T-joints and the previously discussed T-joints reinforced with Z-pins.

However, the application of stitching, tufting and Z-pins is limited to co-cured composite joints where the reinforcements can be applied to the uncured material.

2.3 Fatigue behaviour of bonded joints

For industrial applications it is essential to guarantee failure-free operation for the service life of components. It is well known that materials tend to fail at much lower stresses when subjected to fatigue loading compared to their static strength. Therefore, investigations of the fatigue limits are important in many engineering areas although experiments simulating the entire service life of structures are time-consuming and expensive.

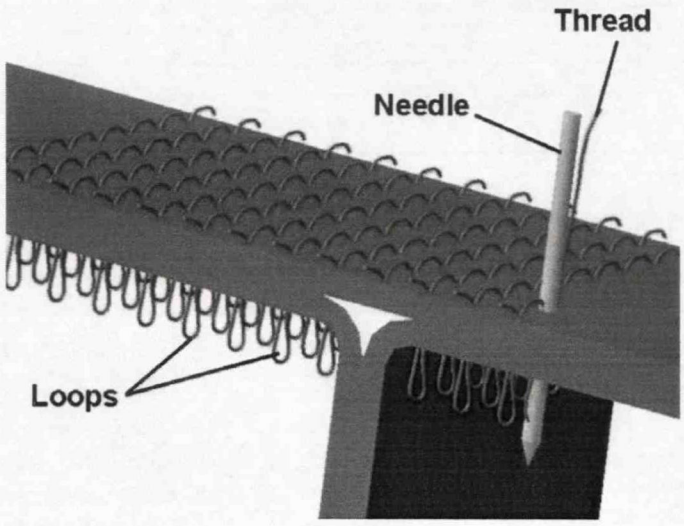

Figure 2.26: Reinforcement by tufting
(Cartie et al. 2006)

Work has been carried out to investigate the fatigue behaviour of bonded joints and to predict the fatigue life of which the main approaches are briefly described in the following section.

2.3.1 Prediction methods

For the prediction of fatigue life two approaches have been established: The *Stress-life approach* uses experimental data to define an endurance limit where the joint is not supposed to fail. *Fatigue crack propagation analysis (FCP)* is used to predict the propagation of cracks initiated by voids or flaws within the material.

Stress-life approach

The traditional Stress-life approach is commonly used to analyse fatigue life, first introduced for determining the failure of metallic rail axes (Wöhler 1870). Adhesive joints can be subjected to fatigue loading at different load levels. The data is usually presented in diagrams where the applied load or load relative to the static strength is plotted versus the number of cycles, which is called an S-N curve. The average shear stress can alternatively be used instead of applied loads which helps to generalise the data although transferability to other joints may be problematic.

A schematic S-N curve is shown in Figure 2.27 where a fatigue limit, also called endurance limit, depicts a limit below which failure does not occur after a large number of cycles, usually in order of $10^6 - 10^8$ fatigue cycles.

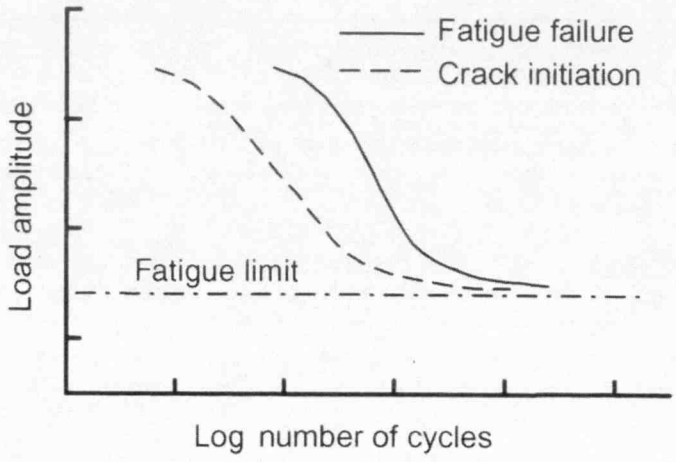

Figure 2.27: Schematic S-N curve
(Harris 2003)

(Matting and Draugelates 1968) applied cyclic loading to a number of lap shear joints using a wide range of variables. Joints were tested at different load levels up to 10^8 cycles. The experimental results matched the Woehler line used for metal fatigue testing. They also recommend to test lap joints up to 1.2 x 10^7 cycles allowing extrapolation to 5 x 10^8 cycles.

Recently, (Zeng and Sun 2004) improved the lap shear joint strength by introducing the wavy joint (see Section 2.2.1). They also compared the fatigue behaviour of the wavy joint with the standard lap shear joint using unidirectional carbon epoxy substrates. The lap shear joint was tested using sinusoidal loads with a maximum of 4.2 kN and 5.6 kN (load ratio $R = 0.1$) producing average failure loads of 336.000 and 77.000 cycles, respectively. At these load levels the wavy joint did not fail within 1.000.000 cycles. Thus, the wavy joint was tested at a higher cyclic load of 10 kN where the joint failed at an average of 211.000 cycles. This shows the great impact an improved stress distribution can have on the fatigue life of bonded joints.

Fatigue crack propagation approach

The Griffith energy approach is based on the strain energy release rate, G', expecting cracks to propagate when the decrease of potential energy due to the growth is equivalent to the increase of surface energy due to the presence of the crack (Griffith 1921). The energy release rate is usually measured using double cantilever beam specimens or lap shear joints both with an existing crack whose propagation is monitored. The recorded crack growth rate can then be plotted versus the energy release rate, as shown in Figure 2.28. The threshold region contains a threshold, G'_{th}, below which the crack does not propagate. Above this value the rate of crack growth increases. The central region describes a linear crack growth rate and in the third region cracks grow rapidly up to the critical value which is called fracture toughness, G'_c, at which the structure is expected to fail.

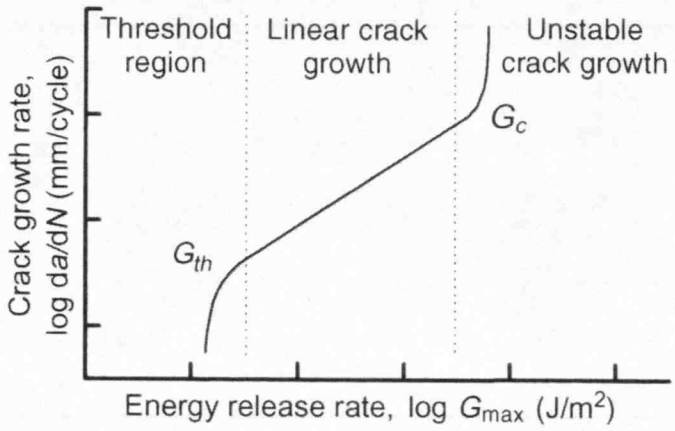

Figure 2.28: Energy release rate: 3 regions of crack growth (Harris 2003)

Numerous fatigue crack growth laws are available in literature. The most widely used approach was introduced by Paris and Erdogan (1963):

$$\frac{da}{dN} = C_1(\Delta K)^{m_1} \tag{2.26}$$

which can alternatively be expressed in terms of the strain energy release rate, G',

as

$$\frac{da}{dN} = C_2(\Delta G')^{m_2} \tag{2.27}$$

where the variables C and m are empirical constants, K the stress intensity factor and da/dN the crack growth rate. The Paris law has been used to describe the crack growth in various materials for the linear area (on a log/log scale) of the crack growth curve, shown in Figure 2.28.

Mostovoy and Ripling (1975) studied the dynamic fatigue behaviour bonded joints first using a fracture mechanics approach. The Tapered Double Cantilever Beam (TDCB) geometry was used to evaluate the the fatigue performance of a number of adhesives using aluminium-alloy substrates.

However, the purpose of this investigation is not to predict failure. In order to compare the performance of various joint types subjected to fatigue a simple comparison of S-N-curves and their endurance limit can show trends in the expected fatigue life using a relatively low number of experiments.

2.3.2 Parameters affecting fatigue tests

Both prediction methods require experimental data which can be obtained from cyclic fatigue testing where specimens are subjected to cyclic loading. Various test parameters can have a significant impact on the results of which the most important are the temperature, the applied stresses, water, and the test frequency. Jethwa (1995) summarised the work that has been done on parameters significantly affecting the fatigue life of bonded joints.

However, this investigation focusses on the impact of various joint configurations on the joint performance. The same test parameters were chosen for all joints to minimise their influence on the test results. It is assumed that variations of the conditions affect every joint with a low dependency on joint design and thus, similar trends are expected.

2.4 Summary

It has been shown that closed-form solutions have been developed to describe the stress distribution along the bondline and to predict joint failure. The characteristic stress profile of lap shear joints was given by Volkersen (1938) and Goland and Reissner (1944) where stress peaks at the overlap ends decreased the potential of the adhesive joint. They analysed the differential straining of the substrates and the nonlinear joint rotation. These were important findings in order to understand the key stresses developed within lap shear joints.

Based upon their analysis various optimisation attempts were made in recent years trying to reduce differential straining and joint rotation. Others reduced the resulting stress concentrations with overlap substrate modification. The various joint configurations are summarised in Table 2.1, although the limited data available complicates the comparison of the methods due to the different materials and geometries used in the experimental investigations. However, a valuation of the potential performance of the metallic and composite joints, the effects on the component weight and the substrate fabrication and assembly costs have been estimated and compared with the the lap shear joint as a reference.

For automotive applications pre-forming of substrates appears to have a great potential for metallic and composite joints as manufacturing and assembly costs are not significantly increased. Hence, joints with prebent substrates, reverse-bent and wavy joints were chosen to be numerically optimised using FEA in the following chapters. Spot welding and rivets were not further investigated due to their limited applicability to composite materials.

Numerical work needs to be validated with experiments using composite and metallic substrates since the different failure modes require a different focus within the optimisation. A joint geometry applicable to both substrate types would be beneficial for hybrid joints.

It is expected that improving the quasi-static joint strength also increases the

Method	**Performance metallic sub.**	**Performance composite sub.**	**Weight**	**Costs**
Lap shear j. (reference)	o	o	o	o
Scarf joint	++	++	++	- -
Stepped scarf joint	+	++	++	- -
Joggle joint	o	o	o	-
Reverse-bent joint	++	++	o	o
Prebent substrates	+	+	o	o
Wavy joints	++	++	o	-
Multi-mod. bondline	++	++	o	-
Rubber toughening	+	+	o	o
Adhesive fillets	+	+	o	o
Tapered sub.	+	+	+	- -
Tapering & fillets	++	++	o	- -
Notched substrates	+	- -	o	-
Nested overlaps	N/A	+	+	-
Bonds + spot welds	+	N/A	-	-
Bonds + bolts	+	o	- -	- -
Bonded columns	o	o	-	- -
Attachments	+	+	- -	- -
Stitched substrates	N/A	+	o	-
Z-pinning	N/A	+	o	–

- disadvantage, o even, + advantage

Table 2.1: Comparison of optimisation methods for overlap joints

fatigue life of bonded joints. Cyclic tests using common test parameters comparing the traditional lap shear joint with the optimised joint will be carried out for the metallic joints to show the potential of the chosen design in terms of fatigue life.

3 Material characterisation

In order to investigate bonded joints numerically and experimentally material properties obtained from experimental tests are required. In this chapter the adhesives and substrate materials used in this work are characterised and relevant failure mechanisms are described.

3.1 Adhesives

Two structural adhesives were chosen for this investigation. A relatively stiff single-part, heat-cured epoxy that is often used in the automotive industry, and a more ductile, two-part epoxy adhesive were used. It was expected that the ductile adhesive would be more suitable for bonding low strengths and composite materials, whereas, the stiffer adhesive would be more suitable for bonding stiff and thick substrates.

Adhesive 1

ESP110, supplied by Bondmaster, was chosen for the stiffer adhesive. According to their technical data sheet (Bondmaster 2001), the silver coloured paste adhesive is metal filled and was designed to provide maximum resistance to impact, shear, cleavage and tensile loads. The durability, chemical resistance and high temperature performance are good. ESP110 will bond to a wide variety of surfaces, including oily steel, and performance is usually limited by the strength of the adherends themselves. In many applications it can replace traditional fixing

techniques to give enhanced appearance and greater design flexibility. The shear strength was given to be 30 MPa, obtained using more ductile metallic substrates, such as copper and its alloys. The recommended service temperature range for this product is −40 to +180°C (Bondmaster 2001).

Adhesive 2

The more ductile adhesive *DP460 Off-White - Scotch Weld*, provided by 3M, is a high performance, two-part epoxy adhesives offering outstanding shear and peel adhesion, and very high levels of durability (3M 2004). The shear strength of 28 MPa is given for copper substrates. The technical data sheet (3M 2004) provides various shear strengths at different temperatures and using different substrate materials.

Dumbbell tests

Despite the dependency of material properties on e.g. temperature, test speed and environmental effects, the adhesives were only tested at ambient room temperature (23°C) conditions. In accordance with BS-2782-3, the Young's modulus was recorded using dumbbell specimens (see Table 3.1 and Figure 3.1) which were cast in moulds. Adhesive 1 was cured in an oven at 100°C for 4 hours. Adhesive 2 was cured for 7 days in a controlled environment at 23 ± 3°C and 50 ± 5% relative humidity. five replicates were made for each adhesive.

Dimension	Adhesive	Steel
l_1	60	75
l_2	170	120
b_1	10	12,5
b_2	20	20
h	4	1.2

Table 3.1: Dimensions of the Dumbbell specimens in mm

The specimens were tested at a crosshead speed of 2 mm/min which corresponds to a stain rate of $\dot{\epsilon}$=3.03E-04 s^{-1}. A Testometric tensile test machine was used fitted with a 25 kN load cell. To record the strains an extensometer with a gauge length of 50 mm was used. The properties of the two adhesives are listed in Table 3.2 and the stress-strain behaviour is shown in Figure 3.2.

The measured ultimate tensile strength (UTS) of adhesive 1 was 54 MPa but was governed by voids in the specimen and was expected to be higher. Other literature reports the following values for adhesive 1: $E = 3.7$ GPa,$G = 1.35$ GPa, $\sigma_{ult} = 70$ MPa, $\tau_{ult} = 50$ MPa (Adams et al. 1997).

Property	**Adhesive 1**	**Adhesive 2**
Tensile Modulus [MPa]	4600	2400
Ultimate tensile strength [MPa]	54*	36*
Ultimate Strain [%]	1.7*	2.6*

*governed by small voids in the dumbbell specimen (approx. 5% of the cross section)

Table 3.2: Material properties of the adhesives

3.2 Metallic substrates

It is well known that the properties of metal substrates (e.g. yielding) can substantially influence the joint strength (Adams et al. 1997). In order to investigate the influence of the substrate yielding on the performance of various joint types, three steel types with different yield strengths and subsequent plastic behaviour were selected for this investigation. Steel 1 is a mild steel with a low yield point and large plastic deformation before ultimate failure. Steel 2 was representative of a typical automotive steel, and exhibits a higher yield point and similar plastic strain to failure. In contrast to the other two steels the ultimate failure of Steel 3 occurs after negligible plastic deformation (see Figure 3.3).

Tensile tests were performed to obtain accurate material behaviour of the three steel types. Dumbbell specimens were made for each steel type, according to the British Standard BS-EN10002 (see Table 3.1 and Figure 3.1). Strain gauges were placed in the centre on both sides of the sample to record the strain of the elastic region. An extensometer (gauge length 50 mm) was additionally used to record strains after the strain gauges peeled off due to the large deformation.

Five replicate specimens were tested for each steel type at a crosshead speed of 2 mm/min ($\dot{\epsilon}$=3.03E-04 s^{-1}) using a Testometric tensile test machine with a 100 kN load cell. The various properties are listed in Table 3.3, and the stress-strain curves are shown in Figure 3.3.

The non linear relationship between stress and strain of Steel 2 which is later used for the numerical analysis can be described using the Power Law:

$$\sigma = C + K\epsilon^n \tag{3.1}$$

where

$$C = -4.77E + 06$$

$$K = -4.771E + 06$$

$$n = 1.727E - 05$$

Property		**Steel 1**	**Steel 2**	**Steel 3**
Young's Modulus	E [GPa]	193	198	206
Yield point (0.2%)	σ_Y [MPa]	219	404	-
Ultimate tensile strength	UTS [MPa]	325	649	678
Ultimate Strain	ϵ [%]	30	25	0.7

Table 3.3: Material properties of the metallic substrates

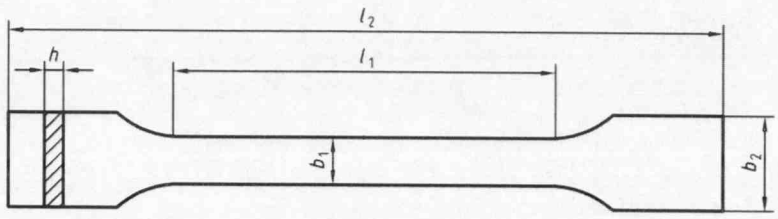

Figure 3.1: Geometry of the Dumbbell specimens

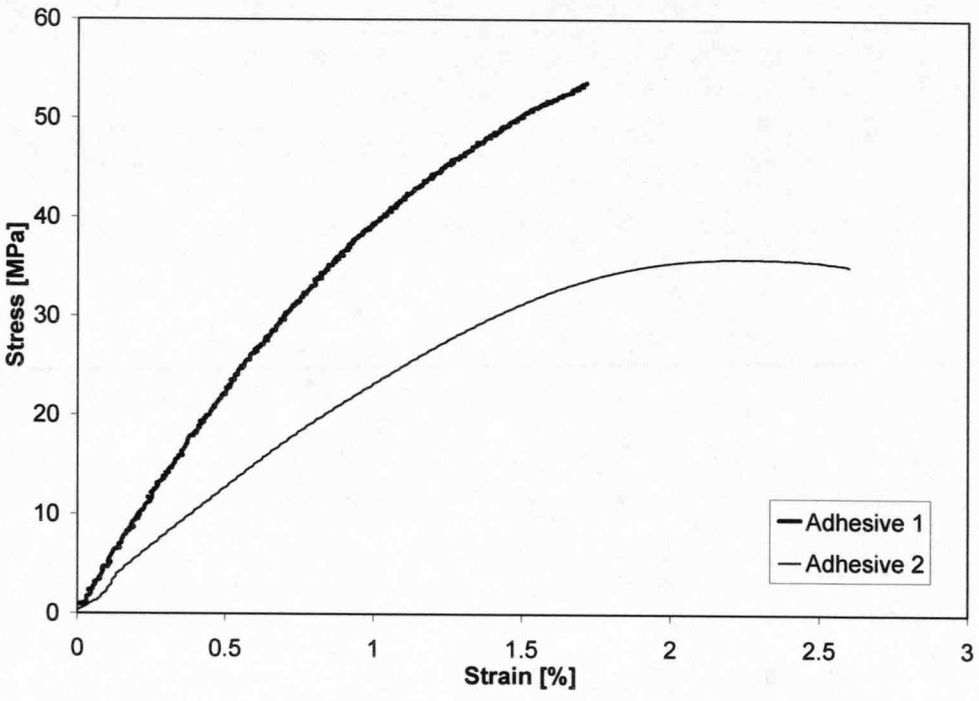

Figure 3.2: Representative tensile (engineering) stress-strain curves of the adhesives obtained from tensile tests

3.3 Composite substrates

The strength of composite joints is often limited by the low through-thickness strength of the substrates where delamination failure occurs before the adhesive fails. The stacking sequence of the composite can influence the delamination failure significantly. Hence, a composite material was used with a variation of different layups to alter these properties.

The chosen carbon fibre reinforced composites for the experimental tests were made of a stack of thin prepreg layers aligned in various directions. However, material properties were obtained using unidirectional (UD) fibre layups in order to provide the material data required for the FEA.

The laminate was laid up between two metallic sheets to gain a similar surface quality for both sides of the composite. The layup was then vacuum-bagged and cured for 2.5 hours at 135°C under a pressure of approximately 1 bar. The samples were then cut with a diamond tipped slitting disc according to the required geometries.

Tensile tests

Tensile tests were carried out using UD-composites made of 15 layers of prepreg resulting in a total thickness of 2.0 mm. Samples were cut to the following dimensions:

- In fibre direction: Length 300 mm; Width 10 mm
- Perpendicular to the fibre direction: 300 mm; Width 25 mm

Strain gauges were used to record strains in the fibre and perpendicular to the fibre direction, which allows the determination of Young's modulus, E, Poisons ratio, ν, and the tensile strength σ_{ult} in relation to the test direction. The results are listed in Table 3.4 where direction 1 of the applied coordinate system is aligned

with the fibres and direction 2 and 3 are perpendicular to the fibres in the through-thickness and width direction, respectively.

Material properties in the through-thickness direction were of particular interest since lap shear joints with composite substrates tend to fail by delamination. The measurement of the mechanical properties in this direction is difficult and hence material properties in the through-thickness and width direction are assumed to be similar.

Aluminium end tabs with a length of 60 mm were bonded on to ensure the specimen did not slip in the jaws during testing. This might have caused stress concentrations initiating early failure of the material in the fibre direction 1, therefore the measured tensile strength, σ_{ult}, is assumed to be a lower bound.

Property	**Tensile test**
E_1 [GPa]	163 ± 0.07
$E_2 \approx E_3$ [GPa]	8.3 ± 0.1
$\nu_{12} \approx \nu_{13}$	0.31 ± 0.04
$G_{12} \approx G_{13} \approx G_{23}$ [GPa]	7.5*
σ_{1ult} [MPa]	>2200**
$\sigma_{2ult} \approx \sigma_{3ult}$ [MPa]	40.7 ± 2.5
ϵ_{1ult}[%]	>1.23**
$\epsilon_{2ult} \approx \epsilon_{3ult}$ [%]	0.5 ± 0.1
ν_f[%]	0.58***

* estimated

** governed by crack initiation at the end tabs

*** according to the manufacturer

Table 3.4: Material properties of the composite substrates obtained from tensile tests

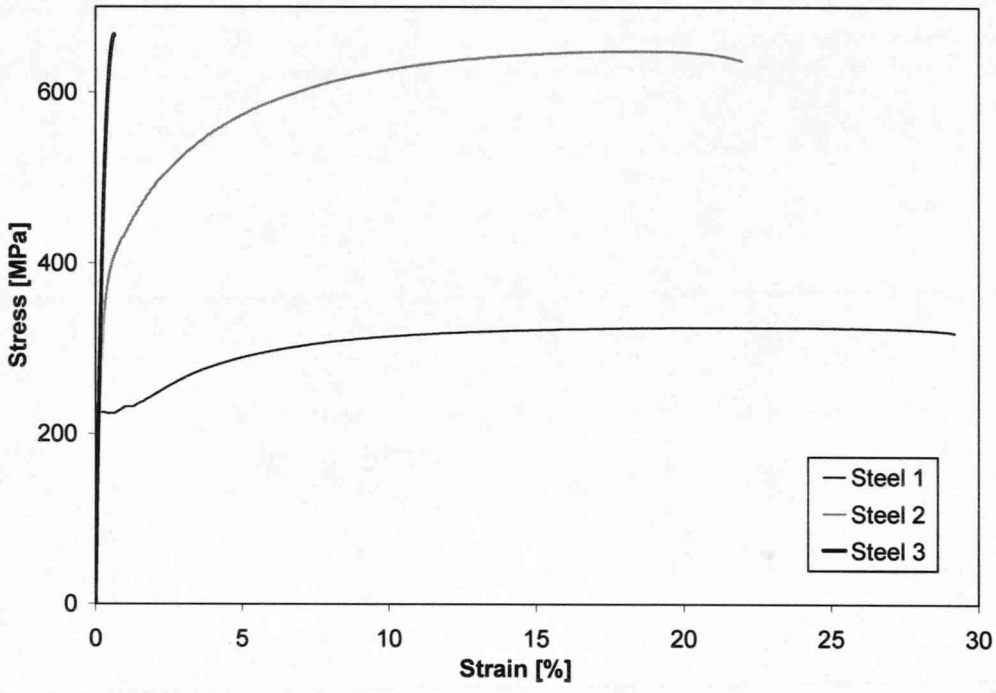

Figure 3.3: Tensile (engineering) stress-strain curves of the substrate material obtained from tensile tests

4 Numerical analysis of lap joints

Experimental investigations of bonded joints, especially geometric optimisations, can be time consuming and subsequently cost intensive. Finite Element Analysis (FEA) is a powerful tool which can be used to gain an understanding of stresses occurring within the joint and to find possibilities to improve the stress distribution. The literature review and selection comparison showed the joints with pre-bent, wavy and the reverse-bent substrates to be most suitable for increasing joint strength with a wide range of substrates and adhesive materials. Thus, a parametric study was performed on these joints to establish optimum stress distributions which were compared with the traditionally used lap shear joint.

Due to the inherent difference in properties of both the metallic and composite substrates they were investigated separately in this chapter.

4.1 Details of FEA models

In order to ensure comparability between the different joint geometries the basic joint dimensions and modeling parameters were set the same.

The various joint types were modelled with the finite element code ANSYS 10.0. Adhesive joints used in reality were assumed to be significantly wider compared to their thickness and overlap length. Thus, 2D-models applying plane-strain conditions were assumed to be adequate to compare stress distributions of the different overlap joints.

As previously mentioned, the geometry of lap shear joints changes under load-

ing conditions. The joint rotation influences the distribution and magnitude of stresses in the adhesive and substrates and thus, nonlinear geometry effects were also considered.

In the following graphs principal, through-thickness and shear stresses are plotted along the centre of the bondline. The plots were normalized to the average shear stress of 24 MPa, which corresponded with the mean failure stress of the traditional lap shear joint. For wavy and reverse-bent joints the direction of through-thickness and shear stresses was aligned for each element along the direction of the bondline using stress transformation equations to allow comparisons of through-thickness stresses that are always perpendicular the bondline.

Basic joint dimensions are listed in Table 4.1. The boundary conditions are given in Figure 4.1. A Young's Modulus of 4.6 GPa and a Poisson's Ratio of 0.4 were used to model the adhesive.

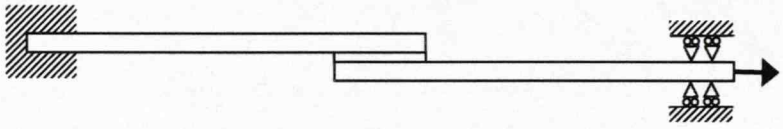

Figure 4.1: Boundary conditions

4.1.1 Joints with metallic substrates

The various 2D-analyses employed eight-node plane-strain elements (Plane82), which are suitable to model curved geometries. The adhesive and the metallic substrates were divided into 11 and 8 elements through the thickness respectively. The length of the bondline consisted of 150 elements. A pressure load of 400 MPa was applied to each joint type in tension, enabling the various graphs to be compared.

Additionally, it is important to take the non-linear behaviour of the substrates into account since joints with metallic substrates often fail due to metal yield at the adhesive interface. The experimentally obtained stress-strain curve of steel 2,

Property	Notation	Value [mm]
Length of the overlap	l_o	10 and 20
Bondline thickness	t_a	0.25
Thickness of metallic substrate	t_s	1.2
Thickness of composite substrate	t_s	2.0
Inner radius of the reverse-bent joint	R'	40
Width	w	25
Length of outer substrates (between overlap and clamped part)	L	50
Length of the clamped area	L_{cl}	>40

Table 4.1: Joint dimensions

shown in Figure 3.3, was used to model the material properties of the substrates. For the plastic deformation incremental theory was used, the stress-strain correlation was based on von Mises. The adhesive was modelled as linear elastic to simplify the analysis.

4.1.2 Joints with composite substrates

The composite substrates were laid up in 15 stacks UD CFRP in various directions. Each of the 15 layers was modelled with one element in the thickness direction. The element type Plane42 was used in this analysis, which allows the material properties to be orientated to the local element coordinate system. This enables the anisotropic properties to follow the shape of the substrates for each joint. The complete set of material properties are given in Table 3.4.

The bondline model geometry was similar to the metallic joints with 11 elements through the thickness and 150 elements along the bondline, and every joint was loaded with a pressure of 240 MPa. The adhesive and composite materials were modelled linear-elastically.

4.1.3 Mesh convergence

In order to obtain mesh convergence three different mesh densities were applied on the lap shear joint.

- Low mesh density: adhesive 90 elements, substrates 360 elements
- Medium mesh density: adhesive 1650 elements, substrates 7200 elements
- High mesh density: adhesive 6300 elements, substrates 12800 elements

The effect of the various element sizes on the stress distribution along the overlap length is shown in Figure 4.2. The distribution of stresses is not affected apart from the outer joint ends where the stress singularity made mesh convergence impossible. The results of low mesh density is not sufficiently accurate for certain analysed details and the highest mesh density is not required. Thus, the medium mesh density was chosen to model joints in this chapter.

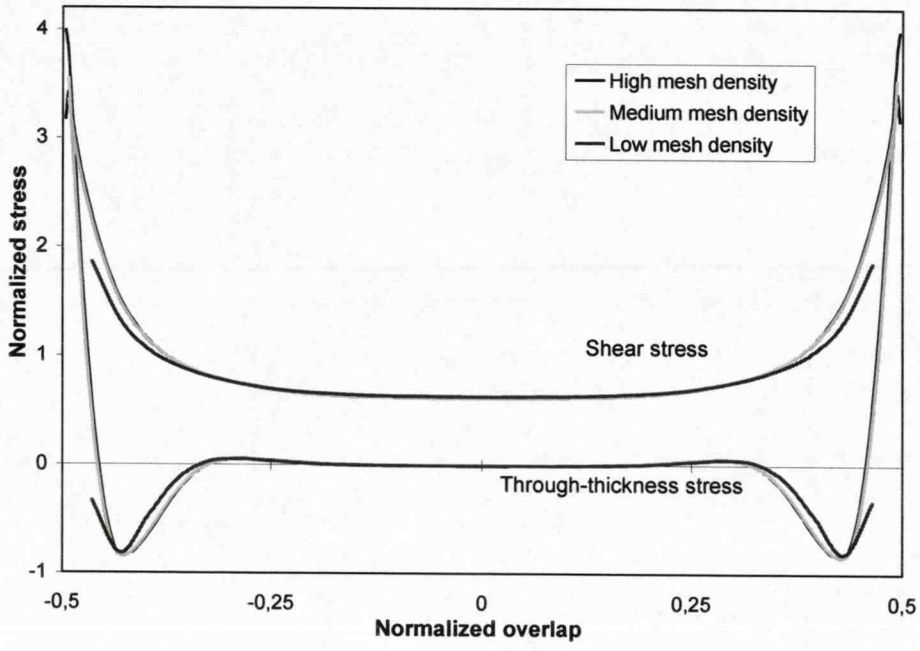

Figure 4.2: Influence of different mesh densities on lap shear joint stress distributions

4.2 Parametric study of lap joints with metallic substrates

This section discusses the main design variables of the joints in order to compare the various geometric variables and possibly develop general design recommendations for bonded overlap joints.

4.2.1 The traditional lap shear joint

In lap shear joints with thin metal substrates, the combined differential straining of the substrates and the rotation of the overlap area, caused by out-of-plane loading, tends to generate excessive stresses at the ends of the overlap in the substrates and the adhesive, as can be seen in Figure 4.3. Plastic deformation within the substrates at the loaded overlap end might occur and introduce high strains at the adhesive interface causing ultimate joint failure.

Generally to maximise joint strength, lap shear joints should meet the following criteria:

- Differential straining should be minimized
- Prevention of high strains or yielding of the substrates adjacent to the adhesive interface
- The joint should be loaded in shear; peel stresses should be minimised
- Eliminate joint rotation
- Stress peaks, especially at the joint ends, should be avoided

4.2.2 Wavy joint

A schematic diagram of the wavy joint, proposed by Zeng and Sun (2000), is shown in Figure 4.4 with the general dimensions listed in Table 4.2. The stress

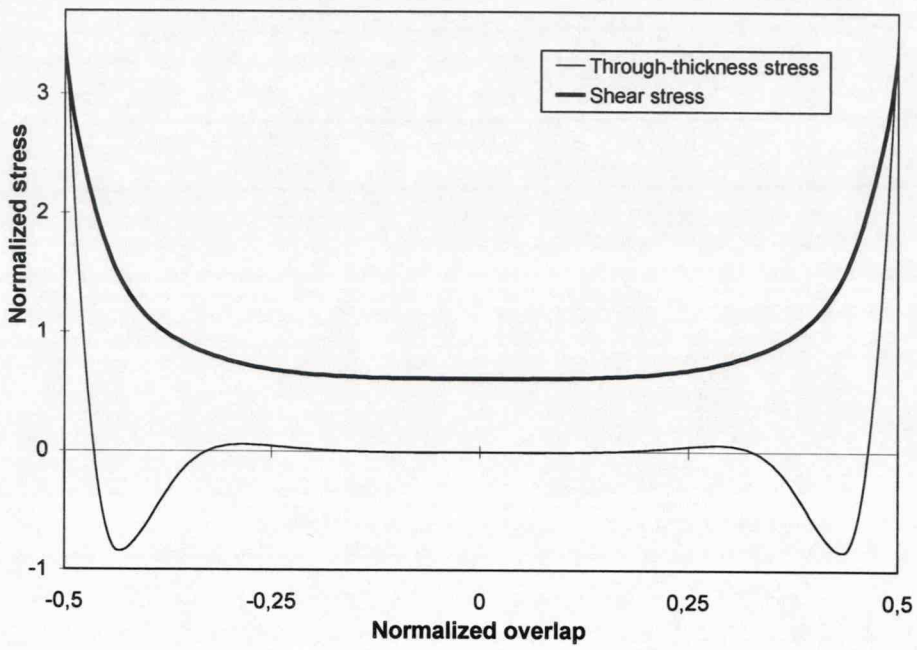

Figure 4.3: Normalized stress distribution in a lap shear joint

distribution, resulting from loading along the horizontal plane in the original wavy joint configuration, is shown in Figure 4.5. The critical through-thickness tensile stress at the end of the overlap, typically associated with lap shear joints, has been replaced by a compressive stress and the remaining tensile stresses are more uniformly distributed within the central region of the joint. The maximum shear stress is also relocated from the end of the overlap and over a greater area within the central region of the overlap.

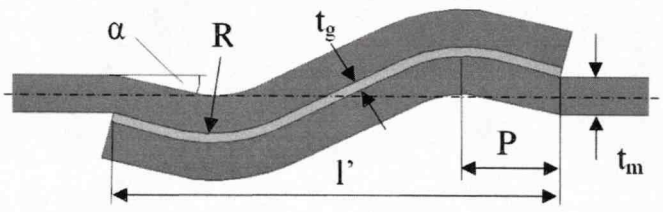

Figure 4.4: Geometry of a wavy joint

Zeng (2001) carried out a parametric study on the wavy joint with composite substrates; the variables included the initial proportion of the overlap, P, the angle, α, and the radius, R. He showed that the best configuration is that of a relatively

Property	Notation	Value
Horizontal length of the overlap	l'	19.7 mm
Angle	α	7°
Initial proportion of the overlap	P	25%
Radius	R	10 mm

Table 4.2: Dimensions of the wavy joint

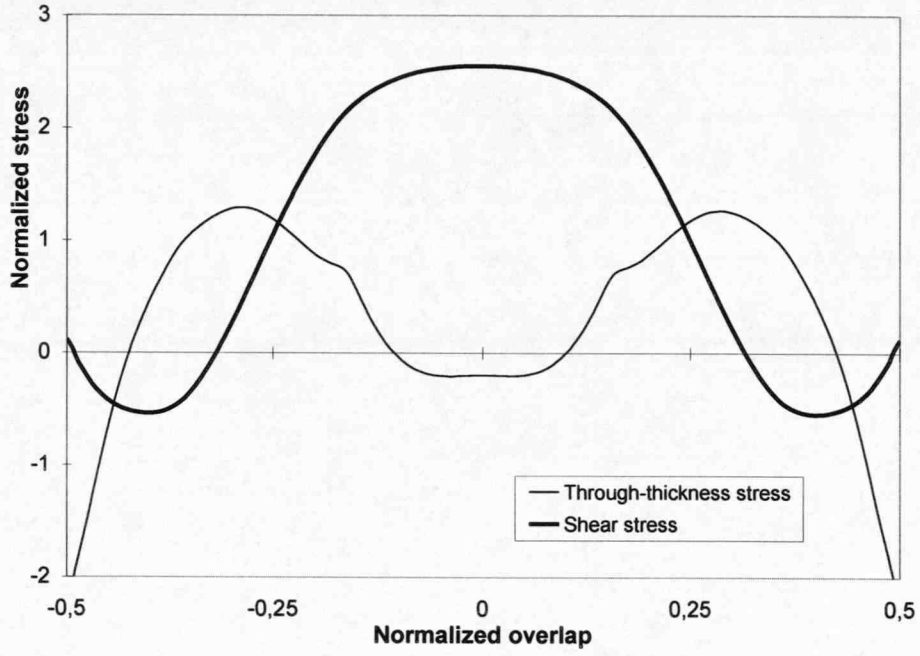

Figure 4.5: Normalized stress distribution of a wavy joint configuration

flat joint with an angle, α, lying somewhere between 0° and 6°. The minimum initial proportion of the overlap, P, was shown to give the best results, indicating an optimum somewhere below 14% of the overall overlap length. Limited by the geometry, the best wave radius would appear to be one that is as large as practically possible.

Figure 4.6 displays the stress distribution at the adhesive interface as a result of varying the angle, α, and keeping all other variables constant (refer to Table 4.2). Large angles increased both the tensile through-thickness stresses and the beneficial

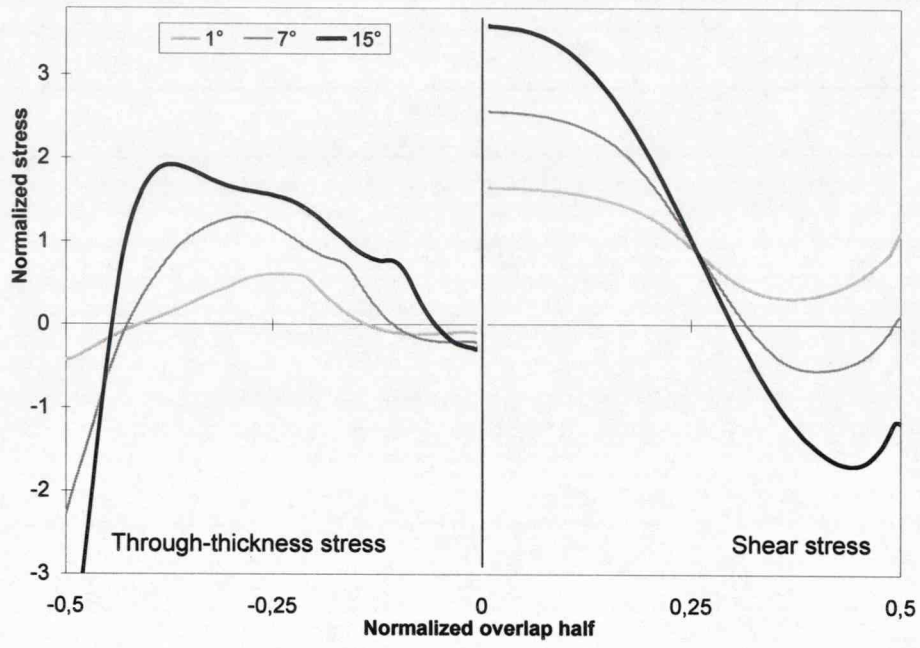

Figure 4.6: Normalized stress distribution of a wavy joint configuration generated by different angles α ($P = 25\%$, $R = 10\ mm$)

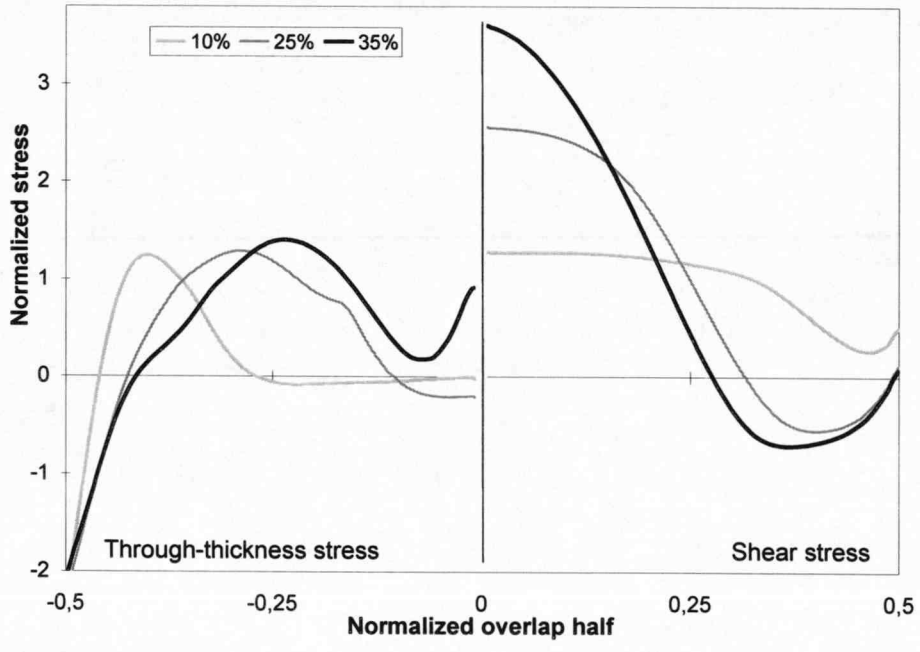

Figure 4.7: Normalized stress distribution of a wavy joint configuration generated by varying the length of the initial proportion of the overlap P ($\alpha = 7°$, $R = 10\ mm$)

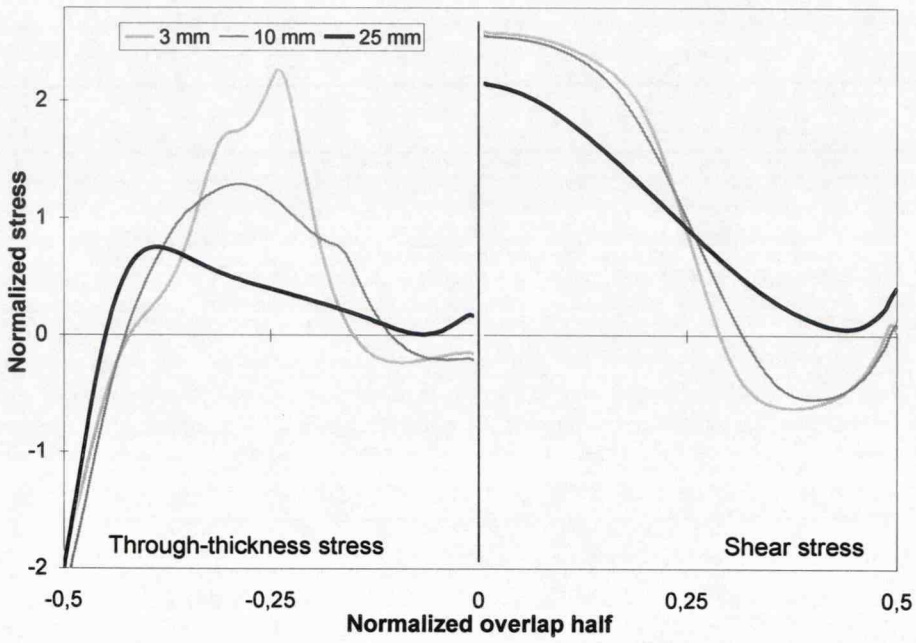

Figure 4.8: Normalized stress distribution of a wavy joint configuration generated by different radii R ($\alpha = 7°$, $P = 25\%$)

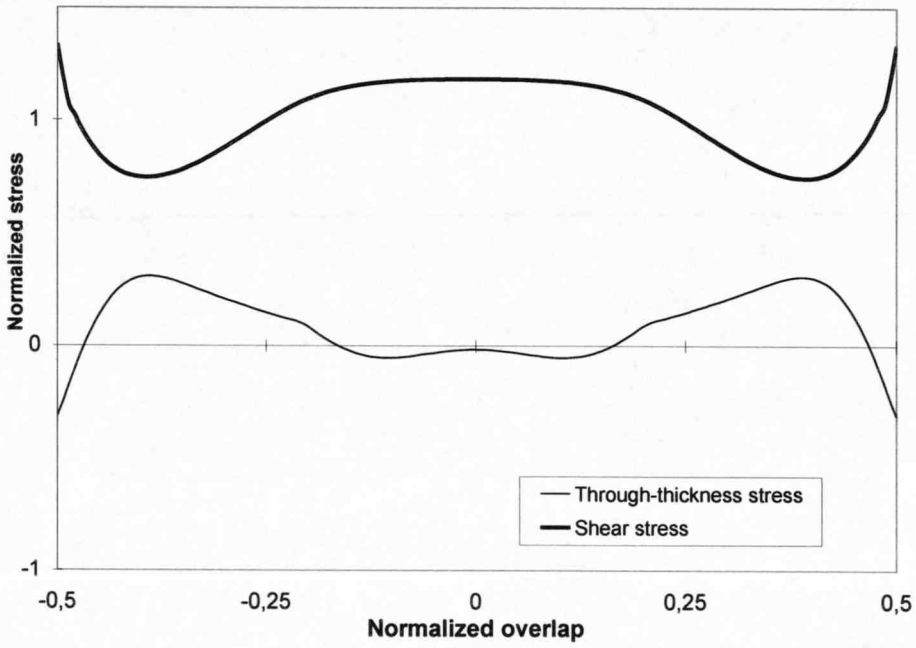

Figure 4.9: Normalized stress distribution of an improved wavy joint ($\alpha = 1°$, $P = 15\%$, $R = 45\ mm$)

compressive through-thickness stresses at the overlap ends, whereas smaller angles generated a more uniform stress distribution due to the reduced joint deformation. A similar trend appears in the shear stress distribution; in joints with an angle of 1° the shear stress is more evenly distributed and does not change the direction. The effect of varying the initial proportion of the overlap, P, on the stress distribution is shown in Figure 4.7. In this case, the smaller the magnitude of P, the lower the resulting maximum shear stress. The distribution of the through-thickness stresses changed but the magnitude remained almost constant.

The radius, R, also had a significant influence on the through-thickness stress, as can be seen in Figure 4.8. The larger radius distributed the shear stress over a greater area and subsequently reduced the magnitude of both peak shear and peak through-thickness stresses.

For comparison with the other joint types, it was decided to model a wavy joint with the initial proportion of the overlap, P, set to 15% of the overlap, the angle, α, was chosen to be 1° and the radius R set to 45 mm. The resulting stresses are shown in Figure 4.9. Shear stress was substantially more dominating than the through-thickness stress, but both demonstrate a highly uniform stress distribution along the entire overlap length.

4.2.3 Joint with prebent substrates

The idea of bending the substrates outside of the overlap area was first suggested by DasGupta and Sharma (1975) and investigated using closed-form solutions. Sawyer and Cooper (1981) performed a parametric study on joints with prebent substrates varying a number of different joint parameters. In this investigation only the following parameters, which were described in Figure 4.10, were altered:

- Angle β (7.7°)
- Distance between overlap and substrate-bend a (1 mm)

- Radius R'' (2 mm)

The values in parentheses represent the actual parameters used in the joint model.

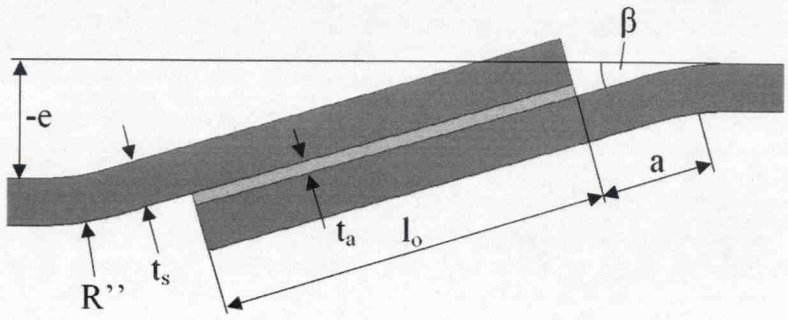

Figure 4.10: Geometry of a joint with prebent substrates

Figure 4.11 shows the effect of varying the bend angle on the stress distribution within the adhesive layer. When the joint is designed with large bend angles the substrates tend to flatten under loading conditions which decreases the bend angle. This reduces tensile stresses within the substrates adjacent to the adhesive. The differential straining, normally occurring in flat lap shear joints, is reduced resulting in more evenly distributed shear stresses along the bondline, as can be seen in Figure 4.11. The peak through-thickness stresses appear to minimize between an angle of 3.8° and 11.7°. Sawyer and Cooper (1981) found an optimum bend angle between 12° and 18° but this is expected to be strongly dependent on the general joint dimensions and the chosen materials.

The distance between the substrate bend and the overlap area, a, also affects the stress distribution within the adhesive. When the parameter, a, is chosen to be large, the bending stresses within the substrates at the point where the substrates was preformed only marginally influence adhesive stresses. Thus, the distance, a, should be minimized, as shown in Figure 4.12, which is in agreement with the conclusions of Sawyer and Cooper (1981).

The influence of the radius, R'', on the adhesive stress distribution is small. A minimal radius of 2 mm was chosen to avoid the radius affecting the bondline

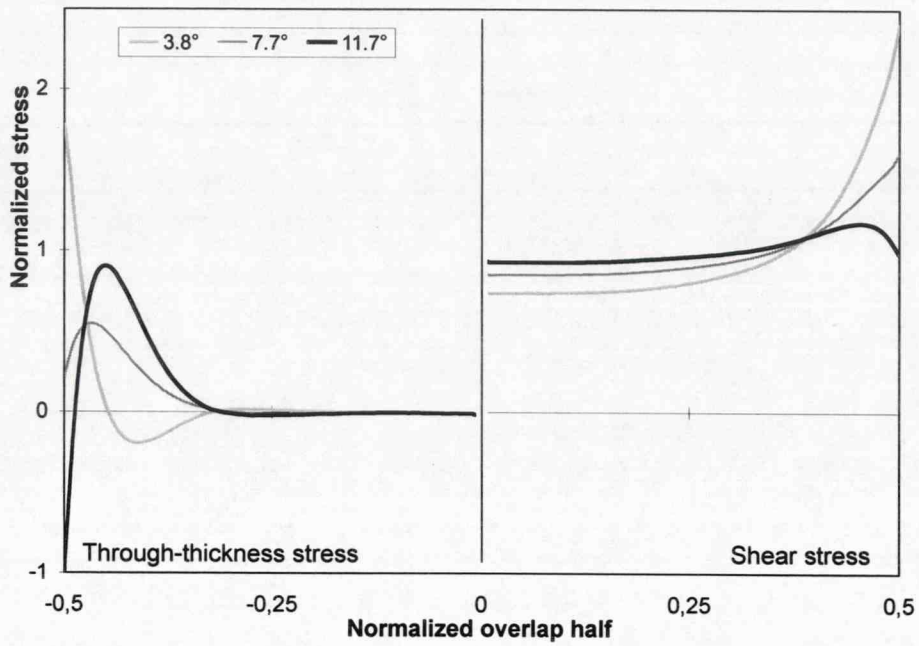

Figure 4.11: Normalized stress distribution of a joint with prebent substrates generated by varying the bend angle β ($a = 1\ mm$, $R" = 2\ mm$)

thickness when small distances, a, are used.

To summarize, the joint with prebent substrates was modelled using dimensions of $a = 1$ mm, $\beta = 7.7°$ and $R" = 2$ mm, which resulted in the stress distribution shown in Figure 4.13. Compared to stresses within the traditional lap shear joint, stress peaks were reduced and through-thickness stresses decreased. However, the optimum joint with prebent substrates may be found with the distance, a, approaching null, which can subsequently be seen as a reverse-bent joint.

4.2.4 Reverse-bent joint

The overlap area of a traditional lap shear joint rotates under loading conditions and a bending moment factor, k, can be used to describe the resulting moment introduced in the substrates. McLaren and MacInnes (1958) suggested negative values of k (see Figure 4.15) to improve the stress distribution and to avoid stress peaks at the overlap ends; this was achieved by bending the substrates at the beginning of the overlap, reminiscent of a deformed flat lap shear joint, as shown

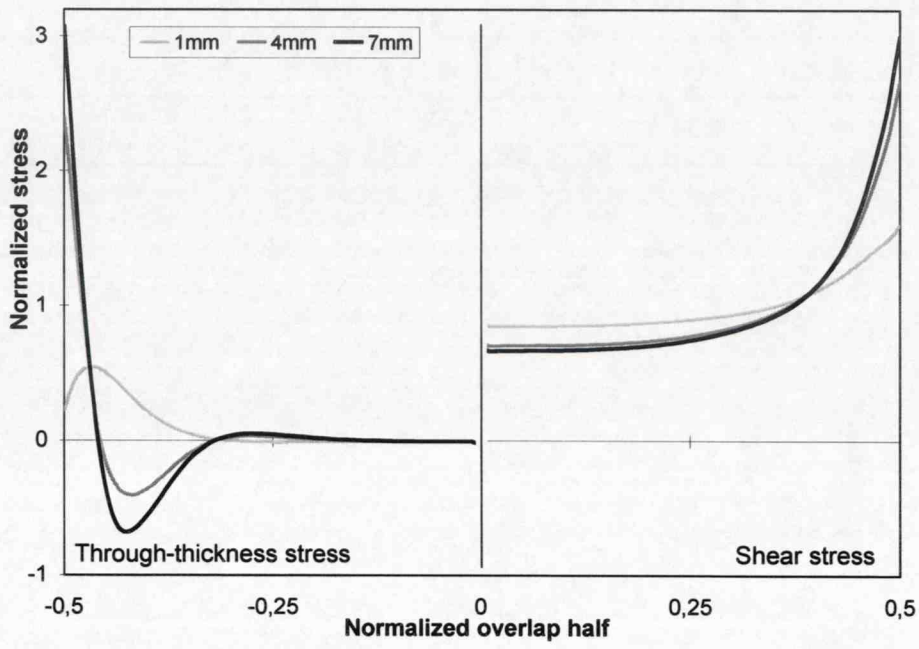

Figure 4.12: Normalized stress distribution of a joint with prebent substrates generated by varying distance between overlap and substrate-bend, a ($\beta = 7.7°$, R" $= 2$ mm)

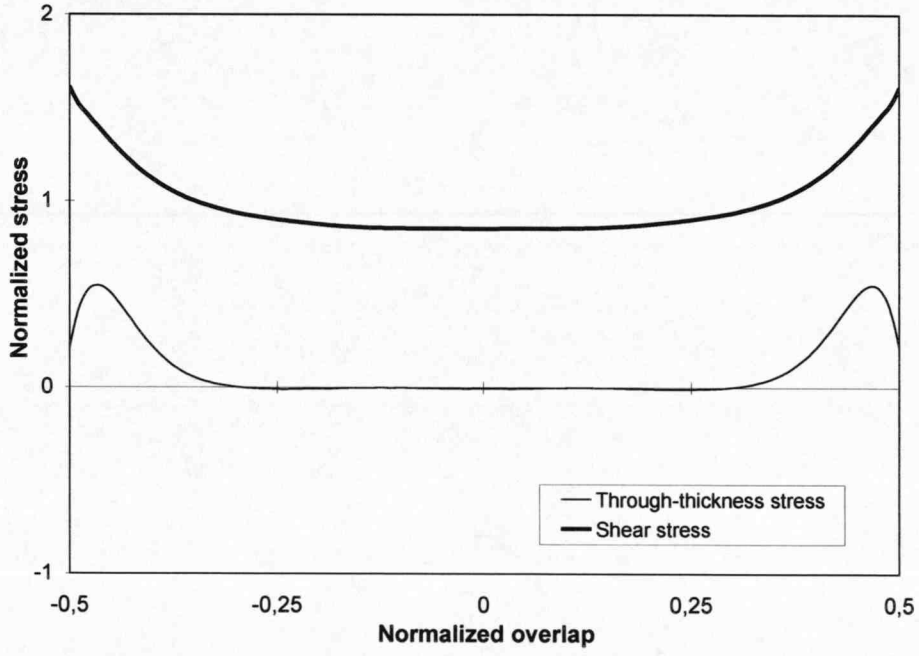

Figure 4.13: Normalized stress distribution of an improved joint with prebent substrates ($a = 1$ mm, $\beta = 7.7°$, R" $= 2$ mm)

in Figure 4.14.

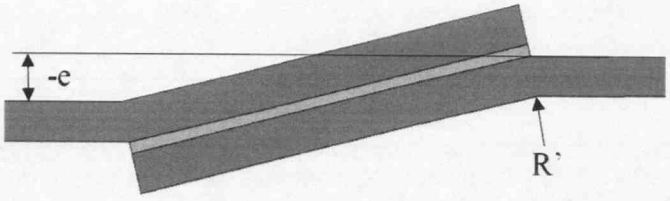

Figure 4.14: Geometry of the original reverse-bent joint

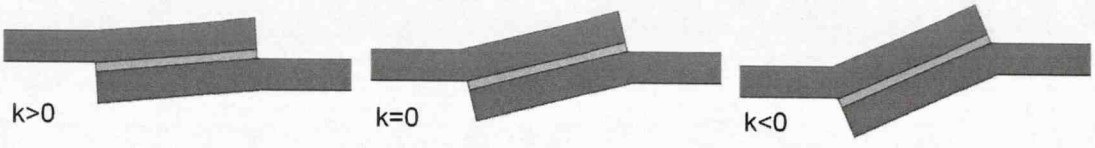

Figure 4.15: Effect of the bending moment factor k on the overlap geometry

As part of this investigation, various positive and negative k-values were studied, where the substrates were misaligned opposite to the traditional lap joint. Assuming $k = 0$ for aligned substrates and $k = 1$ for the flat lap shear joint the bending moment factor k for unloaded joints is given by:

$$k = \frac{e}{t_s + t_a} \tag{4.1}$$

where e is the eccentricity of the substrates, t_s the substrate thickness and t_a the adhesive thickness.

Introducing eccentricity, e, to the alignment of the substrates reduces the tensile through-thickness stress at the end of the overlap. Increasing the eccentricity relocates the tensile through-thickness stress peaks closer to the central region and generates compressive stresses at the outer ends, as illustrated in Figure 4.16. Due to the reduction of the differential substrate straining, the shear stress distribution improved with larger eccentricities.

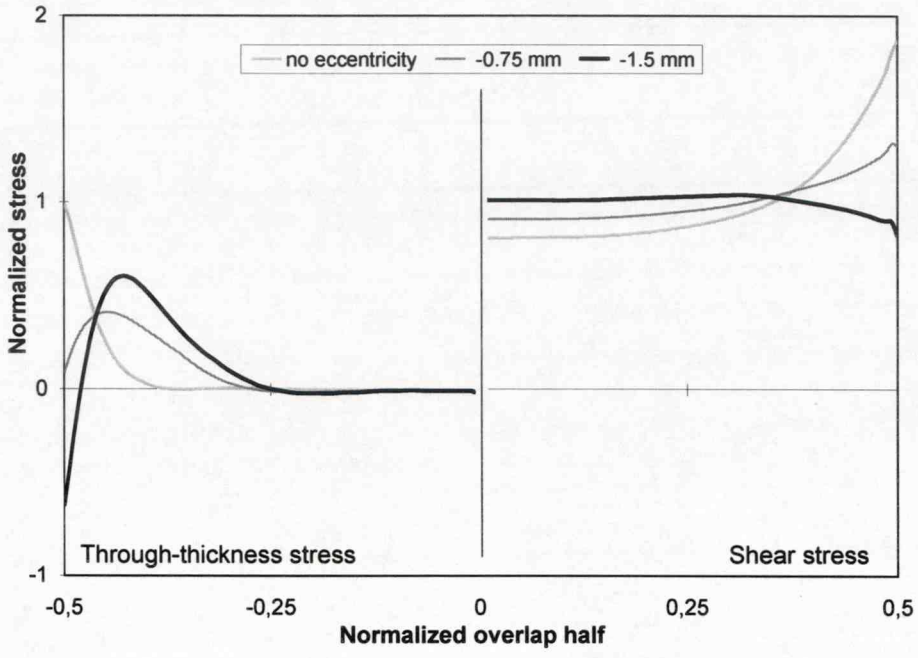

Figure 4.16: Normalized stress distribution of a reverse-bent joint generated by different eccentricities e ($l_f = 15\%$, $R' = 15\ mm$)

4.2.5 Improvements to the reverse-bent joint

The improved wavy joint configuration gives the best stress distribution within the adhesive layer but bending the substrates at two locations is expensive and may require tight tolerances during the assembly process. Thus, bending the substrate only once, as shown in Figure 4.17, could enable simpler implementation into the production processes. The generated *internal fillet* further helps to reduce the stresses at the end of the overlap area, especially for composite joints as discussed in the literature review.

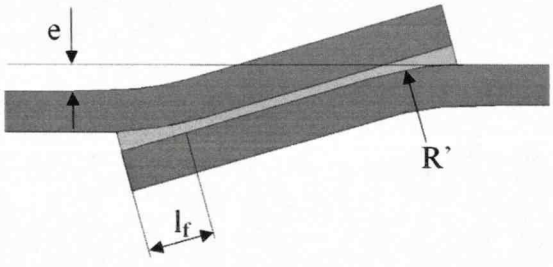

Figure 4.17: Geometry of a reverse-bent joint

The optimisation of the joint with prebent substrates also resulted in the same joint configuration as shown in Figure 4.17. The distance between the overlap end and the substrate-bend, a, (see Figure 4.10) should be minimized to reduce stress peaks within the adhesive layer. Negative values for a lead to the improved reverse-bent joint, where $a = -l_f$.

In Figure 4.18, the general effect of various internal fillet sizes with aligned substrates ($e = 0, k = 0$) on peel and shear stresses is illustrated. Larger internal fillets reduced the stress peaks at the overlap ends but tended to increase more uniformly towards the joint centre. An internal fillet size of 15% provided an even distribution of shear and through-thickness stresses for aligned substrates.

The effect of the bend radius on the stress distribution is relatively small. Similar to the wavy joint, large radii distribute stress peaks over a greater area, as shown in Figure 4.19.

For comparison with the other joint types investigated, the length of each internal fillet, l_f, was set to 10% of the overlap length of the joint, the bend radius, R', was 50mm and the eccentricity, e, was set to 0.25 mm. The distribution of the shear stress, as shown in Figure 4.20, is approximately uniform over the overlap area. The through-thickness stress is low, compared to the shear stress, and it is well distributed.

4.2.6 Discussion of the parametric study

It has been shown that the geometry of an overlap joint has a significant influence on the resulting stress distribution in the adhesive bondline. In particular the effect of-out-of-plane-loading can be much reduced by incorporating the wavy joint design. However, the substrates at the overlap area tend to flatten under loading conditions, generating uneven stress distributions. By comparison, the improved wavy joint configuration ($P = 15\%$, $\alpha = 1°$, $R = 45$ mm), the joint with prebent substrates ($e = -0.75$ mm, $k = -0.52$, $a = 1$ mm, $R'' = 2$ mm) and the improved reverse-bent

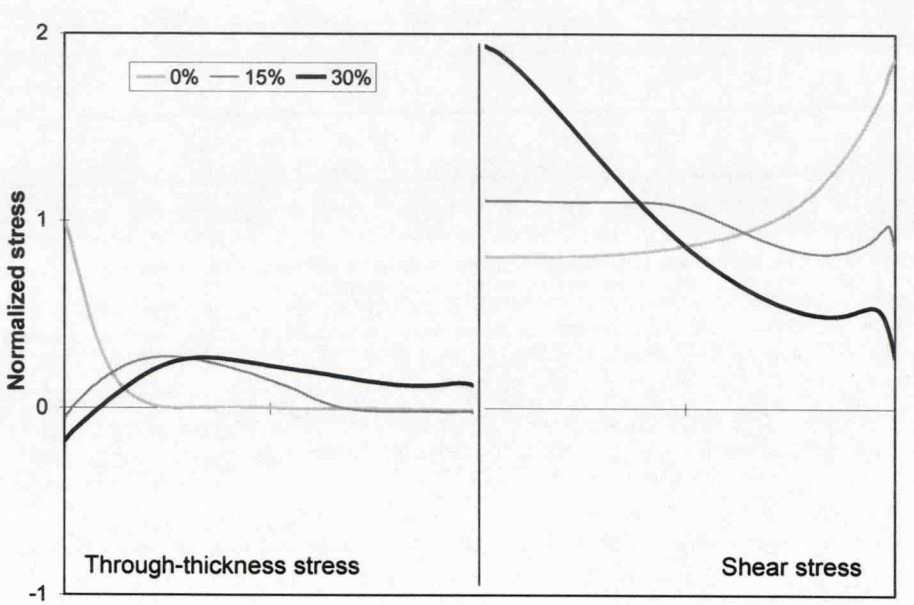

Figure 4.18: Normalized stress distribution of a reverse-bent joint generated by different internal fillet sizes l_f (as a proportion of the bond line length; $e = 0$, $R' = 15\ mm$)

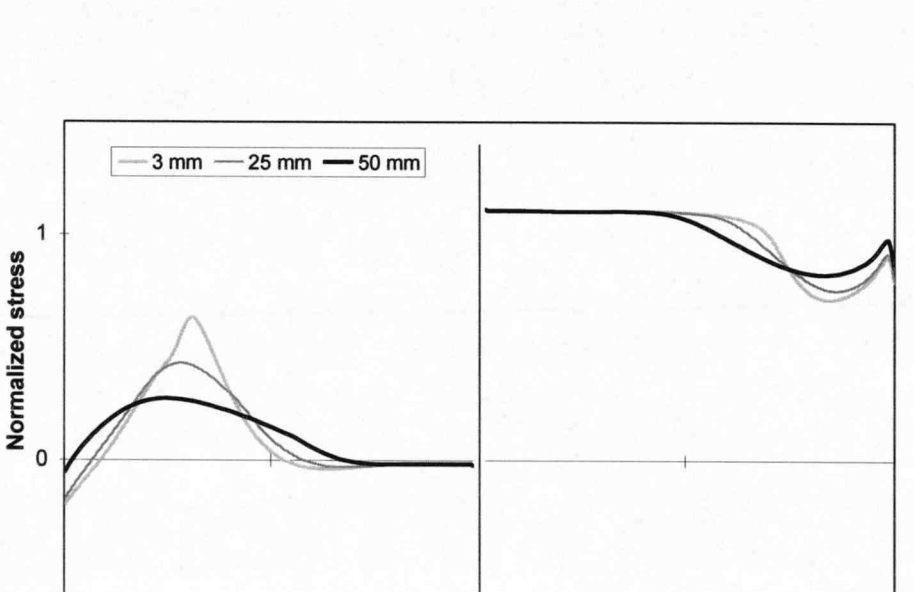

Figure 4.19: Normalized stress distribution of a reverse-bent joint generated by different substrate bend radii of the substrates R' ($e = 0$, l_f=15%)

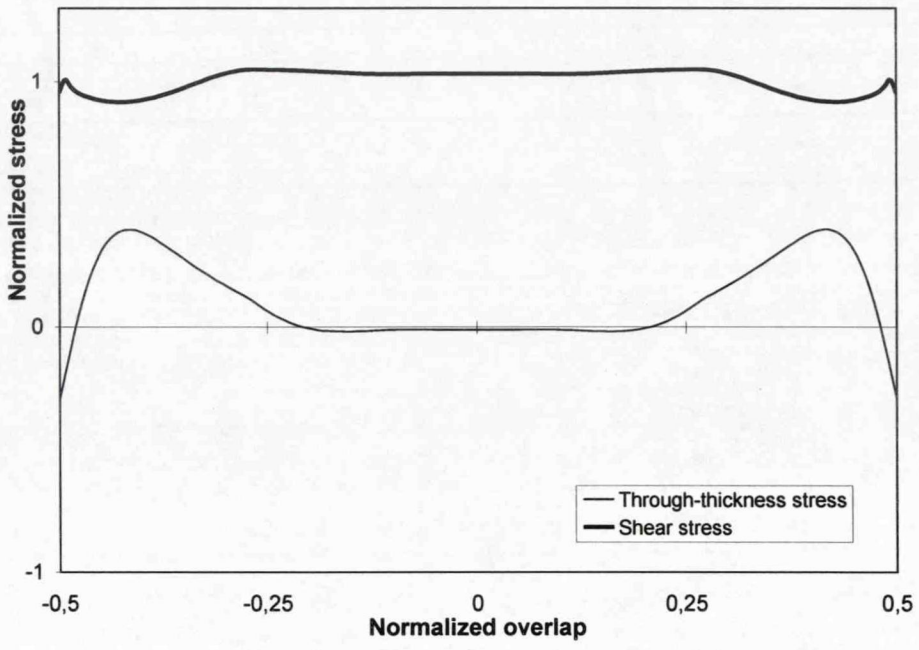

Figure 4.20: Normalized stress distribution of an improved reverse-bent joint ($e = 0$, $l_f = 15\%$, $R = 50$ mm)

joint ($e = -0.25$ mm, $k = -0.17$, $l_f = 10\%$, $R' = 50$ mm) provide a highly uniform stress distribution along the entire bondline. Notably, Figure 4.21 shows that for the reverse-bent joint with $e = -0.75$ mm ($k = -0.52$) and the joint with prebent substrates, both with negative eccentricities ($e < 0$), provide a maximum stress in the substrate that is localised to the outer surface at the bend radius, away from the critical interface between adhesive and substrate. In common with the lap shear joint, the overlap area rotated to balance the eccentricity and thus deformed the substrates in bending. The combined tensile and bending deformation are likely to cause high strains and eventual yielding of the substrate at the tension surface, which, in this case, is not adjacent to the adhesive. Compressive stresses (as a result from bending the substrate) at the adhesive interface minimize the general tensile stresses and help to reduce the differential straining of the substrate at the bonded surface, giving a more uniform shear stress distribution. This effect decreases when the substrates are bent outside the overlap area, which means the distance a should be minimized in the case of the joint with prebent substrates. In general,

the optimised substrate eccentricity will be dependent on the material properties of the adhesive and especially that of the substrates. Metals with low yield strengths may require greater eccentricity to avoid plasticity within the substrate adjacent to the adhesive interface, which would otherwise begin under relatively small loads in traditional lap shear joints.

The FE analysis also showed reduced through-thickness stresses in the substrates of the joints with prebent substrates, the improved wavy and the improved reverse-bent joints; this is likely to be more favourable for composite applications.

In wavy joints the unfavourable peel stress concentrations at the overlap ends change into compressive stresses, though relatively high tensile through-thickness stresses occur closer to the joint centre. The improved reverse-bent joint and, similarly, the improved configuration of the wavy joint lead to more evenly distributed stresses along the bondline. Although the amount of through thickness stress was reduced, more shear stress was exhibited. Figure 4.22 shows a comparison of the joint types discussed.

Assuming, that tensile through-thickness stresses at any location along the bondline are the main cause of failure in composite joints, bending deformations of the substrates should be avoided at all costs in order to decrease the magnitude of tensile through-thickness stresses and thus, presumably, increase joint strength. The improved configuration of the reverse-bent and wavy joint therefore appear appropriate for bonding both, metallic and composite materials. Due to the ease of manufacturing, the improved reverse-bent joint seems to be the most promising for practical applications and hence, a numerical investigation of only this joint configuration was carried out for a comparison with the traditional lap shear joint.

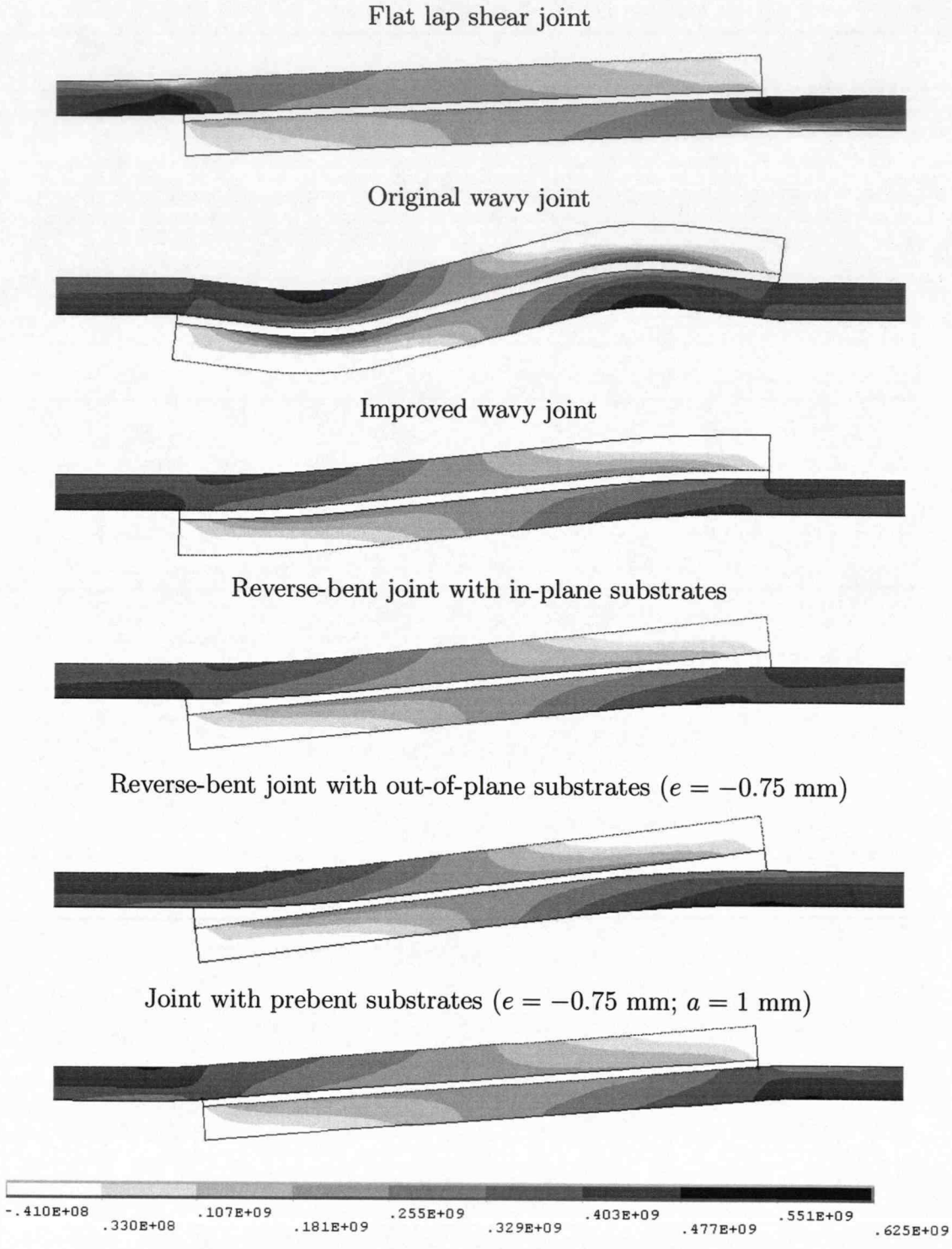

Figure 4.21: Influence of different joint configurations on principal stresses in metal substrates

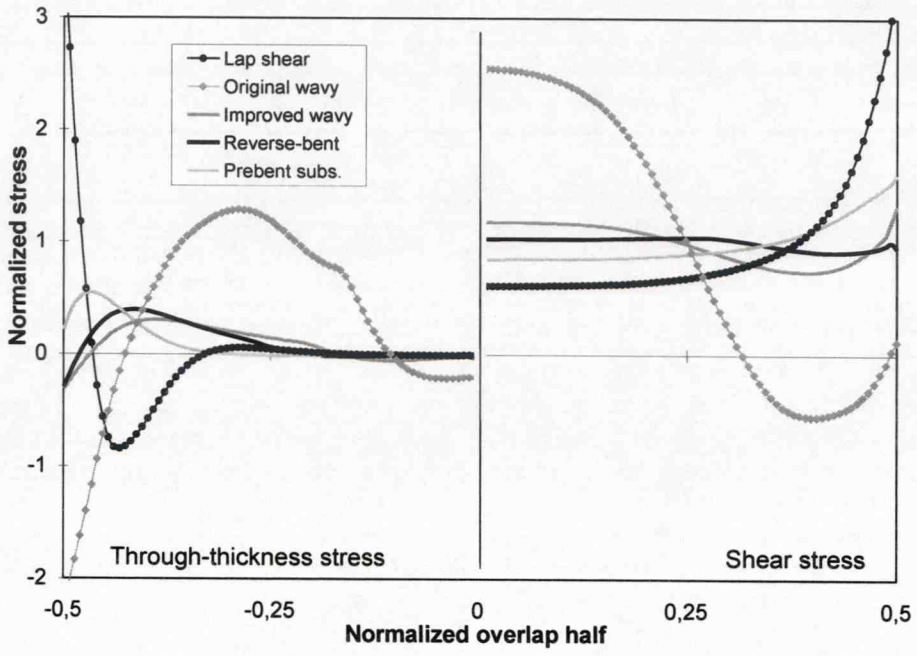

Figure 4.22: Normalized stress distribution of different joint types

4.3 Lap shear and reverse-bent joints with composite substrates

In contrast to metallic joints, where the metal yielding significantly influences joint strength, composite joints often fail in delamination of the substrates, which should ideally be avoided. Figure 4.23 shows the stress distribution within the adhesive bondline of a lap shear joint with unidirectional composite substrates. As in metallic joints the uneven stress distribution is caused by the differential straining and out-of-plane-loading of the substrates, generating peak stresses at the overlap ends.

The reverse-bent joint, first introduced by McLaren and MacInnes (1958), was developed further for metallic substrates to the final shape shown in Figure 4.17. Due to the more uniform stress distribution and the low through-thickness stresses this joint appears particularly suitable for composite joints. Figure 4.24 shows through-thickness, shear and principal stresses within the adhesive bondline for reverse-bent joints with zero and -2 mm eccentricities. In the latter case, the angle

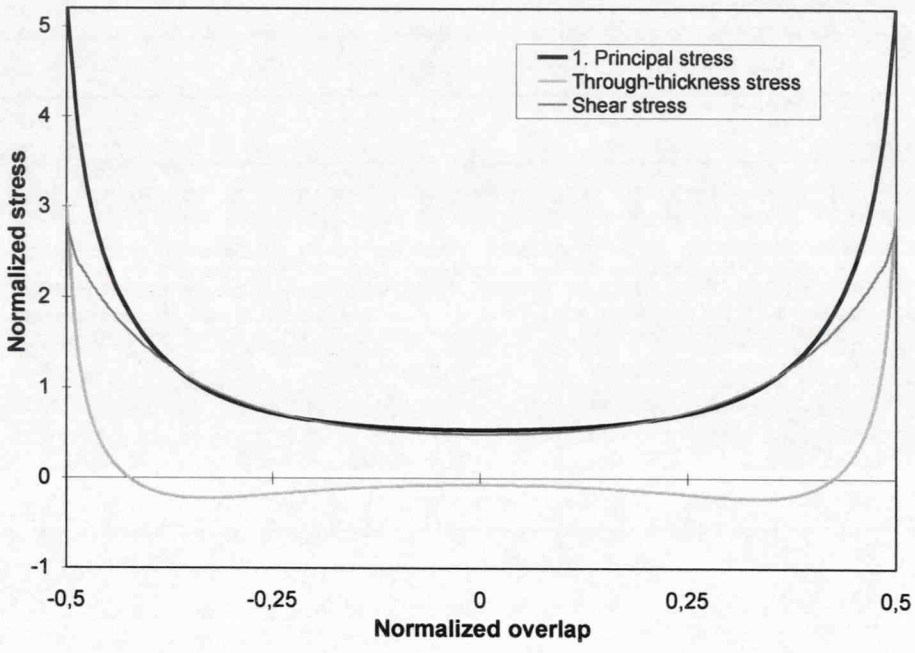

Figure 4.23: Normalized stress distribution within a traditional flat lap shear joint with UD-substrates.

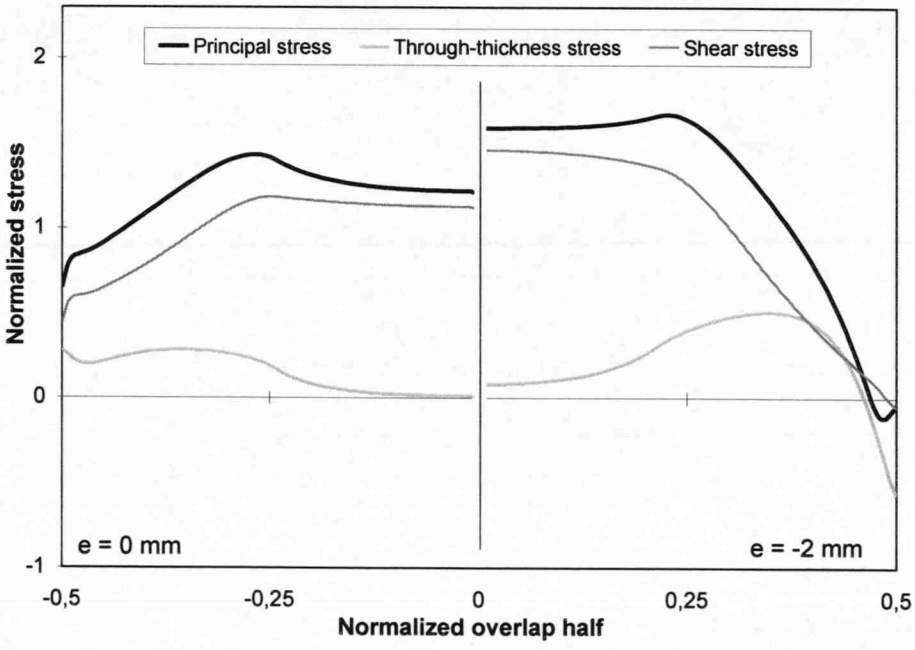

Figure 4.24: Normalized stress distribution of reverse-bent joints with no eccentricity ($l_f = 15\%$) and $e = -2$ mm ($l_f = 10\%$) using UD-substrates ($R = 50$ mm)

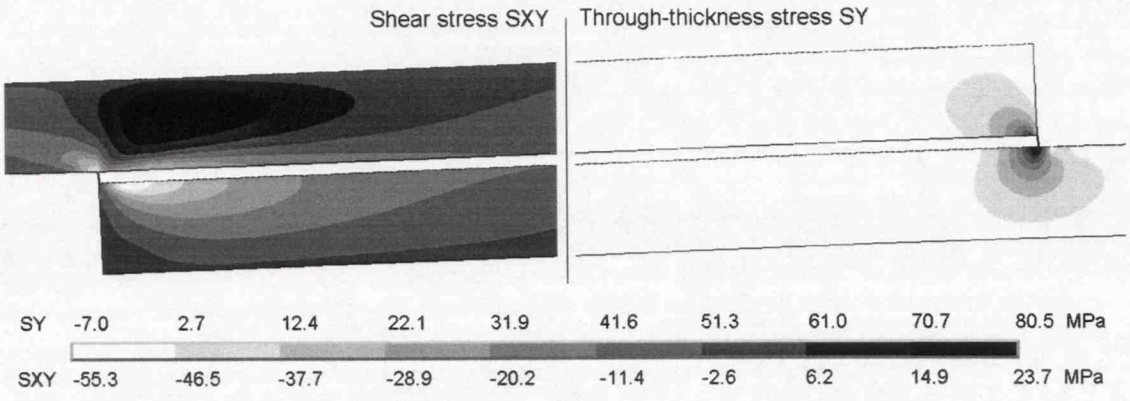

Figure 4.25: Shear (SXY) and through-thickness stress (SY) distribution within UD-substrates of a lap shear joint.

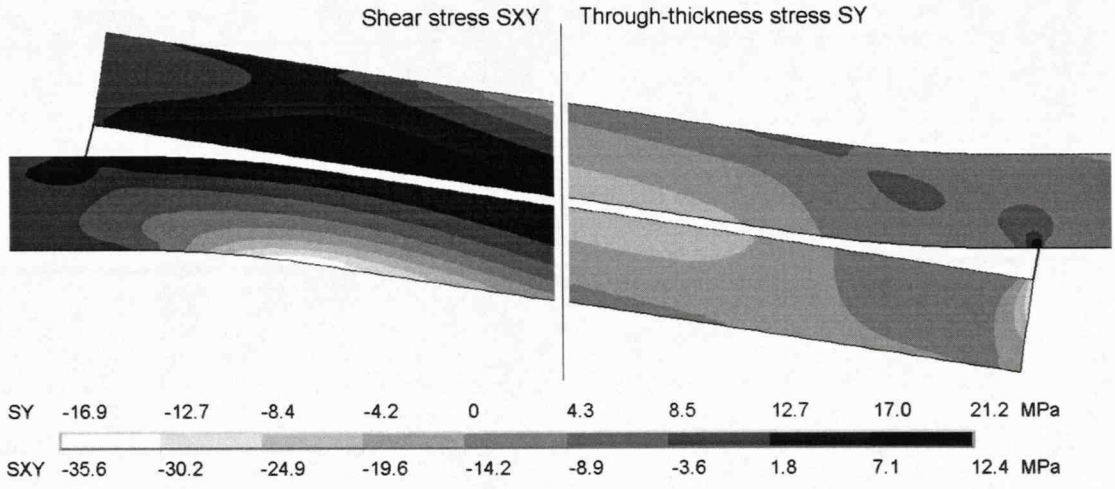

Figure 4.26: Shear (SXY) and through-thickness stress (SY) distribution within UD-substrates of a reverse-bent joint ($e = 0$; $l_f = 15\%$, $R = 50$ mm).

to which the substrates were bent ($e = -2$ mm, $k = -0.89$) was larger than with the aligned substrates ($e = 0$, $k = 0$) and, subsequently, the adhesive fillets at the overlap ends were also larger. Therefore, to allow a better comparison of both cases, the fillet size was reduced from 3 mm ($e = 0$, $k = 0$) to 2 mm ($e = -2$ mm, $k = -0.89$). Applying a negative eccentricity rotates the overlap area under load and reduces the stresses at the overlap ends, generating compressive through-thickness stresses at the end of the overlap. On the other hand, this increases the stresses nearer the centre of the overlap, though, as shown in Figure 4.24 the peaks were significantly reduced compared to the traditional lap shear joint. Maximum stresses were relocated towards the centre of the overlap length and, due to the lack of a

stress singularity in this area, the distribution across the thickness is relatively constant.

Figure 4.25 and 4.26 show shear and through-thickness stresses within the unidirectional FRP substrates of the lap shear joint and the reverse-bent joint with no eccentricity, respectively. Both joint types were modelled with sharp edges at the ends of the adhesive layer. Due to stress singularities at the overlap ends, direct comparisons between the magnitudes are not therefore possible. However, shear and especially through-thickness stresses within the reverse-bent substrates are more uniform, distributing the high stresses over a greater area compared to the lap shear joint. Figure 4.24 illustrates that stresses in the bondline of the reverse-bent joint tend to decrease towards the overlap ends indicating that the joint may not initially fail in the neighbourhood of the stress singularity.

4.4 Summary and conclusions

It was shown that the stress distribution of the lap shear joint is uniform with stress concentrations occurring at the overlap ends. Plastic deformation of the substrates is critical for metallic joints whereas high through-thickness stresses within the substrates of fibre reinforced composites often cause delamination of the substrates.

Wavy joints require a more complex forming process but peel stresses at the overlap ends are replaced by compressive stresses which can result in increased strength of composite joints (Zeng and Sun 2000). However, a parametric study suggested a flatter design, which appears to be very similar to the improved reverse-bent joint. Also, the investigation of the joint with prebent substrates resulted in an optimum similar to the design of the reverse-bent joint.

For the improved reverse-bent joint FEA showed a more uniform stress distribution within the bondline, lower through-thickness stresses within the FRP substrates and a reduction of plastic deformations of metallic substrates within the

overlap area. This makes the reverse-bent joint particularly suitable for metallic and composite joints. The actual effect on joint strength was therefore investigated further experimentally using various metallic and composite materials in the following chapters.

5 Experimental results

The FEA has shown that the reverse-bent joint has great potential due to the uniform stress distribution within the bondline and the substrates. Hence, metallic and composite reverse-bent joints were investigated experimentally for comparison with the standard lap shear joint. A number of metallic joints were also loaded in fatigue.

5.1 Strategy for the experimental testing

The overall aim of the experimental work was to prove the higher joint strength of the reverse-bent joint over the lap shear joint predicted by the FEA results. A parametric experimental study was also conducted based upon the best configurations defined by the FEA results. Due to the ease of bending metallic sheets to various different shapes the parametric study was carried out using steel substrates. The configuration found was used for different materials and joint geometries even though it may not be optimised for these different configurations. For comparison, similar reverse-bent and lap shear joints were produced with various adhesives, substrate materials and overlap lengths.

In practice, the fatigue performance is often more important than the static strength. Hence, both joint types were subjected to cyclic loading at different load levels producing S-N-curves that could be used for comparison.

Composite joints were tested to show the potential of the reverse-bent joint. Due to

the strong impact that the composite material properties can have on joint failure, various layups where made in order to examine their different effect.

5.2 Fabrication of the joints

Metal joints

Joints using various substrates, adhesives and geometries were manufactured consistently to ensure a comparability of the results. The basic joint dimensions used for all experiments are listed in Table 4.1.

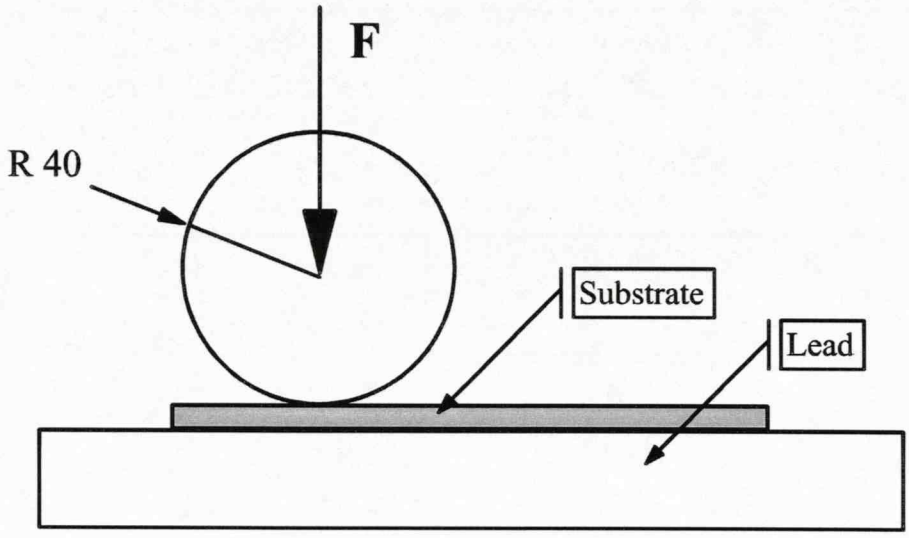

Figure 5.1: Bending tool

The steel sheets used for the substrates materials were cut with a guillotine. The specimens for the reverse-bent joint were bent using a tool, shown schematically in Figure 5.1. After bending the steel substrates to form the appropriate shape the bonding surfaces were grit blasted and then solvent wiped using acetone.

Composite joints

Unidirectional carbon fibre epoxy prepregs were manufactured in a straight and bent shape. Each UD lamina had a thickness of about 0.13 mm, 15 lamina gave a total substrate thickness of 2.0 mm. The properties of the UD-properties are listed

in Table 3.4 . Different fibre layups were produced to simulate materials which were more sensitive to through-thickness stresses and strains and thus more likely to fail in delamination within the substrates. It was assumed that joints with substrates of a $[90_2 - 0_2 - 90 - 0 - 90 - 0_{1/2}]_S$ stack are weaker than joints of composites where fibres are orientated in the reverse, with the 0 fibres located at the surface layer.

The bond surfaces were lightly grit blasted and then solvent wiped using Ethanol. Aluminium end tabs were bonded onto the substrates to ensure the joint did not slip in the jaws during testing.

Bonding and testing

End tabs were bonded onto the flat lap shear joints to compensate for the misalignment of the substrates. In order to ensure a constant thickness of the adhesive layer one percent weight ballotini of 0.25 mm was added. Subsequently the corners and especially the fillets were fashioned, carefully, with a small file to give a consistent fillet profile. The joint geometry was checked before testing to ensure consistency of shape to minimize the scatter.

Finally, the joints were tested at 23±2°C using a Testometric tensile test machine, fitted with a 25 kN load cell, at a crosshead speed of 1 mm/minute. Five replicate specimens were made for each test.

Fatigue tests

For the investigation of the fatigue behaviour the automotive steel 2 was chosen together with the stiffer adhesive 1. For the cyclic loading a hydraulic test machine with a 10 kN and 20 kN load cell was used. Tests were performed using sinusoidal loads of constant amplitude with a load ratio of 0.1 and a frequency of 10 Hz. Temperature was not controlled. Four replicate specimens were tested for each load level. Tests were stopped once the specimen lasted more than one million cycles.

5.3 Static test results using metal substrates

Steel 2 and adhesive 1 were used to investigate various eccentricities and internal fillet sizes. End tabs were not used for the reverse-bent joints to investigate the effect of substrate eccentricity. The overlap length was fixed at 20 mm. Figure 5.2 displays the influence of different eccentricities on the failure load of the joint. The eccentricities, e, of the substrates, varying from $e = -2.13$ mm to $e = 1.45$ mm, are equivalent to bending moment factors, k, where k varies from -1.47 to 1, see Figure 5.2. The best result was obtained with aligned substrates ($e = 0$; $k = 0$). The influence of internal fillet sizes is shown in Figure 5.3, using aligned substrates. Highest failure loads were achieved with a joint configuration exhibiting an internal fillet size of 3 mm each side, which corresponds to 15% of the bondline length; this joint configuration was subsequently used for further testing and comparison.

Figure 5.4 and 5.5 show experimental results comparing reverse-bent and lap shear joints with a 10 mm and 20 mm overlap each and different substrate materials. Reverse-bent joints with steel 2 substrates and a 20 mm overlap show the highest improvement of 40% compared to flat joints. The load-displacement graph, shown in Figure 5.7, indicated a large difference in total joint strain between both joint types. All 6 samples of the 20 mm overlap configuration, using steel 3 substrates and adhesive 1, failed in the substrate outside the overlap area. Test results comparing the joints utilizing the more ductile adhesive 2 are shown in Figure 5.6. Fractured surfaces of several joints can be seen in Figure 5.8.

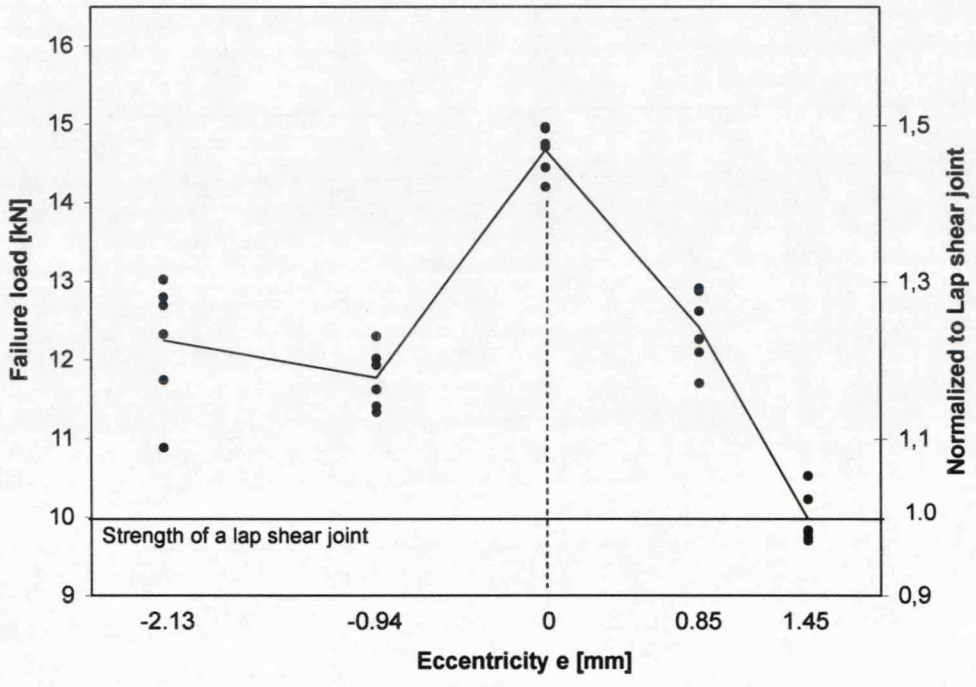

Figure 5.2: Failure loads resulting from various eccentricities, e, of the reverse-bent joint (20 mm overlap, steel 2, adhesive 1, $l_f = 0$, $R' = 40$ mm)

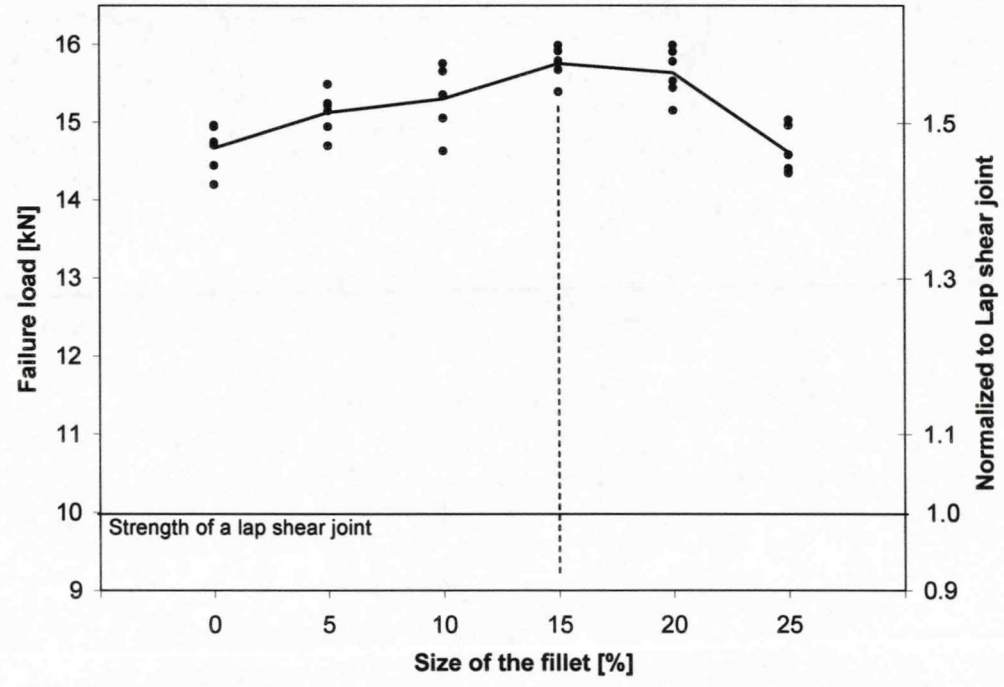

Figure 5.3: Failure load of various fillet sizes of the reverse-bent joint (20 mm overlap, steel 2, adhesive 1, $e = 0$, $R' = 40$ mm)

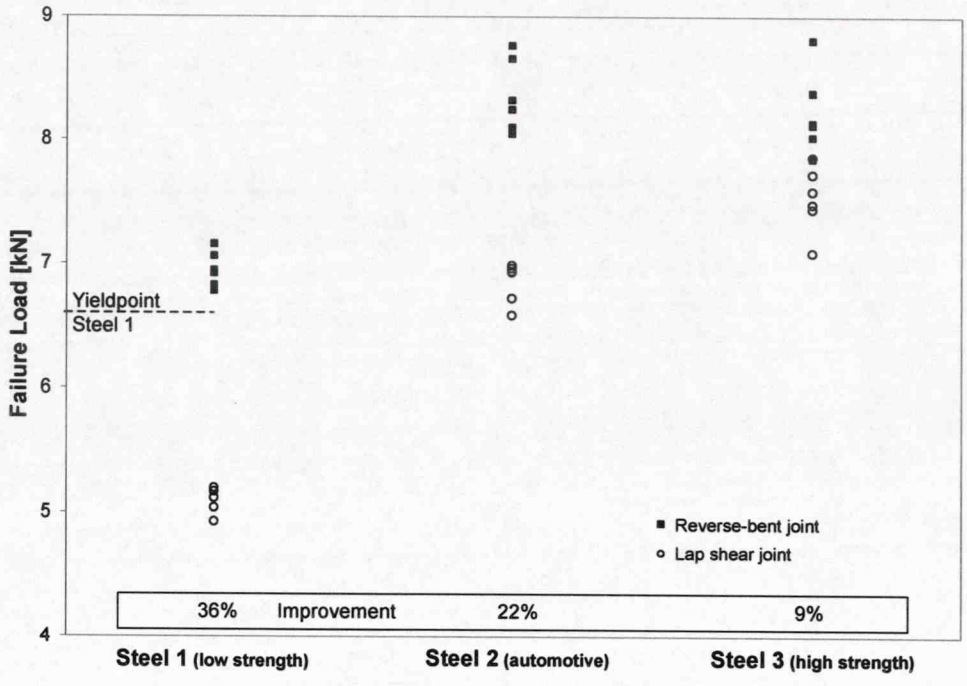

Figure 5.4: Failure load of reverse-bent and lap shear joints with an overlap length of 10 mm (adhesive 1)

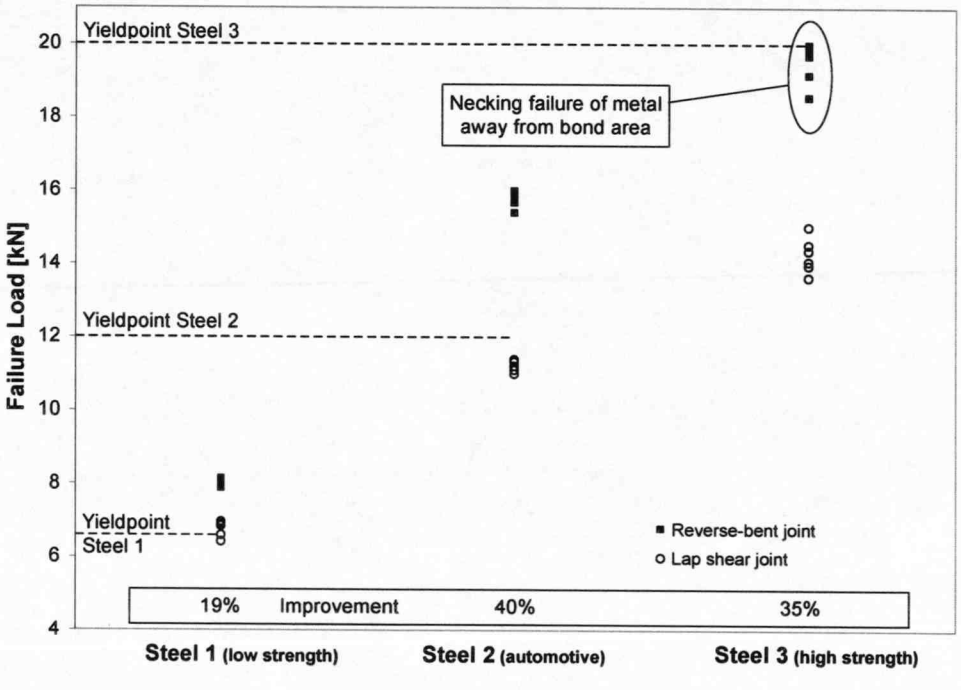

Figure 5.5: Failure load of reverse-bent and lap shear joints with an overlap length of 20 mm (adhesive 1)

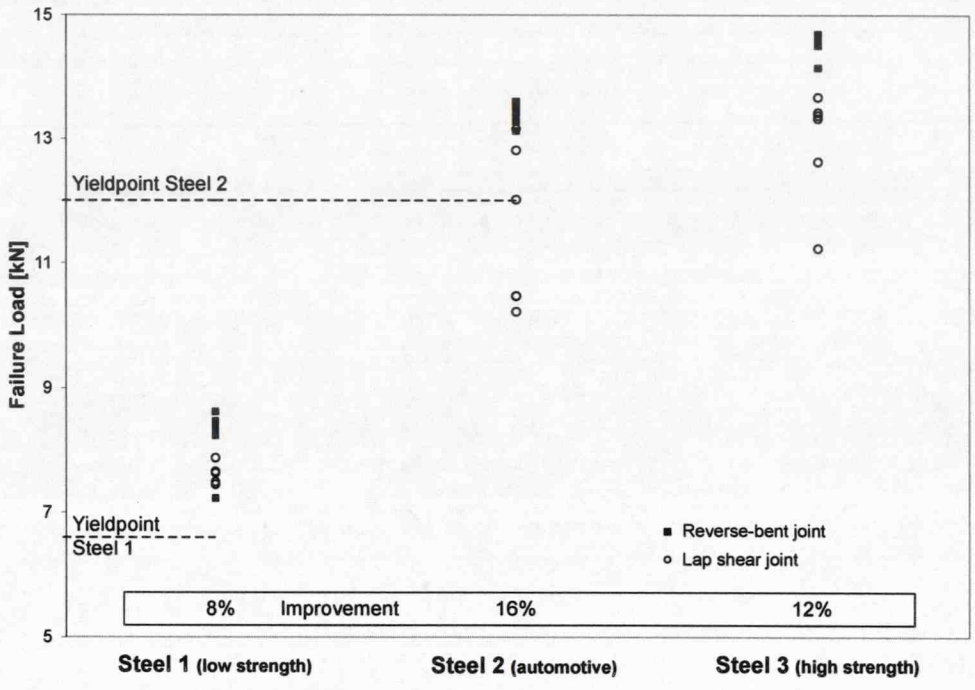

Figure 5.6: Failure load of reverse-bent and flat lap shear joints with an overlap length of 20 mm (adhesive 2)

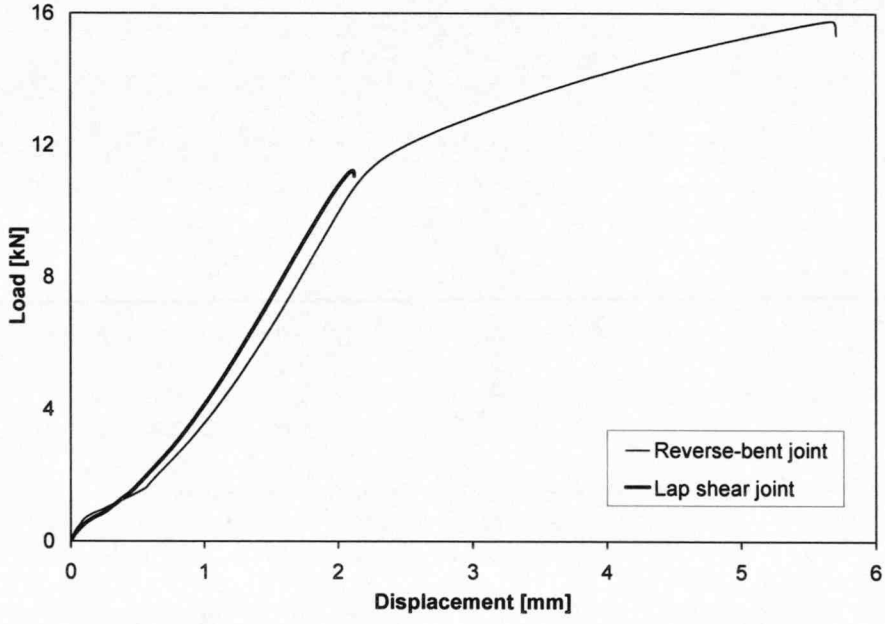

Figure 5.7: Load-displacement graph of the lap shear and reverse-bent joint (20 mm overlap, steel 2, adhesive 1); cross head displacement measured

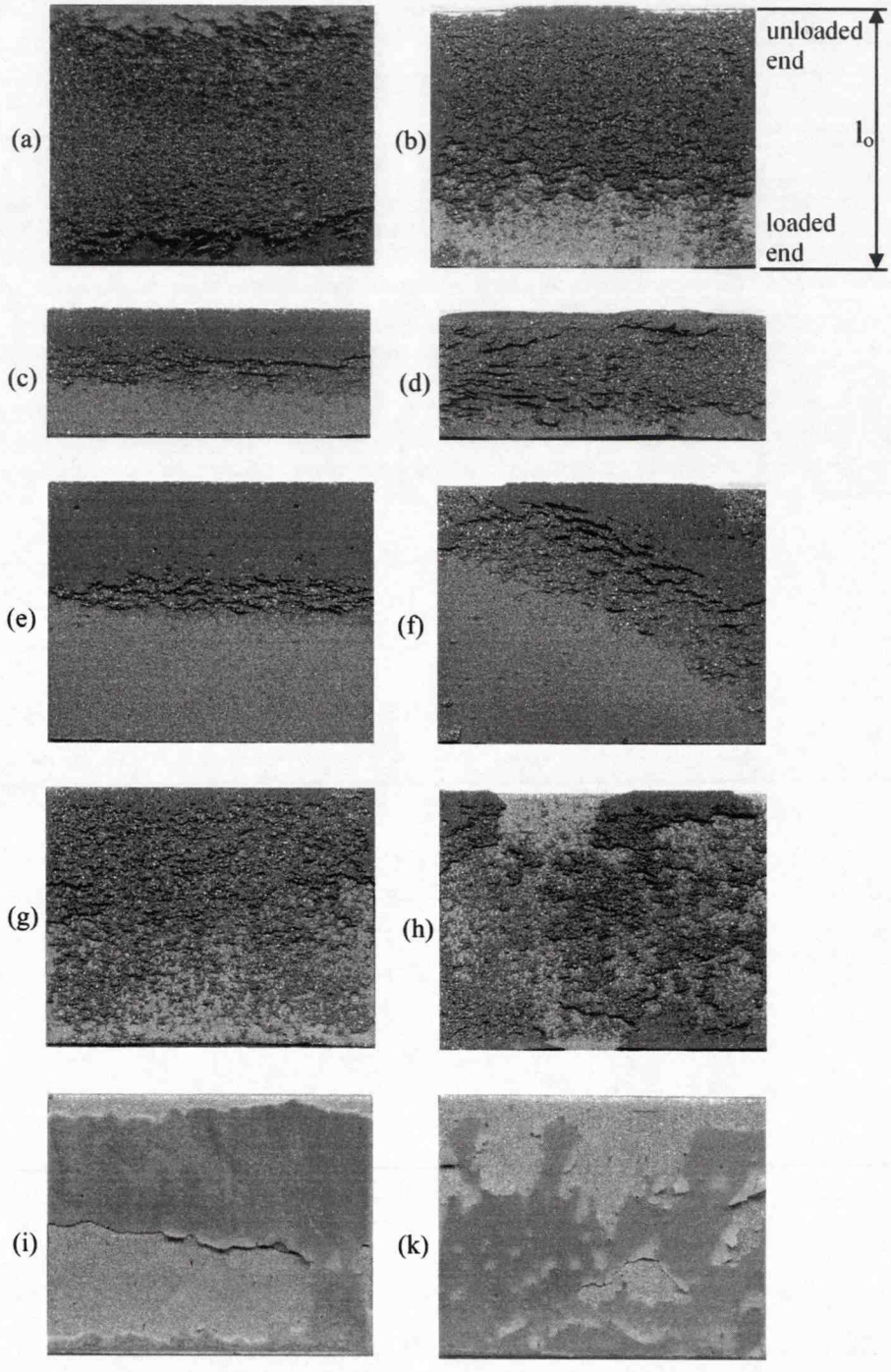

Figure 5.8: Interface after failure of various joint configurations (see (b) for orientation): (a) Fillet optimization: fillet size 25%; Adhesive 1, steel 2, 20 mm overlap, (b) Fillet optimisation: fillet size 0%; Adhesive 1, steel 2, 20 mm overlap, (c) Adhesive 1, steel 1, 10 mm overlap, flat; (d) Adhesive 1, steel 1, 10 mm overlap, reverse-bent; (e) Adhesive 1, steel 1, 20 mm overlap, flat; (f) Adhesive 1, steel 1, 20 mm overlap, reverse-bent; (g) Adhesive 1, steel 2, 20 mm overlap, flat; (h) Adhesive 1, steel 2, 20 mm overlap, reverse-bent; (i) Adhesive 2, steel 2, 20 mm overlap, flat; (k) Adhesive 2, steel 2, 20 mm overlap, reverse-bent

5.4 Fatigue test results using metal substrates

The results of the fatigue tests are presented in Figure 5.9 and also separately in Figure 5.10 for the lap shear joint and in Figure 5.11 for the reverse-bent joint. Four lap shear joint specimens did not fail within the maximum range of one million cycles when a maximum load of 3.25 kN was applied; equivalent to 29% of the static load. In contrast, reverse-bent joint specimens exceeded one million cycles at a load level of 8.5 kN, which corresponds to 54% of the static failure load. In comparison to static strength improvements of 40%, cyclic loading produced improvements of 160%, when load levels are compared where no failure occurred after one million cycles.

The fractured surfaces of lap shear and reverse-bent joints subjected to fatigue loading are shown in Figure 5.12 (a) and (b).

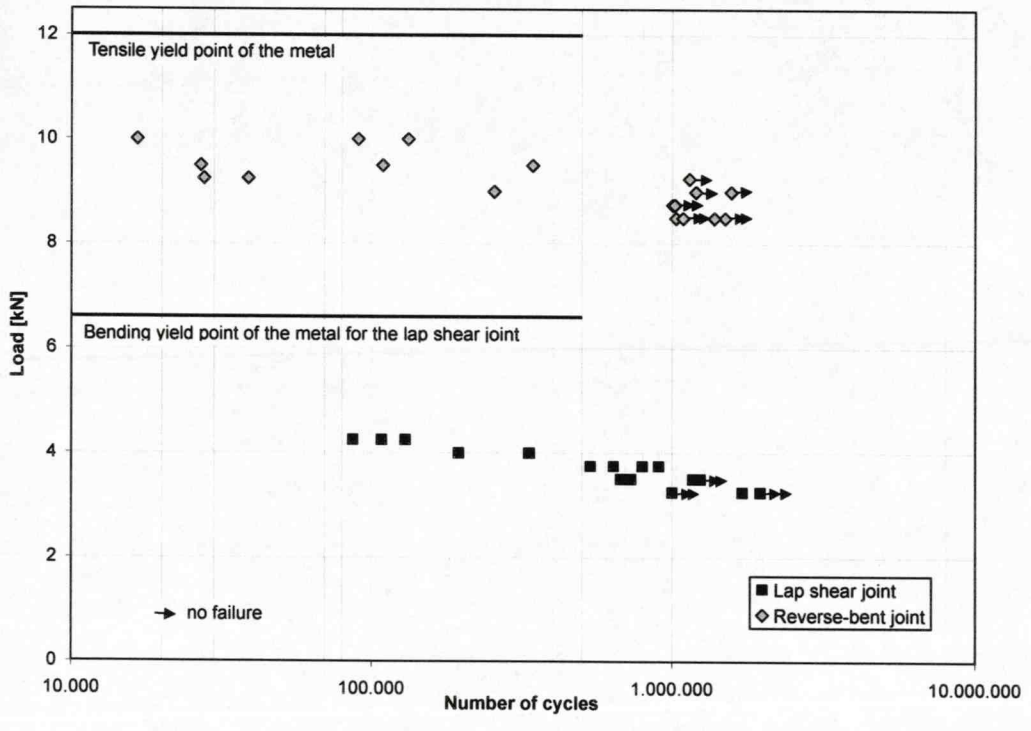

Figure 5.9: Fatigue results: comparison of flat lap shear with reverse-bent joint

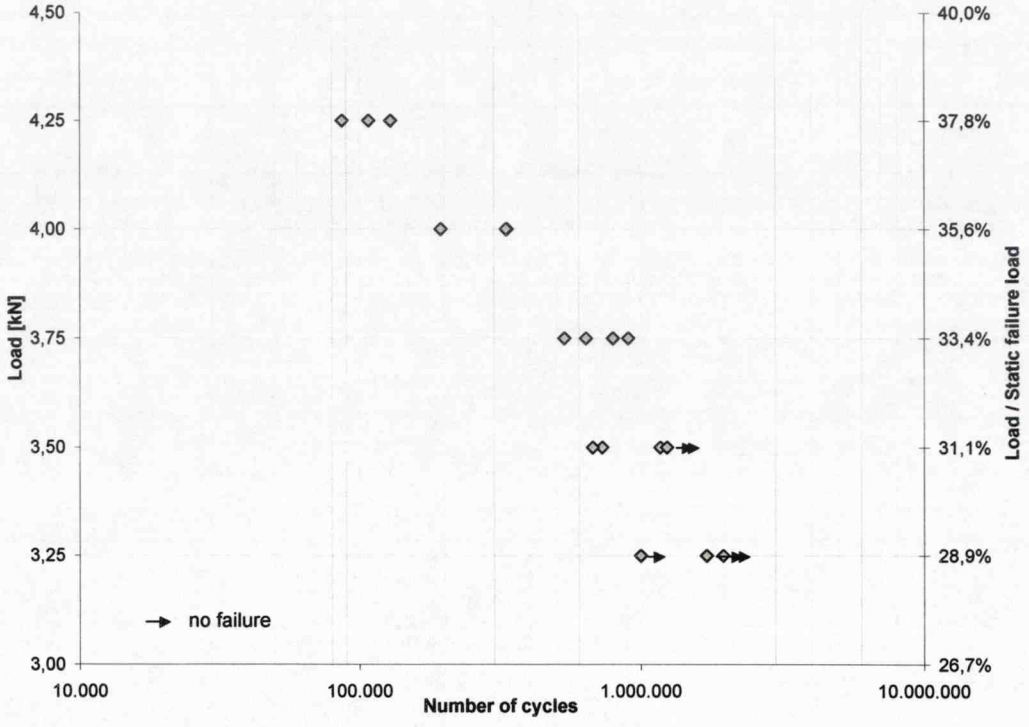

Figure 5.10: Fatigue results of the flat lap shear joint

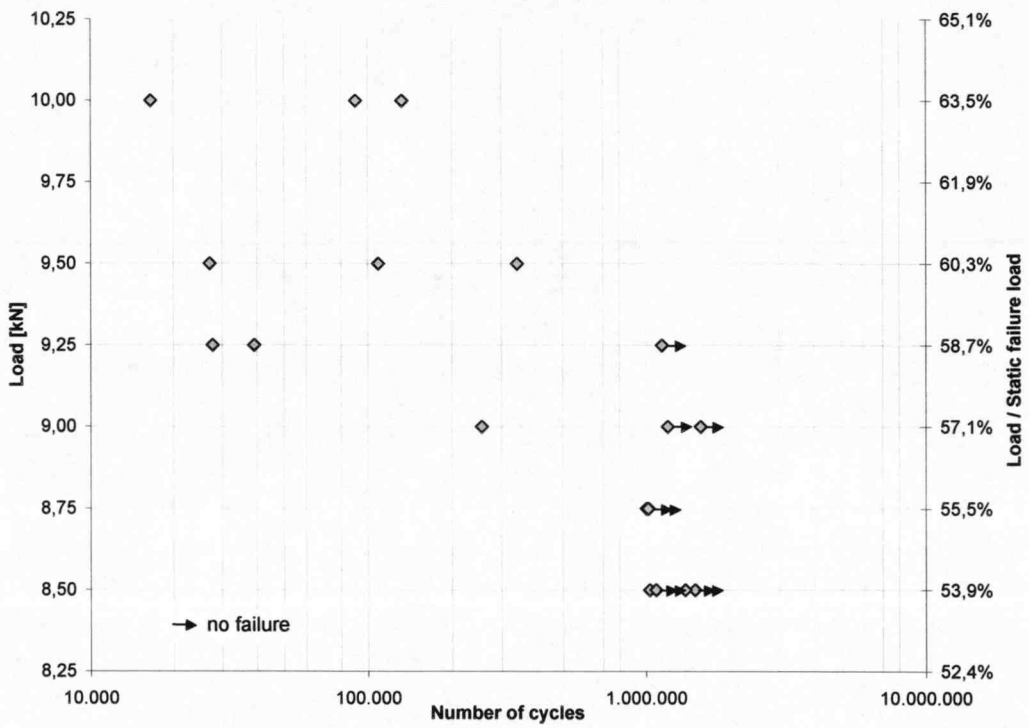

Figure 5.11: Fatigue results of the reverse-bent joint

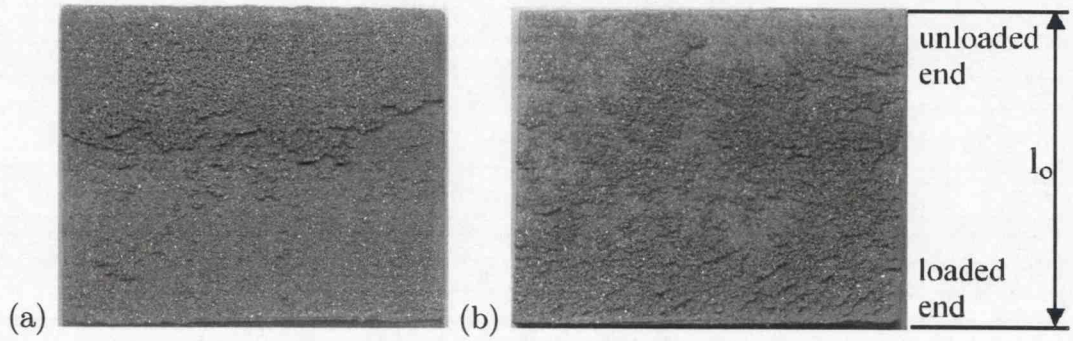

Figure 5.12: Fractured surfaces of (a) the lap shear joint and (b) the reverse-bent joint that were subjected to cyclic loading

5.5 Static test results using composite substrates

For comparison with the FEA models, two sets of UD reverse-bent joints were made, a) using aligned substrates ($e = 0$) and b) with an eccentricity of $e = -2$ mm. The fillet size was also reduced from 3 mm to 2 mm. Despite the varied eccentricity the joint strength decreased by only 6% for the case of $e = -2$ mm. Yet, compared to flat lap shear joints the failure load of the reverse-bent joint with aligned substrates was approximately 70% higher. It may be argued that introducing large external fillets of adhesive can also increase the lap shear joint strength, hence, lap shear joints were also produced with large adhesive fillets fashioned to approximately 45° at the overlap ends. This improved the strength of the lap shear joint by 24%.

Joints with substrates made of varied fibre directions showed a joint strength increase from 88% to 193% when compared to a lap shear joint with similar substrates, whilst joints made with the more ductile adhesive showed only a small improvement in strength of 11%. Detailed test results with pictures of the fractured surfaces are summarised in Table 5.1.

	Joint type	Substrate	Adhesive	FEA: max. Stress* [MPa]	Average failure load [kN] (StDev)	Fractured surfaces, scale 1:0.93
a)	Lap shear joint	UD	1	N/A	12.21 (0.52)	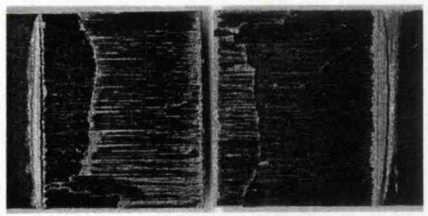
b)	Lap shear joint with large fillets	UD	1	N/A	15.18 (0.46)	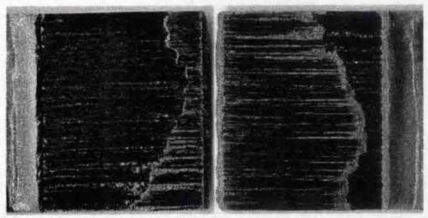
c)	Reverse-bent joint $e = 0$	UD	1	$S1_a$59.6; SY_c5.2; SXY_c21.6	20.73 (0.65)	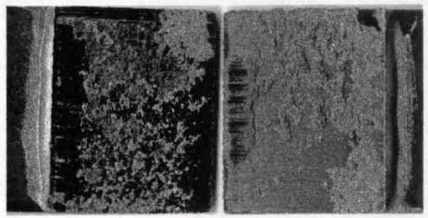
d)	Reverse-bent joint $e = -2$	UD	1	$S1_a$64.1; SY_c10.3; SXY_c12.1	19.49 (0.84)	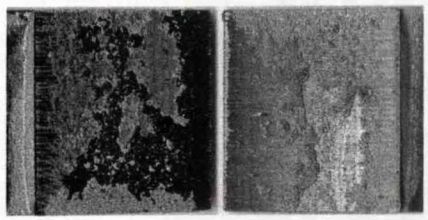

continued on next page

	Joint type	Substrate	Adhesive	FEA: max. Stress* [MPa]	Average failure load [kN] (StDev)	Fractured surfaces, scale 1:0.93
e)	Lap shear joint	0-0-90-90-0-90...	1	N/A	9.73 (0.88)	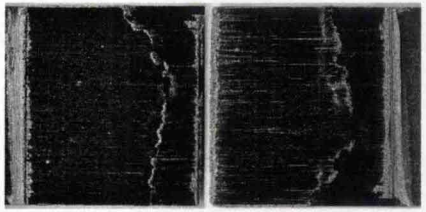
f)	Reverse-bent joint $e = 0$	0-0-90-90-0-90...	1	$S1_a$53.7; SX_c230; SY_c6.8; SXY_c33.0	18.34 (0.96)	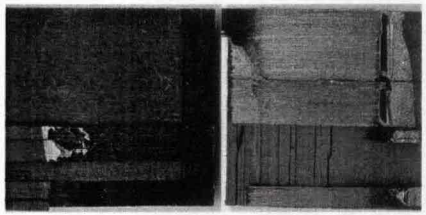
g)	Lap shear joint	90-90-0-0-90-0...	1	N/A	3.72 (0.37)	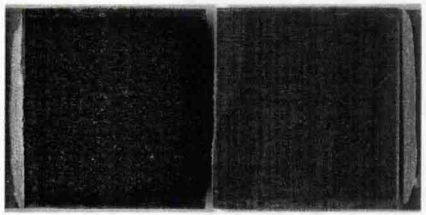
h)	Reverse-bent joint $e = 0$	90-90-0-0-90-0...	1	$S1_a$32.5; SX_c19.4; SY_c4.0; SXY_c23.4;	10.89 (0.85)	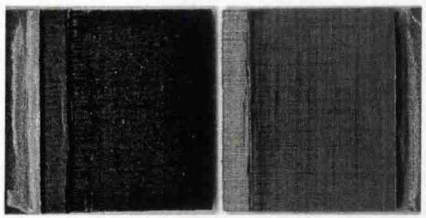

continued on next page

	Joint type	Substrate	Adhesive	FEA: max. Stress* [MPa]	Average failure load [kN] (StDev)	Fractured surfaces, scale 1:0.93
i)	Lap shear joint	UD	2	N/A	12.86 (1.17)	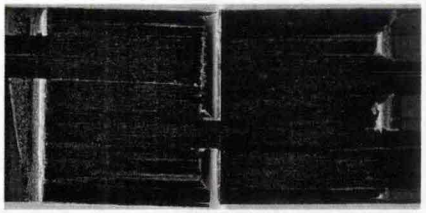
k)	Reverse-bent joint $e = 0$	UD	2	$S1_a$40.8; SY_c3.6; SXY_c15.6	14.3 (0.41)	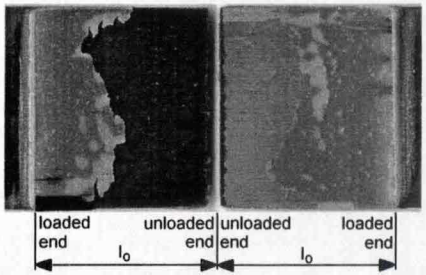

* c=composite; a=adhesive; S1=principal stress; SX=stress in loading direction; SY=through-thickness stress; SXY=shear stress

Table 5.1: Composite joints: Test results

6 Discussion

FEA showed great potential for the reverse-bent joint which was confirmed, experimentally, with increased static and fatigue performance compared to the lap shear joint. This chapter explains the experimental results in more detail, also drawing upon the knowledge gained from the FEA results.

6.1 Metallic substrates

6.1.1 Parametric study

A nonlinear FE Analysis was applied to obtain various stress distributions for the reverse-bent joint configuration and to identify general trends for improvements. It was assumed that any improvements in the stress distribution within the joint would result in improvements in experimental joint strength. To validate this assumption, reverse-bent joints with different eccentricities and internal fillet sizes, were tested. Aligned substrates, i.e. $e = 0$; $k = 0$, gave the highest failure loads, as a result of minimum joint rotation. FEA showed that the stress distribution improved with a small eccentricity, due to a reduction in substrate deformation at the adhesive interface (see Figure 4.16) but no evidence was found to evaluate this experimentally. However, further testing of eccentricities close to aligned substrates, $e = 0$, may result in higher failure loads. Greenwood et al. (1966) suggested an optimum k-factor of $k = -0.5$ for an overlap length of 76 mm and a substrate thickness of 13 mm. Due to the high thickness of the substrates, almost no plastic

deformation in a pure tension mode occurred in the substrates, whereas, in this study, the metal yielding, distinguishable in Figure 5.7, influenced the failure mode significantly. This may be why the optimum for this investigation, lying somewhere between $k = -0.65$ and $k = 0.59$, differs from that found by Greenwood.

Figure 4.16 also shows a higher scatter for joints with an eccentricity of $e = -2.13$ mm. This is expected to be caused by the production process which became more difficult with greater substrate bends.

Various internal fillet sizes were investigated using FEA to see the effect on stresses at the overlap ends of the joint. Compared to the eccentricity, the influence of the internal fillet size on the failure load was much less significant. Figure 5.3 indicates an optimum lying somewhere between 10% and 20%. The failure surfaces of the extreme cases, 25% and 0% (no internal fillet), which is shown in Figure 5.8(a) and (b) respectively, point to an altered crack path and thus a change in failure mode. In joints with large internal fillets the crack appeared to initiate and then propagate from the outer ends of the overlap close to or at the interface to the unloaded substrate. In joints with no additional internal fillet the crack appeared to run from the loaded substrate end. In the best configuration (15% internal fillet) a crack path was not distinguishable, as can be seen in Figure 5.8(h). From the FE Analysis the stress distribution was expected to be very uniform, so much so that apparently no distinguishable stress peaks at particular points initiate failure.

It is expected that there will be interactions between internal fillet size and eccentricity, and a dependency of these design variables on material properties and general geometry of the joint is assumed. Nevertheless the comparative investigation of various overlaps, substrate and adhesive materials was performed with the reverse-bent joint configuration of aligned substrates, $e = 0$, and an internal fillet size of 15% only.

6.1.2 Performance comparison of lap shear and reverse-bent joints

The various joint configurations showed improvements in joint strength of between 8% and 40% for the reverse-bent joint compared to the equivalent lap shear joint. As might be expected, the difference is more significant with the more brittle adhesive 1 as it is not ductile and therefore does not yield significantly which in the lap shear joint would reduce the effect of the stress peaks.

Figure 5.4 and 5.5 show a reverse in trends between the overlap length and the yield strength of the substrates. In the case of the smaller 10mm overlap, reverse-bent joints with substrates of the low yield strength, steel 1, gave the greatest improvement over the lap shear joint (36%). The overlap area of the lap shear joint exhibited large rotation and bending deformation; hence the outer areas of the joint failed due to the high amount of straining of the metal at the interface to the adhesive, distinguishable in Figure 5.8(c). Only a small part in the overlap centre failed cohesively in apparent shear, whereas, in the reverse-bent joint, this area was much increased, see Figure 5.8(d), as a result of the reduced substrate yielding due to bending. As expected, joints with the higher strength steel 2 and 3 substrates failed at higher loads. The amount of substrate yield was reduced and the area subjected to shear increased. The failure load of the reverse-bent joint with steel 2 and 3 substrates is approximately the same (Figure 5.4), which indicates that in both cases the adhesive failed before the yield point of the metal was reached. This was also reflected in the experimental scatter, which is typically reduced when substrate yield affects the joint failure.

Increasing the overlap from 10 to 20 mm improved the joint strength of the low strength steel 1 only marginally, as failure was dominated by substrate yielding. Comparing the failure surfaces of the mild steel 1 in Figure 5.8(c) and (e) shows that the area of adhesive failing in shear was almost constant whereas the area failing interfacially, apparently due to metal yielding and peel stresses, increased

significantly. The equivalent reverse-bent joint with the 10 mm overlap appeared to fail mainly in shear, whereas reverse-bent joints with 20 mm overlaps failed predominantly due to metal yielding and peel stresses in the adhesive. The aligned substrates of the reverse-bent joint delayed yielding further, as can be seen in the load vs. displacement graph plotted in Figure 5.7, but at higher loads the metal starts to yield outside of the overlap area in a tension mode resulting in lateral straining of the steel sheets. This introduces large straining in the corners of the joint. Figure 5.8(f) shows the crack running from one corner diagonally through the overlap area. In reality, automotive joints would be much wider and thus the predominant lateral straining would be initiated only in the through-thickness direction, which would tend to result in higher joint strengths than were observed in this investigation.

Increasing the yield point of the substrates further (steel 3), the strength improvement of the reverse-bent joint was at least 35%, in this case limited by the ultimate failure of the metal, away from the bond area.

Adhesive 2 is more ductile and, as can be seen in Figure 3.2, the strain to failure is greater compared to adhesive 1. Hence, this adhesive should be more suited for bonding the low-strength steel 1, resisting more metal yielding before failure. In lap shear joints with a 20 mm overlap and mild steel 1 substrates, adhesive 2 performed 12% better compared to adhesive 1, whereas, using reverse-bent joints with the same substrates both adhesives produced similar failure loads, despite the contrasting properties of the adhesives. Both joint types benefit from the increased strain to failure of adhesive 2 but due to the decreased shear strength the failure load of the reverse-bent joint did not increase significantly.

With the use of adhesive 2 the joint strength comparison of both joint types shows a less significant improvement for the reverse-bent joint of 8% to 16% depending on the steel type. The adhesive failed predominantly interfacially, as can be seen in Figure 5.8(i) and (k). The crack path in the lap shear joint typically ran along

the loaded substrate interface initially, and then changed to the loaded part of the other substrate, in the joint centre. The reverse-bent joint also failed interfacially but a representative crack path was undistinguishable, pointing perhaps to a more uniform stress distribution. The lack of stress peeks and substrate yielding in bending in reverse-bent joints appears to allow the application of more brittle adhesives with higher shear strength, even for metallic substrates with low yield points.

Adams et al. (1997) presented a simple tool to predict the joint strength of lap shear joints based on the shear or yield strength of the adhesive and the yielding of the metallic substrates due to the overlap rotation. An adoption of this model for reverse-bent joints, which takes the adhesive shear strength, τ_u, and the tensile yield point of the substrates, σ_y, into account, seems to give a good approximation for the load at which the joint can be expected to fail:

$$P = \min\{\begin{matrix}\tau_u l_o w \\ \sigma_y t_s w\end{matrix} \tag{6.1}$$

where l_o is the overlap length, t_s is the thickness of the substrate and w is the with of the joint.

The uniform shear stress distribution and low through-thickness stresses of the reverse-bent joint enable the application of failure criteria based on average adhesive shear strength, τ_u (or yield strength, τ_y).

6.1.3 Fatigue loading

The reduction of stress concentrations in the reverse-bent joint seems to affect the fatigue behaviour (see Figure 5.9) much more significantly, compared to the increase obtained in the static tests (Figure 5.5). The absolute load level increased but also the load relative to the static strength. The endurance limit of the lap shear joint was expected for loads between 20% and 40% of the static joint strength, which agrees with the test results shown in Figure 5.10. Using the reverse-bent

joint configuration, the limit appears to rise to 55% of the static strength for the joints investigated (Figure 5.11). Figure 5.11 also shows a large scatter for the test results of the reverse-bent joint (logarithmic standard deviation $s_{log} = 0.5$), which is three times higher compared with the normal lap shear joint, where $s_{log} = 0.1$ (Figure 5.10).

Literature suggests that the fatigue life of bonded lap shear joints is dominated by crack propagation, with the initiation of the crack occurring after 15% of the entire fatigue life (Taylor 1997). Crack initiation occurs at the ends of the overlap at the location of high stress peaks. In the reverse-bent joints it is difficult to locate a point of initial crack initiation due to the much more uniform stress distribution. Thus, the fatigue life is dominated by the crack initiation phase, which apparently results in higher scatter compared to the lap shear joint where the crack propagation produces smaller scatter. The fractured surfaces of lap shear and reverse-bent joints subjected to fatigue loading are shown in Figure 5.12 (a) and (b). In the tested lap shear joints the crack initiated along the adhesive-substrate interface at the loaded overlap end, running towards the centre of the joint. By contrast, it would appear that the crack in the reverse-bent joint propagates along the outer areas of the overlap length adjacent to the unloaded substrate-interface. Within the large central area there is no crack path visible. Because of the high stresses at the overlap centre and the lack of substrate yielding for the fatigue load levels, the crack may initiate within the central region of the overlap, running outwards towards the joint-ends.

Figure 5.9 shows a comparison of the fatigue life of both joint types and the load where the substrates are expected to deform plastically. The load at which the metal substrate starts to yield was simply estimated by $P = \sigma_y t_s w/4$ (Adams et al. 1997) for the lap shear joint and $P = \sigma_y t_s w$ for the reverse-bent joint. Also plotted in Figure 5.9 were the substrate yield points, in order to provide an estimate of the yield load whereby plastic deformation of the substrate will start to significantly

influence joint strength. From this plot it is plausible that the endurance limit is governed by the adhesive and not the substrate for the reverse-bent joint.

An advantage of the non-uniform stress distribution in traditional lap shear joints is, however, a good resistance to creep. Due to the low shear stresses in the central region of the overlap, creep is less likely to occur. When reverse-bent joints are subjected to fatigue loading the adhesive may have the tendency to creep, depending on the load level and R-ratio, as the entire bondline is equally stressed.

6.2 Composite substrates

In comparison to the traditional lap shear joint, the numerical study of the reverse-bent joint showed a more uniform stress distribution, reduced peak stress values and relocation of maximum stresses to less critical areas (i.e. away from the overlap ends), as can be seen in Figure 4.24. The experimental study subsequently showed significantly improved failure loads for the reverse-bent joint over the lap shear joint. In Table 5.1, the fractured surfaces of the reverse-bent joint show a general trend of an increased central area of the overlap that appeared to fail cohesively in the adhesive rather than by delamination of the CFRP substrates, suggesting lower shear and through-thickness stresses within the CFRP. Notably, the reverse-bent joint always exhibited delamination at the unloaded end of the substrate, which was in contrast to the lap shear joint where, as is usually expected, delamination initiated at the loaded end.

6.2.1 UD Substrates

The lap shear joint with UD substrates failed at a load of 12 kN. Apparently, the crack initiated at the loaded substrate end and delaminated the composite. The introduction of a large external fillet of adhesive increased the failure load by only 24%, although the failure mode remained the same as that obtained without external fillets. The reverse-bent joint failed at loads 37% and 70% higher compared

to single lap joints with and without external fillets, respectively. Only a small part of the unloaded reverse-bent substrate appeared to be delaminated whereas the major central area failed cohesively within the adhesive, as can be seen in joints c and d in Table 5.1.

FEA predicted reduced stresses at the overlap end when an eccentricity of -2 mm was used but also higher stresses located more centrally compared to reverse-bent joints with aligned substrates. The eccentricity of -2 mm decreased the strength by 6%, which is in accordance with the small increase in stresses predicted by FEA.

The fractured surfaces of reverse-bent joints with and without eccentricities show a central cohesive failure of the adhesive and delamination of the composite at the ends of the unloaded substrate. Failure did not occur at the overlap end at the interface adjacent to the loaded substrate where stresses, predicted by FEA, appeared to be singular. Figure 4.26 shows the through-thickness stress distribution within reverse-bent substrates. Apart from the area affected by the stress singularity, high through-thickness and shear stresses were predicted at the unloaded substrate end which correlates with the failure mode observed from the experiments.

To help distinguish the initial locus of failure, reverse-bent joints were modelled according to the CFRP stacking sequence and loaded up to failure loads exhibited in the experimental work. Maximum principal stresses within the adhesive layer ($S1_{adhesive}$) and maximum through-thickness ($SY_{composite}$), longitudinal ($SX_{composite}$) and shear stresses ($SXY_{composite}$) within the unloaded end of the composite substrates are listed in Table 5.1. Failure prediction within composite materials remains an extremely complex field, and thus within the scope of this project the following discussion relates only to a comparison of the stresses in the joint to that of the material strength data listed in Table 3.4.

In reverse-bent joints with UD substrates, adhesive 1 and eccentricities of 0 and -2 mm the maximum principal stress within the adhesive bondline was relatively high, higher than the strength obtained from bulk tensile tests, but lower than

values found in the literature (Adams, Comyn, and Wake 1997). Maximum tensile through-thickness stresses within the composite substrates were less than 25% of the failure stresses obtained from transverse tensile tests, where fibres in the specimen were aligned perpendicular to the loading direction. Thus, the reverse-bent joint presumably initially failed in the adhesive due to the high principal stresses that are shown in Figure 4.24. It is likely thereafter that the crack propagated towards the overlap centre within the adhesive and towards the overlap end within the composite substrates. This assumption is drawn from the fact that the stresses in the adhesive are much lower at the overlap ends whereas through-thickness stresses in the composite are at their maximum. The failure of lap shear joints, as is often the case, is more complicated to determine due to singular stresses at the overlap ends where maximum stresses within the adhesive and substrate occur. Hence, for lap shear joints, a simple comparison of FEA predictions with experimental data was not undertaken.

6.2.2 Orthotropic substrates

When composites with orthotropic fibre layups were used, both their tensile and bending stiffness (in direction x) was reduced, causing higher peel and shear strains, which ultimately resulted in lower failure loads in the lap shear joints. The drop in strength of the lap shear joints was 20% and 70%, respectively, for $[0_2-90_2-0-90-0-90_{1/2}]_S$ and $[90_2-0_2-90-0-90-0_{1/2}]_S$ substrates. Due to the configuration of the reverse-bent joint, the substrates only bend marginally causing lower through-thickness stresses/strains. Subsequently, the performance of the reverse-bent joint only dropped by 12% and 47%, respectively for the two layup configuration.

The stress distribution within the orthotropic substrates and the adhesive layer of the reverse-bent joint showed similar trends to those of reverse-bent joints using unidirectional CFRP substrates: the highest through-thickness stresses in the composites are located at the outer regions of the overlap and principal stress peaks

of the adhesive occur more centrally. In reverse-bent joints with $[0_2 - 90_2 - 0 - 90 - 0 - 90_{1/2}]_S$ substrates, the principal stresses in the adhesive layer were only slightly lower compared to the maximum principal stress in reverse-bent joints with UD-substrates, but shear and through-thickness stresses within the unloaded substrates were high, causing the joint to fail by delamination of the composite. The substrate failed at the interface between the 0^o and 90^o layer without breaking the fibres at the bonding surface orientated in the loading direction. The crack then propagated beyond the overlap end, reaching the end tabs, before finally breaking the the fibres of the surface layer (joint f in Table 5.1).

In reverse-bent joints with $[90_2 - 0_2 - 90 - 0 - 90 - 0_{1/2}]_S$ substrates, longitudinal stresses ($SX_{composite}$) need to be taken into account because the fibres at the surface layer are orientated perpendicularly to the loading direction. These longitudinal stresses reach 50% of the composite strength in the transverse direction and are five times higher than stresses occurring in the through-thickness direction. The fractured surface of joint h in Table 5.1 shows the typical crack path of reverse-bent joints with $[90_2 - 0_2 - 90 - 0 - 90 - 0_{1/2}]_S$ substrates, where the composite delaminates at the interface between the 0^o and 90^o layer at the unloaded side, and switches to the other side of the bondline at the point of maximum stress. Thus, the initiation of failure is expected at the point of highest stress within the composite, then, due to high longitudinal stresses, propagating to the other side of the bondline and, subsequently, delaminating the substrate towards the unloaded end.

The same substrates bonded together using the lap shear configuration experience higher stresses in the surface layer due to the reduced bending stiffness and the rotation of the overlap which causes additional longitudinal stresses. Thus, it would appear that the strength of the reverse-bent joint was much less dependent on the delamination characteristics of the composite. For example, the largest difference when comparing the performance of lap shear and reverse-bent joints was obtained

with substrates having fibres oriented at 90^o at the outer layers, where delamination occurred early and caused the lap shear joint to fail at 3.7 kN. Reverse-bent joints with the same substrates, benefiting from a more uniform stress distribution, failed at a load of 10.89 kN (193% higher). Hence, this joint type is likely to be highly beneficial for materials which are particularly weak in the through-thickness direction.

6.2.3 Adhesive type

The application of high strength, high stiffness, adhesives for bonding composite materials is not very common. More flexible adhesives are favourable because, although they exhibit lower shear capacities, they are more capable of reducing stress concentrations and thus avoiding an early delamination failure of the composite. Consequently, the use of the more flexible adhesive 2 increased the joint strength of lap shear joints by only 5% compared to lap shear joints with the stiffer adhesive 1. However, the strength of the reverse-bent joint with adhesive 1 decreased by 31% when adhesive 2 was used. In this case, the joint strength was only limited by the low shear capacity of the flexible adhesive as no delamination of the composite occurred. Notably, the maximum principal stress within the bondline of adhesive 2 also correlates with the tensile material strength listed in Table 3.2.

6.3 Summary

FEA has been used to investigate the parameters that influence joint strength for three different joint configurations. Trends found from FEA to improve joint strengths were validated experimentally. A comparison of strength between the reverse-bent and standard lap shear joint showed an improvement of up to 40%. The static joint strength of the standard lap shear joint appeared to be strongly dependent upon bending and subsequent yielding of the metallic substrates. However, in the case of the reverse-bent joint, failure was predominantly cohesive shear

in the adhesive layer, or else, ultimate failure was due to lateral straining of the substrates away from the overlap.

The fatigue life of similar lap shear joints was improved significantly when the reverse-bent configuration was used. The applied loads, at which no failure occurred after one million cycles, increased from 3.25 kN for the standard lap shear joint to 8.5 kN for the reverse-bent joint. Notably, the joint failure load was less than that to cause yielding in the substrates.

Also for joints with composite substrates the experimental work appeared to validate the numerical results with higher failure loads resulting from the reverse-bent joint. Depending on the materials, and especially the composite layup, an increase in joint strength of up to 193% was obtained. Locations of highest stress within the adhesive and composite substrates of the reverse-bent joint were deduced not to be adjacent to points of singular stresses, enabling a simpler evaluation of stresses using FEA. When reverse-bent joints predominantly failed cohesively within the adhesive, maximum predicted principal stresses in the adhesive correlated with experimental strength values. Compared to a brittle adhesive, a more flexible adhesive is generally better capable of bonding composite materials using lap shear joints, yet, high strength brittle adhesives were shown to be better using the reverse-bent joint configuration, as through-thickness stresses were reduced, whilst the shear stresses within the bondline and substrates were more uniformly distributed.

7 General conclusions

This chapter briefly draws some general conclusions about lap joints in automotive applications and the potential of the reverse-bent joint. Finally, some recommendations for future investigations are given.

7.1 Improvements of lap joints

There are various different ideas available in the literature aiming to increase the performance of traditional lap shear joints, such as bending the substrates prior to bonding, increasing the adhesive thickness in certain areas or varying the adhesive properties along the bondline. All of these attempts may be beneficial for certain applications, however, three joint designs were chosen that were expected to produce higher joint strengths without increasing cost significantly. A parametric study using FEA resulted in a new joint where stresses within the overlap area are uniformly distributed and, due to simplistic design, no significant additional costs are expected for industrial implementations. The design of the new reverse-bent joint can be used for metal and composite joints and thus, benefits are also expected for hybrid joints.

7.2 Performance comparison of reverse-bent and lap shear joints

The parametric study of three different joints using FEA showed trends to reduce and to relocate maximum stress to less critical areas in the overlap area by changing the design variables. Stress peaks at the overlap ends, high through-thickness stresses and deformations of the substrates could be reduced. The more uniform stress distribution within substrates and the adhesive layer of the improved reverse-bent joint produced an increase in joint strength of up to 40% for metallic substrates. However, it was shown that the joint strength is strongly dependent on the yield point of the metallic substrates. The lap shear joints failed mostly due to bending of the substrates, whereas the reverse-bent joints failed predominantly in shear or due to lateral straining of the substrates away from the overlap. When the reverse-bent joint was subjected to fatigue the performance increase was even more significant. The applied loads, at which no failure occurred after one million cycles, increased from 3.25 kN for the standard lap shear joint to 8.5 kN for the reverse-bent joint. Using composite substrates the joint strength increased up to 190% depending upon the composite layup. The advantage of the reverse-bent joint over the lap shear joint increased with the sensitivity of substrates subjected to delamination failure. Generally, it was shown that stiffer adhesives with greater shear strengths can be used for reverse-bent joints due to reduced stress concentrations.

For metallic joints it was also demonstrated that the simple formula for estimating the joint strength of lap shear joints presented by Adams et al. (1997) can also be applied to reverse-bent joints. For joints with composite substrates the application of failure criteria based upon maximum stresses or strains within adhesive and composite are expected to produce good results due to the fact that the maximum stresses in reverse-bent joints do not occur at the points of singular stresses at the overlap ends.

7.3 General recommendations for the use of lap joints

The design of lap joints in industrial applications may vary from the simplified lap shear joint that this investigation was based upon. However, the FE Analysis and the experimental work has yielded some general design recommendations for the practical use of adhesive overlap joints:

- Eccentricities of the substrates should be avoided.
- Plastic deformations of the metallic substrates adjacent to the adhesive can cause failure at the metal interface and should be avoided.
- Concentrations of adhesive can help to reduce local stress peaks (i.e. adhesive fillets)
- Varying the overlap geometry can be a simple way to increase the joint strength significantly
- Reverse-bent joints enable the use of stiffer and therefore typically stronger adhesives to be used.

7.4 Recommendations for future work

It has been shown that the reverse-bent joint exhibited superior performance for the chosen materials and overlap geometries. Further investigations using a wider range of substrate and adhesive materials could refine the use of the design variables and validate the performance increase over the traditional lap-shear joint.

Sandwich materials with foam cores are increasingly used, however, their strength in the through-thickness direction is particularly weak, and which complicates joining sandwich structures to other components. Through thickness stresses were minimised in the reverse-bent joint avoiding peel stress peaks, and modifications

to the sandwich joints using the concept of the reverse-bent joint may increase their strength significantly. Numerical and experimental analyses need to validate this.

The more uniformly distributed stresses of the reverse-bent joint make the prediction of initial failure location difficult and subsequent crack propagation when the reverse-bent joint is subjected to fatigue loading. This can be clarified using appropriate experimental tools.

A continuation of the work would be to focus upon the prediction of both static and fatigue strengths of the reverse-bent joint. This should be less complicated as failure does not seem to initiate at points of singular stresses, which therefore allows a more reliable application of failure criteria.

Bibliography

3M (2004). Technical information sheet Scotch-Weld DP460 Off-White. 3M.

Adams, R. (2001). The design of adhesively-bonded lap joints: Modelling considerations. *International SAMPE Symposium and Exhibition (Proceedings) 46 I*, 402 – 414.

Adams, R., J. Comyn, and W. Wake (1997). *Structural Adhesive Joints in Engineering* (2 ed.). London: Chapman & Hall.

Adams, R. D. and J. A. Harris (1987). Influence of local geometry on the strength of adhesive joints. *International Journal of Adhesion and Adhesives 7*(2), 69 – 80.

AEROBOLTS (2007). Aerobolts webpage. http://www.aerobolt.com.au.

Avila, A. F. and P. d. O. Bueno (2004). An experimental and numerical study on adhesive joints for composites. *Composite Structures 64*(3-4), 531 – 537.

Bondmaster (2001). Technical information sheet ESP110. Bondmaster.

Cartie, D. D., G. Dell'Anno, E. Poulin, and I. K. Partridge (2006). 3D reinforcement of stiffener-to-skin T-joints by Z-pinning and tufting. *Engineering Fracture Mechanics 73*(16), 2532 – 2540.

Chamis, C. and P. Murthy (1991). Simplified procedures for designing adhesively bonded composite joints. *Journal of Reinforced Plastics and Composites 10*(1), 29 – 41.

Chang, B., Y. Shi, and S. Dong (1999). Comparative studies on stresses in weld-bonded, spot-welded and adhesive-bonded joints. *Journal of Materials Processing Technology 87*(1-3), 230 – 236.

Cherry, B. and N. Harrison (1970). Optimum profile for a lap joint. *Journal of Adhesion 2*, 125 – 8.

Coates, C. W. and E. A. Armanios (2000). An assessment of nested overlap and transverse interfacial layer in co-cured composite single lap joints. *Proceedings of 15th American Society of Composites, September 24-27, Texas A&M University, College Station, Texas, US*, 1161 – 1171.

Da Silva, L. F. M. and R. Adams (2007). Adhesive joints at high and low temperatures using similar and dissimilar adherends and dual adhesives. *International Journal of Adhesion and Adhesives 27*(3), 216–226.

DasGupta, S. (1979). Stresses in adhesive lap joints with pre-bent adherends. *American Society of Mechanical Engineers (Paper)* (79-DET-105), 1 – 4.

DasGupta, S. and S. P. Sharma (1975). Stresses in an adhesive lap joint. *American Society of Mechanical Engineers (Paper)* (75-WA/DE-18), 2 – 7.

Drucker, D. C. and W. Prager (1952). Soild mechanics and plastic analysis for limit design. *Quarterly of Applied Mathematics 10*(2), 157 – 165.

Fitton, M. and J. Broughton (2005). Variable modulus adhesives: An approach to optimised joint performance. *International Journal of Adhesion and Adhesives 25*(4), 329 – 336.

Givler, R. C. and R. B. Pipes (1981). Analysis of the 'joggle-lap' joint for automotive applications. *ASTM Special Technical Publication*, 61 – 74.

Gleich, D., M. Van Tooren, and P. De Haan (2000). Shear and peel stress analysis of an adhesively bonded scarf joint. *Journal of Adhesion Science and Technology 14*(6), 879 – 893.

Goland, M. and E. Reissner (1944). The stresses in cemented joints. *Journal of Applied Mechanics 11*(1).

Greenwood, L., T. R. Boag, and A. S. McLaren (1966). Stress distribution in lap joints. pp. 273 – 279. MacLaren and Sons LDT; London.

Griffith, A. A. (1921). The phenomenon of rupture and flow in solids. *Philosophical Transactions of the Royal Society of London. Series A, Containing Papers of a Mathematical or Physical Character 221*, 163 – 198.

Groth, H. and P. Nordlund (1991). Shape optimization of bonded joints. *International Journal of Adhesion and Adhesives 11*(4), 204 – 212.

Harris, B. (2003). *Fatigue in composites.* Woodhead Publishing Limited, Cambridge England.

Hart-Smith, L. (1973a). Adhesive-bonded double-lap joints. Technical Report CR-112235, NASA.

Hart-Smith, L. (1973b). Adhesive-bonded single-lap joints. Technical Report CR-112236, NASA.

Hashin, Z. (1981). Fatigue failure criteria for unidirectional fiber composites. *Journal of Applied Mechanics, Transactions ASME 48*(4), 846 – 852.

Hennig, G. (1965). Festigkeitsuntersuchungen an Metallklebverbindungen. *Plaste und Kautschuk 12*(8), 459–464.

Hildebrand, M. (1994). Non-linear analysis and optimization of adhesively bonded single lap joints between fibre-reinforced plastics and metals. *International Journal of Adhesion and Adhesives 14*(4), 261 – 267.

Hu, N., B. Wang, H. Sekine, Z. Yao, and G. Tan (1998). Shape-optimum design of a bi-material single-lap joint. *Composite Structures 41*(3-4), 315 – 330.

Jethwa, J. K. (1995). *The fatigue performance of adhesively bonded metal joints.* Ph. D. thesis, Imperial College of Science Technology and Medicine, London.

Krueger, R., I. L. Paris, T. K. O'Brien, and P. J. Minguet (2002). Comparison of 2D finite element modeling assumptions with results from 3D analysis for composite skin-stiffener debonding. *Composite Structures 57*(1), 161 – 168.

Liu, J. and T. Sawa (2002). Strength and finite element analysis of single-lap joints with adhesively filled columns. *American Society of Mechanical Engineers, Design Engineering Division (Publication) DE 115*, 547 – 552.

Matting, A. and U. Draugelates (1968). Die schwingfestigkeit von metallklebverbindungen. *Adhaesion 12*, 5–22.

McLaren, A. and I. MacInnes (1958). The influence on the stress distribution in an adhesive lap joint of bending of the adhering sheets. *British journal of applied physics 9*, 72–77.

Melograna, J. D. and J. L. Grenestedt (2004). Revisiting a wavy bonded single lap joint. *AIAA Journal 42*(2), 395 – 402.

Miller, K., Y. Chao, and P. Wang (1998). Performance comparison of spot-welded, adhesive bonded, and self-piercing riveted aluminum joints. *ASM Proceedings of the International Conference: Trends in Welding Research, Pine Mountain, Georgia, US*, 910 – 915.

Mostovoy, S. and E. J. Ripling (1975). Flaw tolerance of a number of commercial and experimental adhesives. *Adhesion Science and Technology 9b*, 513–562.

Nirantar, P. and E. Sancaktar (2002). Optimization of adhesively bonded single lap joints by tapering of adherends. *American Society of Mechanical Engineers, Design Engineering Division (Publication) DE 115*, 575 – 588.

Ojalvo, I. U. (1985). Optimization of bonded joints. *AIAA Journal 23*(10), 1578 – 1582.

Paris, P. C. and F. A. Erdogan (1963). A critical analysis of crack propagation laws. *Journal of Basic Engineering, Transactions of the American Society of Mechanical Engineers 85*, 528–534.

Pires, I., L. Quintino, J. Durodola, and A. Beevers (2003). Performance of bi-adhesive bonded aluminium lap joints. *International Journal of Adhesion and Adhesives 23*(3), 215 – 223.

Raphael, C. (1966). Variable-adhesive bonded joints. In *Applied Polymer Symposia*, 3, pp. 99–108.

Renton, W. J. and J. R. Vinson (1975). Efficient design of adhesive bonded joints. *Journal of Adhesion 7*(3), 175 – 193.

Richardson, G., A. Crocombe, and P. Smith (1993). Comparison of two- and three-dimensional finite element analyses of adhesive joints. *International Journal of Adhesion and Adhesives 13*(3), 193 – 200.

Rispler, A., L. Tong, G. Steven, and M. Wisnom (2000). Shape optimization of adhesive fillets. *International Journal of Adhesion and Adhesives 20*(3), 221 – 231.

Sancaktar, E. and S. Kumar (2000). Selective use of rubber toughening to optimize lap-joint strength. *Journal of Adhesion Science and Technology 14*(10), 1265 – 1296.

Sancaktar, E. and P. O. Lawry (1980). Photoelastic study of the stress distribution in adhesively bonded joints with prebent adherends. *Journal of Adhesion 11*(3), 233 – 241.

Sancaktar, E. and S. R. Simmons (2000). Optimization of adhesively-bonded single lap joints by adherend notching. *Journal of Adhesion Science and Technology 14*(11), 1363 – 1404.

Sawyer, J. W. (1985). Effect of stitching on the strength of bonded composite single lap joints. *AIAA Journal 23*(11), 1744 – 1748.

Sawyer, J. W. and P. A. Cooper (1981). Analytical and experimental results for bonded single lap joints with preformed adherends. *AIAA Journal 19*(11), 1443 – 1451.

Taylor, A. (1997). *The impact and durability performance of adhesively-bonded metal joints PhD.* Ph. D. thesis, University of London.

Tong, L., L. Jain, K. Leong, D. Kelly, and I. Herszberg (1998). Failure of transversely stitched rtm lap joints. *Composites Science and Technology 58*(2), 221 – 227.

Tsai, S. (1965). Strength characteristics of composite materials. Technical Report CR-224, NASA.

Tsai, S. and E. Wu (1971). General theory of strength for anisotropic materials. *Journal of Composite Materials 5*, 58 – 80.

Turaga, U. and C. Sun (2003). An investigation of adhesive single-lap joints with attachments. *Collection of Technical Papers - AIAA/ASME/ASCE/AHS/ASC Structures, Structural Dynamics and Materials Conference 7*, 5061 – 5071.

Volkersen, O. (1938). Die Nietkraftverteilung in zugbeanspruchten Nietverbindungen mit konstantem Laschenquerschnitt. *Luftfahrtforschung 15*, 41–47.

Wöhler, A. (1870). Über die Festigkeitsversuche mit Eisen und Stahl. *Zeitschrift für Bauwesen 20*, 74–106.

Yamada, S. E. and C. T. Sun (1978). Analysis of laminate strength and its distribution. *Journal of Composite Materials 12*, 275 – 284.

Zeng, Q. (2001). *A study on composite adhesive lap joints.* Ph. D. thesis, Purdue University.

Zeng, Q. and C. Sun (2000). New bonded composite wavy lap joint. *Collection of Technical Papers - AIAA/ASME/ASCE/AHS/ASC Structures, Structural Dynamics and Materials Conference 1*(II), 995 – 1003.

Zeng, Q. and C. Sun (2004). Fatigue performance of a bonded wavy composite lap joint. *Fatigue and Fracture of Engineering Materials and Structures 27*(5),

413 – 422.

A Publications

1 **Shape optimisation of lap shear joints**

G. Fessel, N.A. Fellows, J.G. Broughton

Adhesion '05; 9th International Conference on the Science and Technology of Adhesion and Adhesives, Oxford, UK, 2005, 198-201.

2 **Evaluation of different lap shear joint geometries for automotive applications**

G. Fessel, J.G. Broughton, N.A. Fellows, J.F. Durodola, A.R. Hutchinson

International Journal of Adhesion and Adhesives, 2007, 27, 574-583

3 **A numerical and experimental study on reverse-bent joints for composite substrates**

G. Fessel, J.G. Broughton, N.A. Fellows, J.F. Durodola, A.R. Hutchinson

48th AIAA/ASME/ASCE/AHS/ASC Structures, Structural Dynamics, and Materials Conference, Honolulu, Hawaii, US, 2007

4 **Fatigue performance of metallic reverse-bent joints**

G. Fessel, J.G. Broughton, N.A. Fellows, J.F. Durodola, A.R. Hutchinson

Fatigue and Fracture of Engineering Materials and Structures, 2009, 32, 704-712

The contents of four papers, listed on page 114, have been removed from this thesis due to copyright restrictions